

Design and Performance of Open-Graded Friction Course Mixtures Containing Epoxy Asphalt

by

Anurag Anand

A thesis submitted to the Graduate Faculty of
Auburn University
in partial fulfillment of the
requirements for the Degree of
Master of Science

Auburn, Alabama
December 11, 2021

Keywords: OGFC Mix Design, FC-5, Epoxy-Modified Asphalt, OGFC Mixture Performance Testing, Optimal Epoxy Dosage, EMA Binder Image Analysis

Copyright 2021 by Anurag Anand

Approved by

Fan Yin, Chair, Assistant Director, National Center for Asphalt Technology
Nam Tran, Assistant Director, National Center for Asphalt Technology
Raquel Moraes, Assistant Research Professor, National Center for Asphalt Technology

ABSTRACT

Open-Graded Friction Course (OGFC) is a type of pavement primarily composed of coarse aggregates and high asphalt content. Higher permeability, better friction resistance, improved visibility, reduced pavement noise, and reduced hydroplaning are some of the benefits associated with the uniform aggregate structuring with an extensive, interconnected air void system. However, a severe limitation of OGFC to date is surface raveling leading to reduced service life. This thesis aims to determine the viability of using epoxy-modified asphalt (EMA) to improve the long-term durability and life span of OGFC mixtures. To that end, a comprehensive literature review and experimental laboratory plan were conducted. The chemical compatibility of EMA binders was evaluated using fluorescence microscopy and image analysis. EMA OGFC mixtures were prepared at different epoxy dosage rates (EDR) with epoxy materials from domestic (U) and foreign sources (J), and 30% EDR was determined as optimum with respect to mixture performance and cost estimation. The EMA mixtures showed improved raveling resistance and durability as EDR increased between 15% and 40%. After extended long-term aging, the EMA mixtures at 30% EDR and high polymer (HP) mixtures showed significantly better raveling resistance and durability than the polymer-modified asphalt (PMA) mixtures. All OGFC mixtures had acceptable Tensile Strength Ratio results regardless of the type of asphalt binder used. Two EMA mixtures prepared with the domestic epoxy materials exhibited high severity stripping failures in the Hamburg Wheel Tracking Test (HWTT), possibly due to the lack of cohesive strength of the not fully cured EMA binder. Additional HWTT testing conducted on U-EMA mixtures cured for one to four weeks at room temperature indicated that the performance of the mixture improved with time as the EMA binder cured.

ACKNOWLEDGMENTS

I would like to sincerely thank my advisor, Dr. Fan Yin, for supporting me constantly and standing inspirational. I would like to extend my gratitude to Dr. Nam Tran and Dr. Raquel Moraes for serving as my committee members and providing their invaluable guidance throughout the project.

I would also like to thank the incredible faculty, staff, and friends at NCAT who never failed to share knowledge and warmth from day one. I would not have had a smooth journey of two and a half years without their help.

Special thanks to Dr. Sridhar Raju and Dr. Anasua Guharay from BITS, Pilani, for playing a significant role in my life by mentoring me and motivating me to pursue research.

Finally, I would like to express my gratitude to my family and friends, especially Buddy, Chen Chen, and PD, for their unwavering support and encouragement.

TABLE OF CONTENTS

ABSTRACT.....	2
ACKNOWLEDGMENTS	3
LIST OF TABLES	7
LIST OF FIGURES	9
LIST OF ABBREVIATIONS.....	14
CHAPTER 1. INTRODUCTION	17
1.1 Background	17
1.2 Objectives.....	18
1.3 Research Approach	18
CHAPTER 2. LITERATURE REVIEW	21
2.1 State of the Practice on Use of OGFC.....	21
2.2 OGFC Mix Design and Performance Testing	24
2.2.1 Selection of Suitable Materials	26
2.2.2 Selection of Design Gradation	29
2.2.3 Determination of Optimum Binder Content	29
2.2.4 Performance Testing.....	31
2.3 Approaches to Improve OGFC Durability	33
2.4 Epoxy-Modified Asphalt Binders and Mixtures	42
2.4.1 Epoxy Asphalt Binders	42
2.4.2 Epoxy-Modified Asphalt Mixtures	46
CHAPTER 3. SELECTION OF CHEMICALLY COMPATIBLE EA BINDERS	51
3.1 Experimental Plan	51
3.1.1 Materials	51
3.1.2 Preparation of EMA Binders	53

3.1.3	Fluorescence Microscopy Testing and Analysis.....	54
3.2	Test Results and Discussion.....	56
3.3	Summary of Findings.....	63
CHAPTER 4. DETERMINATION OF OPTIMUM EPOXY DOSAGE RATE		65
4.1	Experimental Plan	66
4.1.1	Materials and Mix Designs	66
4.1.2	Preparation of EMA Binders and Mixtures	67
4.1.3	Mixture Testing Plan.....	70
4.2	Test Results and Discussion.....	74
4.2.1	Mixture Testing Experiment Results	74
4.2.2	Selection of Optimum EDR.....	91
4.3	Summary of Findings.....	95
CHAPTER 5. MIX DESIGN OF EMA OGFC MIXTURES.....		96
5.1	Experimental Plan	96
5.1.1	Materials and Mix Design.....	96
5.1.2	Proposed Mix Design Procedure for EMA OGFC Mixtures.....	98
5.1.3	Modified Pie Plate Test Procedure for OGFC Mixtures with EMA Binders	100
5.2	Test Results and Discussion.....	102
5.2.1	GRN1 Mix Design	103
5.2.2	GRN2 Mix Design	104
5.2.3	GRN3 Mix Design	106
5.2.4	LMS Mix Design	108
5.3	Summary of Findings.....	109
CHAPTER 6. PERFORMANCE CHARACTERIZATION OF EMA OGFC MIXTURES		111
6.1	Experimental Plan	111

6.1.1	Materials and Mix Design.....	111
6.1.2	Laboratory Testing.....	112
6.2	Test Results and Discussion.....	113
6.2.1	Cantabro Loss Results.....	113
6.2.2	IDT Strength Results.....	119
6.2.3	IDT Fracture Energy (G_f) Results.....	124
6.2.4	TSR Results	129
6.2.5	HWTT Results	134
6.3	Summary of Findings.....	141
CHAPTER 7. CONCLUSIONS AND RECOMMENDATIONS		144
7.1	Conclusions	144
7.2	Recommendations	147
REFERENCES		148

LIST OF TABLES

Table 2-1. Summary of OGFC Requirements for U.S. Agencies (Source: Jackson et al., 2008)	25
Table 2-2. Coarse Aggregate Requirements for OGFC Mix Designs (Source: Bennert and Cooley, 2014; FDOT, 2022)	27
Table 2-3. Fine Aggregate Requirements for OGFC Mix Designs (Source: Bennert and Cooley, 2014; FDOT, 2022)	27
Table 2-4. FC-5 Gradation Design Range (Source: FDOT, 2022)	29
Table 2-5. Optimum Asphalt Content Properties for OGFC Mixtures	30
Table 2-6. Range of FDOT Design Binder Contents	31
Table 2-7. Proposed OFGC Mixture Specification Requirements (Source: Watson et al., 2018)	32
Table 2-8. Testing Procedures to Investigate Chemistry and Rheology of Epoxy Asphalt Binders (Source: Yin et al., 2021)	43
Table 3-1. Proposed Testing Matrix for Experiment 1	53
Table 3-2. Blending Proportions of Component Materials for J-EMA Binders	53
Table 3-3. Blending Proportions of Component Materials for U-EMA Binders	54
Table 3-4. Summary of Epoxy Particle Sizes of EMA Binders at 15% and 25% EDRs	59
Table 4-1. Proposed Mixture Testing Matrix for Experiment 2	66
Table 4-2. Job Mix Formula Summary of GRN1 and LMS Mixtures	67
Table 4-3. Blending Proportions of Component Materials for J-EMA Binders	68
Table 4-4. Blending Proportions of Component Materials for U-EMA Binders	69
Table 4-5. Statistical Comparison for Cantabro Loss Results of GRN1 Mixtures with PMA and J-EMA Binders	75
Table 4-6. Statistical Comparison for Cantabro Loss Results of GRN1 Mixtures with PMA and U-EMA Binders	76
Table 4-7. Statistical Comparison for Cantabro Loss Results of LMS Mixtures with PMA and J-EMA Binders	78
Table 4-8. Statistical Comparison for Cantabro Loss Results of LMS Mixtures with PMA and U-EMA Binders	78
Table 4-9. Statistical Comparison for IDT Strength Results of GRN1 Mixtures with PMA and J-EMA Binders	82

Table 4-10. Statistical Comparison for IDT Strength Results of GRN1 Mixtures with PMA and U-EMA Binders	83
Table 4-11. Statistical Comparison for IDT Strength Results of LMS Mixtures with PMA and J-EMA Binders	84
Table 4-12. Statistical Comparison for IDT Strength Results of LMS Mixtures with PMA and U-EMA Binders	85
Table 4-13. Statistical Comparison for IDT Fracture Energy Results of GRN1 Mixtures with PMA and J-EMA Binders.....	87
Table 4-14. Statistical Comparison for IDT Fracture Energy Results of GRN1 Mixtures with PMA and U-EMA Binders	88
Table 4-15. Statistical Comparison for IDT Fracture Energy Results of LMS Mixtures with PMA and J-EMA Binders.....	89
Table 4-16. Statistical Comparison for IDT Fracture Energy Results of LMS Mixtures with PMA and U-EMA Binders	91
Table 4-17. Selection of Optimum EDR for J-EMA Binders.....	93
Table 4-18. Selection of Optimum EDR for U-EMA Binders	94
Table 5-1. Job Mix Formula Summary of GRN1, GRN2, GRN3, and LMS Mixes	97
Table 5-2. Testing Matrix of Experiment 3	97
Table 6-1. Summary of Cantabro Loss and Cantabro Aging Index (CAI) Results	114
Table 6-2. Summary of IDT Strength Results	120
Table 6-3. Summary of IDT G_f Results	125
Table 6-4. Summary of TSR Test Results	130
Table 6-5. Summary of HWTT Results.....	135

LIST OF FIGURES

Figure 1-1. Graphical Illustration of Research Approach.....	19
Figure 2-1. Responses of State DOTs for: a) Discontinuing the Use of OGFC, and b) Not Implementing OGFC (Source: Onyango and Woods, 2017).....	23
Figure 2-2. Types of Additives used in the U.S. (Source: Onyango and Woods, 2017).....	28
Figure 2-3. Curing Reaction of Epoxy Resin (Source: Tian et al., 2021).....	46
Figure 3-1. Epoxy Material Samples from Two Different Sources: (a) Domestic Source – <i>Part A</i> : Liquid Epoxy Resin, <i>Part B</i> : Blend of Asphalt Binder and Curing Agent, and (b) Foreign Source – <i>Part A</i> : Liquid Epoxy Resin, <i>Part B</i> : Curing Agent.....	52
Figure 3-2. Zeiss Axiovert 200 Inverted Fluorescence Microscope.....	56
Figure 3-3. Major Steps of Analyzing Fluorescence Micrographs in ImageJ (Source: Yin et al., 2021).....	56
Figure 3-4. Fluorescence Micrographs of J-EMA Binders at 15% EDR: (a) Base Binder A, (b) Base Binder C, (c) Base Binder G, (d) Base Binder Z	57
Figure 3-5. Fluorescence Micrographs of J-EMA Binders at 25% EDR: (a) Base Binder A, (b) Base Binder C, (c) Base Binder G, (d) Base Binder Z	57
Figure 3-6. Fluorescence Micrographs of U-EMA Binders at 15% EDR: (a) Base Binder A, (b) Base Binder C, (c) Base Binder G, (d) Base Binder Z	58
Figure 3-7. Fluorescence Micrographs of U-EMA Binders at 25% EDR: (a) Base Binder A, (b) Base Binder C, (c) Base Binder G, (d) Base Binder Z	58
Figure 3-8. Cumulative Distribution Curves of Epoxy Particle Sizes for J-EMA Binders at 15% EDR.....	60
Figure 3-9. Cumulative Distribution Curves of Epoxy Particle Sizes for J-EMA Binders at 25% EDR.....	60
Figure 3-10. Cumulative Distribution Curves of Epoxy Particle Sizes for U-EMA Binders at 15% EDR.....	61
Figure 3-11. Cumulative Distribution Curves of Epoxy Particle Sizes for U-EMA Binders at 25% EDR.....	61
Figure 3-12. Difference in the Residue of Top and Bottom Portions after Storage Stability Test Followed by Soxhlet Asphalt Extraction: (a) J-EMA Binders, (b) U-EMA Binders (Source: Yin et al., 2021)	63

Figure 3-13. SARA Fractions of the Base Asphalt Binders (Source: Yin et al., 2021).....	63
Figure 4-1. Aging of Compacted OGFC Mixture Samples in the Environmental Chamber.....	70
Figure 4-2. Weighing an OGFC Mixture Sample after the Cantabro Test.....	71
Figure 4-3. IDEAL CT Equipment and Sample after Testing.....	72
Figure 4-4. Example of Load-Displacement Curve from the IDT Test.....	73
Figure 4-5. Cantabro Mass Loss Results of GRN1 Mixtures with PMA and J-EMA Binders at Different Mix Aging Conditions.....	75
Figure 4-6. Cantabro Mass Loss Results of GRN1 Mixtures with PMA and U-EMA Binders at Different Mix Aging Conditions.....	76
Figure 4-7. Cantabro Mass Loss Results of LMS Mixtures with PMA and J-EMA Binders at Different Mix Aging Conditions.....	77
Figure 4-8. Cantabro Mass Loss Results of LMS Mixtures with PMA and U-EMA Binders at Different Mix Aging Conditions.....	79
Figure 4-9. Cantabro Aging Index Results of GRN1 Mixtures.....	80
Figure 4-10. Cantabro Aging Index Results of LMS Mixtures.....	81
Figure 4-11. IDT Strength Results of GRN1 Mixtures with PMA and J-EMA Binders at Different Mix Aging Conditions.....	82
Figure 4-12. IDT Strength Results of GRN1 Mixtures with PMA and U-EMA Binders at Different Mix Aging Conditions.....	83
Figure 4-13. IDT Strength Results of LMS Mixtures with PMA and J-EMA Binders at Different Mix Aging Conditions.....	84
Figure 4-14. IDT Strength Results of LMS Mixtures with PMA and U-EMA Binders at Different Mix Aging Conditions.....	85
Figure 4-15. IDT G_f Results of GRN1 Mixtures with PMA and J-EMA Binders at Different Mix Aging Conditions.....	87
Figure 4-16. IDT G_f Results of GRN1 Mixtures with PMA and U-EMA Binders at Different Mix Aging Conditions.....	88
Figure 4-17. IDT G_f Results of LMS Mixtures with PMA and J-EMA Binders at Different Mix Aging Conditions.....	89
Figure 4-18. IDT G_f Results of LMS Mixtures with PMA and U-EMA Binders at Different Mix Aging Conditions.....	90

Figure 5-1. Proposed Mix Design Procedure for EMA OGFC Mixtures	98
Figure 5-2. Reference Pie Plate Pictures of OGFC mixtures with PG 67-22 Unmodified Binder at Different Binder Contents: (a) 5.5%, (b) 6.0%, (c) 6.5% (FDOT, 2020)	99
Figure 5-3. Pie Plate Pictures (with loose mixture) of GRN1 Mixtures with PG 67-22 Binder at: (a) JMF OBC-0.5% (6.3%), (b) JMF OBC (6.8%), (c) JMF OBC+0.5% (7.3%)	103
Figure 5-4. Pie Plate Pictures (without loose mixture) of GRN1 Mixtures with PG 67-22 Binder at: (a) JMF OBC-0.5% (6.3%), (b) JMF OBC (6.8%), (c) JMF OBC+0.5% (7.3%)	103
Figure 5-5. Pie Plate Pictures of GRN1 Mixture with U30C EMA Binder at JMF OBC (6.8%): (a) with Loose Mixture, (b) without Loose Mixture	104
Figure 5-6. Pie Plate Pictures (with loose mixture) of GRN2 Mixtures with PG 67-22 Binder at: (a) JMF OBC-0.5% (6.1%), (b) JMF OBC (6.6%), (c) JMF OBC+0.5% (7.1%)	105
Figure 5-7. Pie Plate Pictures of GRN2 Mixtures with PG 67-22 Binder at: (a) JMF OBC-0.5% (6.1%), (b) JMF OBC (6.6%), (c) JMF OBC+0.5% (7.1%)	105
Figure 5-8. Pie Plate Pictures of GRN2 Mixture with J30Z EMA Binder at JMF OBC (6.6%): (a) with Loose Mixture, (b) without Loose Mixture	106
Figure 5-9. Pie Plate Pictures (with loose mixture) of GRN3 Mixtures with PG 67-22 Binder at: (a) JMF OBC-0.5% (6.0%), (b) JMF OBC (6.5%), (c) JMF OBC+0.5% (7.0%)	106
Figure 5-10. Pie Plate Pictures (without loose mixture) of GRN3 Mixtures with PG 67-22 Binder at: (a) JMF OBC-0.5% (6.0%), (b) JMF OBC (6.5%), (c) JMF OBC+0.5% (7.0%)	107
Figure 5-11. Pie Plate Pictures of GRN3 Mixture with J30Z EMA Binder at JMF OBC (6.5%): (a) with Loose Mixture, (b) without Loose Mixture	107
Figure 5-12. Pie Plate Pictures (with loose mixture) of LMS Mixtures with PG 67-22 Binder at: (a) JMF OBC-0.5% (6.4%), (b) JMF OBC (6.9%), (c) JMF OBC+0.5% (7.4%)	108
Figure 5-13. Pie Plate Pictures (without loose mixture) of LMS Mixtures with PG 67-22 Binder at: (a) JMF OBC-0.5% (6.4%), (b) JMF OBC (6.9%), (c) JMF OBC+0.5% (7.4%)	108
Figure 5-14. Pie Plate Pictures of LMS Mixture with U30C EMA Binder at JMF OBC (6.9%): (a) with Loose Mixture, (b) without Loose Mixture	109
Figure 6-1. Cantabro Mass Loss of GRN1 Mixtures with Different Asphalt Binders at Two Mix Aging Conditions	116
Figure 6-2. Cantabro Mass Loss of GRN2 Mixtures with Different Asphalt Binders at Two Mix Aging Conditions	117

Figure 6-3. Cantabro Mass Loss of GRN3 Mixtures with Different Asphalt Binders at Two Mix Aging Conditions	118
Figure 6-4. Cantabro Mass Loss of LMS Mixtures with Different Asphalt Binders at Two Mix Aging Conditions	119
Figure 6-5. IDT Strength of GRN1 Mixtures with Different Asphalt Binders at Two Mix Aging Conditions	121
Figure 6-6. IDT Strength of GRN2 Mixtures with Different Asphalt Binders at Two Mix Aging Conditions	122
Figure 6-7. IDT Strength of GRN3 Mixtures with Different Asphalt Binders at Two Mix Aging Conditions	123
Figure 6-8. IDT Strength of LMS Mixtures with Different Asphalt Binders at Two Mix Aging Conditions	124
Figure 6-9. IDT G_f Results of GRN1 Mixtures with Different Asphalt Binders at Two Mix Aging Conditions	126
Figure 6-10. IDT G_f Results of GRN2 Mixtures with Different Asphalt Binders at Two Mix Aging Conditions	127
Figure 6-11. IDT G_f Results of GRN3 Mixtures with Different Asphalt Binders at Two Mix Aging Conditions	128
Figure 6-12. IDT G_f Results of LMS Mixtures with Different Asphalt Binders at Two Mix Aging Conditions	129
Figure 6-13. TSR Test Results of GRN1 Mixtures with Different Asphalt Binders	131
Figure 6-14. TSR Test Results of GRN2 Mixtures with Different Asphalt Binders	132
Figure 6-15. TSR Test Results of GRN3 Mixtures with Different Asphalt Binders	133
Figure 6-16. TSR Test Results of LMS Mixtures with Different Asphalt Binders	134
Figure 6-17. HWTT Rutting Curves of GRN1 Mixtures with Different Asphalt Binders	137
Figure 6-18. HWTT Rutting Curves of GRN2 Mixtures with Different Asphalt Binders	138
Figure 6-19. HWTT Rutting Curves of GRN2 Mixtures with U30C Binder at Different Curing Times	138
Figure 6-20. Pictures of GRN2 Mixture Samples prepared with (a) PMA Binder, (b) HP Binder, (c) U30C Binder after Testing in HWTT	139
Figure 6-21. HWTT Rutting Curves of GRN3 Mixtures with Different Asphalt Binders	140

Figure 6-22. Picture of U30C GRN3 Mixture Samples after Testing in HWTT..... 140
Figure 6-23. Picture of HWTT Wheels Stuck with U30C GRN3 Mixture Particles..... 140
Figure 6-24. HWTT Rutting Curves of LMS Mixtures with Different Asphalt Binders 141

LIST OF ABBREVIATIONS

AASHTO	American Association of State Highway and Transportation Officials
ALDOT	Alabama Department of Transportation
ASTM	American Society for Testing and Materials
APWS	Asphalt Pavement Weathering System
CAI	Cantabro Aging Index
CII	Colloidal Instability Index
COV	Coefficient of Variation
CT _{Index}	Cracking Tolerance Index
DOT	Department of Transportation
E'	Storage Modulus
ECMT	European Conference of Ministers of Transport
EDR	Epoxy Dosage Rate
EMA	Epoxy-Modified Asphalt
EMOGPA	Epoxy-Modified Open-Graded Porous Asphalt
FDOT	Florida Department of Transportation
FHWA	Federal Highway Administration
FM	Florida Method
FTIR	Fourier-Transform Infrared
G*	Complex Modulus
G _f	Fracture Energy
GTR	Ground Tire Rubber
GRN	Granite

HP	High Polymer
HVS	Heavy Vehicle Simulator
HWTT	Hamburg Wheel Tracking Test
IDEAL-CT	Indirect Tensile Asphalt Cracking Test
IDT	Indirect Tensile
I-FIT	Illinois Flexibility Index Test
ITM	Indirect Tensile Modulus
J-EMA	Epoxy-Modified Asphalt with Foreign Epoxy Materials Source
JMF	Job Mix Formula
J_{nr}	Non-recoverable Creep Compliance
LAS	Liquid Anti-Strip
LMS	Limestone
LTA	Long-Term Aging
LVE	Linear Viscoelasticity
N_f	Number of Cycles to Failure
NAPA	National Asphalt Pavement Association
NCAT	National Center for Asphalt Technology
NCHRP	National Cooperative Highway Research Program
NMAS	Nominal Maximum Aggregate Size
OBC	Optimum Binder Content
OECD	Organization for Economic Co-operation and Development
OGFC	Open-Graded Friction Course
OGPA	Open-Graded Porous Asphalt

PG	Penetration Grade
PMA	Polymer-Modified Asphalt
RAP	Reclaimed Asphalt Pavement
R-LDPE	Recycled Low-Density Polyethylene
SARA	Saturates, Aromatics, Resins, and Asphaltenes
SBS	Styrene-Butadiene-Styrene
SCB	Semicircular Bending
SFE	Surface Free Energy
SGC	Superpave Gyrotory Compactor
STA	Short-Term Aging
TNZ	Transit New Zeal
TSR	Tensile Strength Ratio
U-EMA	Epoxy-Modified Asphalt with Domestic Epoxy Materials Source
UK	United Kingdom
U.S.	United States of America
UV	Ultraviolet
VCA	Voids in Coarse Aggregates
σ	Tensile Strength
δ	Phase Angle

CHAPTER 1. INTRODUCTION

1.1 Background

Open-graded friction course (OGFC) is a special type of asphalt surface layer with a high percentage of coarse aggregates, air voids, and binder content. The mixture has considerable safety and environmental benefits, such as reduced hydroplaning risk, reduced splash and spray from vehicle tires, higher friction resistance, improved visibility, and reduced noise. OGFC has been adopted since 1950 by state highway agencies in different parts of the United States, primarily southeast. For instance, the Florida Department of Transportation (FDOT) requires OGFC on all multi-lane roadways with a design speed of 50 mph or greater, except for curb and gutter areas. One reported disadvantage of these mixtures is that they are highly prone to raveling and have shorter service lives than dense-graded friction courses. Although some performance improvement was achieved in the past by using polymer-modified asphalt binders, there is still a strong need for alternative technologies that can reduce the raveling of OGFC.

One such potential method is to use epoxy-modified asphalt (EMA) binder since it provides superior resistance to oxidative aging and embrittlement, which are two major contributors to the raveling of OGFC mixtures. Therefore, the EMA binder has the potential to improve the long-term durability and extend the life span of OGFC mixtures. EMA is a premium asphalt material that is modified with thermosetting polymers. Compared to asphalt binders containing thermoplastic elastomers, the EMA binder offers better thermal stability, rigidity, and resistance (Chen et al., 2021). Over the last few years, low-dosage EMA binders with up to 25% epoxy dosage rate (EDR) have been successfully used in OGFC mixtures in New Zealand and the Netherlands (Herrington et al., 2007; Herrington, 2010; Wu et al., 2019; Zegard et al., 2019). Field trials of EMA OGFC mixtures were also constructed, and they have been performing well. However, more research is

necessary to investigate whether EMA binders can be successfully used in OGFC mixtures with different available materials, dosages, and conditions. Although it can be helpful for future research elsewhere, this thesis mainly focuses on the efficiency of an OGFC design in Florida.

1.2 Objectives

The overall objective of this study was to determine the viability of using EMA binders to improve the durability and life span of OGFC mixtures. Specifically, this study sought to: 1) select the optimum EDR for asphalt binder modification considering material cost and mixture performance properties, 2) develop an adequate mix design procedure for OGFC mixtures containing EMA binders, and 3) characterize the performance properties of OGFC mixtures with EMA and styrene-butadiene-styrene (SBS) modified asphalt binders.

1.3 Research Approach

The research approach followed to accomplish the objectives of the study is illustrated in Figure 1-1. First, a thorough literature review was conducted to synthesize existing studies on EMA binders and mixtures. Review topics of particular interest were comparisons in laboratory test results and field performance of OGFC mixtures containing EMA binders *versus* unmodified, SBS modified, and rubber modified binders. The literature review also included mix design procedures, laboratory conditioning, and performance testing of OGFC mixtures. In addition, a few successful approaches to increase the durability of the OGFC mixtures from previous studies are documented in chapter 2. Based on information collected from the literature review, a comprehensive experimental plan was developed, which included four supplementary laboratory experiments.

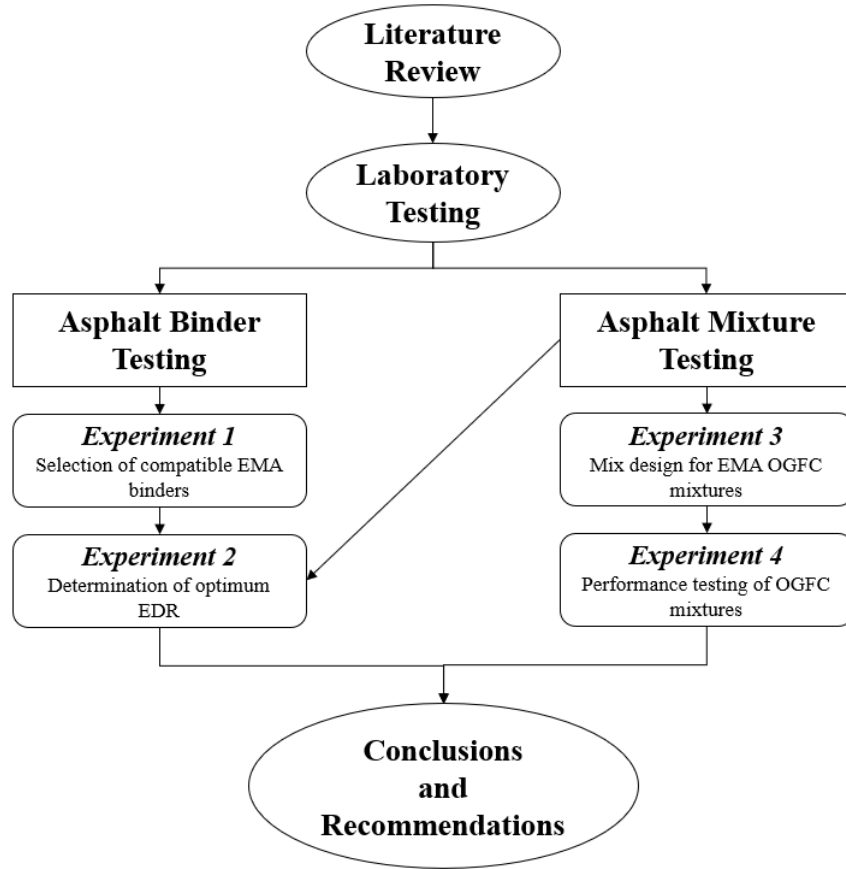


Figure 1-1. Graphical Illustration of Research Approach

Experiment 1 was to screen base asphalt binders from different sources for epoxy modification. Fluorescent microscopy analysis was performed to evaluate the morphology of EMA binders and quantify the network formation of epoxy resin in the modified binder. For each source of epoxy materials, the base binder that yielded the most chemically compatible EMA binders was selected for further evaluation. The experimental procedure and results are discussed in chapter 3.

Experiment 2, which is detailed in chapter 4, was to determine the optimum EDR with respect to material cost and mixture performance properties. This experiment focused on evaluating the raveling resistance, tensile strength, and fracture resistance of OGFC mixtures containing EMA binders at various EDRs *versus* a performance grade (PG) 76-22 PMA binder using the Cantabro

and Indirect Tensile (IDT) tests. Both tests were conducted at three mix aging conditions to account for the impact of mix aging. Finally, the optimum EDR was selected based on the Cantabro and IDT test results, as well as the estimated material cost of OGFC mixtures with EMA binders at various EDRs.

The objective of Experiment 3 was to determine an effective method of designing OGFC mixtures containing EMA binders. Following FDOT's current mix design procedure for friction course (FC-5) mixtures containing polymer-modified asphalt (PMA) or high polymer (HP) binders, a parallel procedure was proposed to design EMA OGFC mixtures based on the pie plate and Cantabro tests. Several modifications were made to the pie plate test procedure as described in FM 5-588 to account for the thermosetting behavior of EMA binders at the optimum EDR determined in Experiment 2. The proposed mix design procedure was then preliminarily validated with EMA OGFC mixtures prepared with four FDOT approved FC-5 mix designs. The details of the experimental matrix, testing, results, and conclusions are presented in chapter 5.

Experiment 4 focused on the performance characterization of OGFC mixtures containing EMA binders at the optimum EDR *versus* PMA and HP binders. Four FC-5 mix designs were included, corresponding to three sources of granite and one source of limestone. The Cantabro, IDT, modified Tensile Strength Ratio (TSR), and Hamburg Wheel Tracking (HWT) tests were conducted to evaluate the raveling resistance, tensile strength, fracture resistance, moisture resistance, and rutting resistance of OGFC mixtures prepared with different types of asphalt binders. Test results were analyzed to determine if the use of EMA binders could improve the long-term durability and extend the life span of OGFC mixtures. An elaboration of this experiment is given in chapter 6. Finally, the key findings and conclusions of the thesis are summarized in chapter 7, which also provides recommendations for future research and implementation.

CHAPTER 2. LITERATURE REVIEW

2.1 State of the Practice on Use of OGFC

OGFC is an open-graded asphalt mixture that contains a high percentage of air voids, typically between 15% and 22% (Alvarez et al., 2006). Depending on the region, it is also called permeable European mix, porous friction course, plant mix seal, popcorn mix, asphalt concrete friction course, and porous asphalt. The OGFC design has been widely used in Europe, Asia, and the United States for decades (Alvarez et al., 2011). The open-type asphalt wearing surfaces were experimented in Oregon in the 1930s, where they observed high skid resistance, less glare from headlights of oncoming vehicles, and better visibility of the centerline stripe when a $\frac{3}{4}$ in the open-type course was laid on a dense, impermeable base (Baldock, 1939). In 1944, California became the first state in the U.S. to construct OGFC as a plant mix seal coat (Huber, 2000). In the early 1970s, several U.S. State Department of Transportation (DOTs) started adopting OGFC when Federal Highway Administration (FHWA) initiated a program to improve the skid resistance of roadway surfaces (Smith et al., 1976). OGFC is usually paved as the final riding surface on roadways because of the safety and environmental benefits associated with this mixture. The interconnection of voids allows water to vertically drain through the OGFC layer to the layers beneath (Kandhal, 2002). The widely recognized benefits of OGFC pavements include (Huber, 2000; Hernandez-Saenz et al., 2016):

- Increase in the permeability of the pavement,
- Good contact between the tires and pavement surface (increased friction resistance),
- Minimization of the risk of hydroplaning,
- Reduction in backsplash and spray, and
- Improved visibility of the pavement markings.

As more OGFC pavements were constructed in multiple places, the noise-reducing benefit (Kayhanian and Harvey, 2020; Kandhal, 2002) and water quality treatment ability also added to the list of benefits associated with these pavements (Ndon, 2017). The influence of OGFC treatment on the reduction of fatalities is debatable as a few studies showed that the number of accidents reduced evidently after the construction of OGFC pavements (Kabir et al., 2012; Chen et al., 2017; Shimento and Tanaka, 2010; Takahashi, 2013). However, other studies stated that due to human dynamics, the driver speed would increase on OGFC surfaces leading to an increase in accidents (Buddhavarupu et al., 2015). Lyon et al. (2018) collected the total, injury, wet-road, wet-road run-off-road, and run-off road, and dry-road crash data from California, North Carolina, Pennsylvania, and Minnesota and performed empirical Bayes before-after analysis to determine the crash modification factors for various low-cost pavement treatments. Of those, mixed results were estimated for OGFC pavements based on the road type. The OGFC treatment was successful in decreasing the crashes on freeways except for dry-road crashes, but the effect was either negative or negligible on multilane and two-lane roads.

Despite the numerous benefits of OGFC pavements, the use of OGFC has diminished over the years mainly due to durability and service life issues (Cooley et al., 2009). The durability issues were generally evidenced by raveling and their rapid progression once the distress begins (Watson et al., 1998). The latest survey of state highway agencies conducted by the University of Tennessee on behalf of Tennessee DOT in 2017 showed that only 45% of the 40 responding state DOTs were using OGFC (Onyango and Woods, 2017). Of the remaining states, 42% used OGFC in the past but are not currently using it, and 13% have never used OGFC. Figure 2-1 summarizes the reasons reported by the state DOTs for not using or discontinuing the use of OGFC. The main issues included poor performance due to raveling, stripping, and clogging high costs compared to benefits

and winter weather maintenance. Raveling exists in two forms: 1) short-term and 2) long-term. Short-term raveling is caused by intense shearing forces at the tire-pavement interface that occurs within newly placed OGFCs, whereas long-term raveling is caused by the segregation of asphalt binder from aggregates due to gravity and dislodging of aggregates with traffic.

Further, most of the agencies using OGFC were in the southeastern and western United States. This was because, in northern states, OGFC tends to freeze and retain the ice longer. And also due to the fact that the application of sand, salt, or other treatments commonly used to prevent ice formation clog the air void structure of the mixture (Watson et al., 2018). Clogging of the pavement subsequently leads to losing permeability and increasing noise levels between the tire and pavement. Other issues reported were the formation of black ice with increased usage of salt in winter weather maintenance, which was unsafe to road users, and OGFC popping off due to freezing water underneath the layer. These challenges, plus lack of suitable aggregates, led to poor performance of OGFC and/or hindered its usage in some states predominantly north of the U.S. The conclusions confirmed the results obtained by previous surveys conducted in National Cooperative Highway Research Program (NCHRP) Project 01-55 and NCHRP Synthesis 284 (Watson et al., 2018).

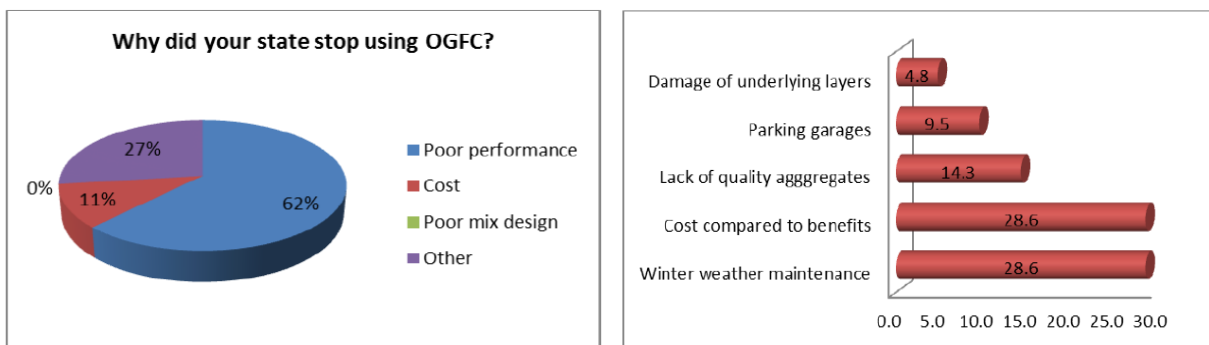


Figure 2-1. Responses of State DOTs for: a) Discontinuing the Use of OGFC, and b) Not Implementing OGFC (Source: Onyango and Woods, 2017)

2.2 OGFC Mix Design and Performance Testing

FHWA developed a Marshall mix design procedure for OGFC in 1974. The design was revised further in 1990 but included the same 12.5 mm maximum sieve size and design steps as follows:

1. Estimating the surface capacity of the predominate aggregate fraction by immersing and draining the aggregate in the Society of Automotive Engineers No. 10 lubricating oil.
2. Determining optimum asphalt content using the oil absorption test.
3. Selecting gradation that yields 15% or higher air voids content.
4. Selecting optimum mixing temperature from Pyrex glass plate test.
5. Evaluating mixture resistance to moisture susceptibility by the immersion-compression test.

However, the designs selected based on these methods lacked good performance and durability. Hence, many state agencies started developing their own OGFC mix design methods, which led to inconsistency in the reported field performance of the friction courses. The National Center for Asphalt Technology (NCAT) recommended a new-generation Superpave OGFC mix design procedure in 2000 (Mallick et al., 2000), which was refined in 2005 to incorporate additional information. The method included:

1. Selection of granular materials, binder, and additives.
2. Selection of design gradation that ensures high air void content and provides stone-on-stone contact within the coarse aggregate fraction retained on the 4.75 mm (No. 4) sieve.

3. Determination of optimum asphalt content based on the Cantabro mass loss before and after aging, air void content, and binder draindown.
4. Evaluation of moisture susceptibility using the modified Lottman method with freeze/thaw cycles.

Currently, there are two OGFC mix design standards available documented based on the NCAT mix design procedure. These two standards, namely ASTM D7064, *Standard Practice for Open-Graded Friction Course Mix Design*, and AASHTO PP 77, *Standard Practice for Materials Selection and Mixture Design of Permeable Friction Courses*, are slightly different in their materials selection and performance criteria. However, the 2014 NCAT survey showed that most of the agencies that responded were using state-specific methods. A summary of the OGFC requirements for U.S. Agencies is given in Table 2-1.

Table 2-1. Summary of OGFC Requirements for U.S. Agencies (Source: Jackson et al., 2008)

Grading	WSDOT Class D	WSDOT OGFC Test	WSDOT OGFC-AR Test	Alabama OGFC	Arizona ARFC	California O-G RAC	Florida FC-5	Georgia OGFC 12.5mm	Idaho PMS-OG	Indiana OGFC OG19.0	Nevada OGFC
3/4"				100		100	100	100		70-98	
1/2"	100			85-100		95-100	85-100	85-100	100	40-68	100
3/8"	97-100	100	100	55-65	100	78-89	55-75	55-75	95-100	20-52	90-100
#4	30-50	35-55	30-45	10-25	30-45	28-37	15-25	15-25	30-50	10-30	35-55
#8	5-15	9-14	4-8	5-10	4-8	7-18	5-10	5-10	5-15	7-23	
#16						0-10					5-18
#200	2-5	0-2.5	0-2.5	2-4	0-3	0-3	2-4	2-4	2-5	0-8	0-4
% Asphalt	4-6	9	9	5.6-9			ARB12	5.75-7.25			
Asphalt	PG 58-22	PG 70-22	A-R	PG 76-22	A-R	A-R	PG 76-22	PG 76-22			
Min Air Temp.	55° F	55° F	55° F	40° F	70° F *	70° F	65° F	55° F	60° F	60° F	
* + 85° F Surface											
Grading	New Jersey OGFC	New Mexico OGFC I & II	New Mexico OGFC III	North Carolina OGFC FC-1 Mod	North Carolina OGFC FC-2 Mod	Oklahoma OGFC	Oregon OGM 1/2" Open	Oregon OGM 3/4" Open	South Carolina OGFC	Texas PGFC	Texas A-R
3/4"		100	100		100		99-100	85-96	100	100	100
1/2"	100	100	70-90	100	85-100	100	90-98	55-71	85-100	80-100	95-100
3/8"	80-100	90-100	40-65	75-100	55-75	90-100			55-75	35-60	50-80
#4	30-50	30-55	15-25	25-45	15-25	25-45	18-23	10-24	15-25	1-20	0-8
#8	5-15			5-15	5-10		3-15	6-16	5-10	1-10	0-4
#10		0-20	6-12			0-10					
#40		0-12	0-8								
#200	2-5	0-6	0-5	1-3	2-4	0-5	1-5	1-6	0-4	1-4	0-4
% Asphalt				5-8	5-8				5-7	5.5-7.0	8-10
Asphalt				PG 76-22	PG 76-22				PG 76-22	PG 76-22	A-R
Min Air Temp	60° F	70° F	70° F			60° F		60° F	60° F	70° F	70° F

FDOT specifies OGFC (FC-5) mix under Section 337 of the Standard Specifications for Road and Bridge Construction. The method for designing FC-5 mixtures is contained in FM 5-588, *Determining the Optimum Asphalt Binder Content of an Open-Graded Friction Course Mixture Using the Pie Plate Method*.

In general, there are four major components of an OGFC mix design (Cooley et al. 2009), which are discussed in detail in the following sections:

1. Selection of suitable materials,
2. Selection of adequate design blend gradation,
3. Determination of optimum binder content, and
4. Evaluation of potential performance.

2.2.1 Selection of Suitable Materials

2.2.1.1 Aggregate

An OGFC mixture primarily consists of coarse aggregate, fine aggregate, asphalt binder, and stabilizing additives. One basic requirement for OGFC is the availability of high-quality non-polishing aggregates. A high friction number cannot be maintained with aggregates that do not have adequate microtexture and resistance to polishing and degradation under traffic (Shuler and Hanson, 1990). FDOT allows the use of an aggregate blend of approved friction coarse aggregates that consists of crushed granite, crushed granitic gneiss, crushed limestone, crushed shell rock, or a combination of the above. The mixtures that contain a minimum of 60% of approved friction coarse aggregates of crushed granite and/or crushed granitic gneiss may also contain up to 40% fine aggregate from other sources of aggregate not approved for friction courses or a combination

of up to 20% reclaimed asphalt pavement (RAP) and the remaining fine aggregate from other sources of aggregate not approved for friction courses. A summary of current aggregate property requirements by ASTM, AASHTO, and FDOT are presented in Tables 2-2 and 2-3.

Table 2-2. Coarse Aggregate Requirements for OGFC Mix Designs (Source: Bennert and Cooley, 2014; FDOT, 2022)

Test Description	Method	ASTM 7064		AASHTO PP 77		FDOT	
		Min.	Max.	Min.	Max.	Min.	Max.
Los Angeles Abrasion, percent loss	AASHTO T 96	-	30	-	30	-	45
Flat or Elongated, percent (5 to 1)	ASTM D 4791	-	10	-	10	-	10
Sodium Sulfate	AASHTO T 104	-	-	-	10	-	12
Magnesium Sulfate		-	-	-	15	-	-
Uncompacted Voids	AASHTO T 326	-	-	45	-	-	-

Table 2-3. Fine Aggregate Requirements for OGFC Mix Designs (Source: Bennert and Cooley, 2014; FDOT, 2022)

Test Description	Method	ASTM 7064		AASHTO PP 77		FDOT	
		Min.	Max.	Min.	Max.	Min.	Max.
Sodium Sulfate	AASHTO T 104	-	-	-	10	-	-
Magnesium Sulfate	ASTM D 4791	-	-	-	15	-	-
Uncompacted Voids	AASHTO T 304	40	-	45	-	-	-
Sand Equivalent	AASHTO T 176	45	-	50	-	-	-

2.2.1.2 Asphalt Binder

Binders with high stiffness are needed for OGFC to prevent asphalt draindown and increase film thickness. Hence, modified binders using rubber, SBS, and styrene-butadiene rubber are mostly

used by agencies in the U.S. For example, FDOT allows the use of PG 76-22 PMA, HP, and asphalt rubber binder that meet the requirements of Section 916 of standard specifications for FC-5 mixtures (FDOT, 2022).

2.2.1.3 Stabilizing Additives

At typical production or construction temperatures, OGFC has a propensity to drain the thick film of asphalt binder from the aggregate structure, termed draindown (Huber, 2000). When draindown occurs during the production and transportation of the OGFC mixture, a significant amount of the asphalt binder is lost from the mix. This loss of binder can cause decreased durability, which may lead to premature raveling or cracking. To reduce the potential for draindown, stabilizing additives are generally incorporated into the OGFC mix design. The two types of stabilizing additives utilized regularly within OGFCs are fibers and asphalt binder modifiers. Figure 2-2 illustrates the percentage of different additives preferred by the state agencies. Other agents include warm mix additives that use a chemical process to lower production temperature while maintaining adequate constructability. FDOT recommends using either mineral or cellulose fibers at a rate of 0.2% to 0.5% by the total weight of the mixture to reduce binder draindown.

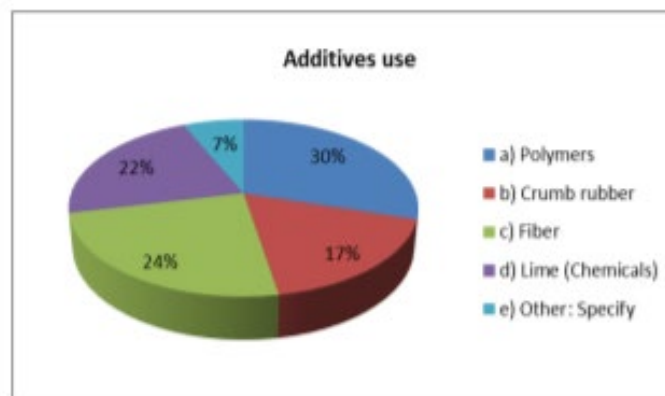


Figure 2-2. Types of Additives used in the U.S. (Source: Onyango and Woods, 2017)

2.2.1.4 Fillers

Fillers or adhesion agents are used to improve the bond between aggregates and the asphalt binder. FDOT requires hydrated lime at a dosage rate of 1% to 1.5% by weight of the total dry aggregate for mixtures containing granite or granitic gneiss or liquid anti-strip (LAS) additive for all mixtures.

2.2.2 Selection of Design Gradation

The optimization of the OGFC mixture can be achieved by utilizing the selected aggregates to develop trial blends that fall on the coarse limit, fine limit, and in the middle of the recommended gradation range. Several agencies provide gradation requirements for a ¾ in (19 mm) maximum aggregate size. Depending on the mix design criteria followed, the most appropriate blend of the trial gradations is selected. The standard OGFC mix design procedures recommend selecting the trial blend with the highest air void content that meets the minimum requirement and provides stone-on-stone contact. FDOT suggests using an aggregate blend that falls within the ranges shown in Table 2-4 and consists of either 100% crushed granite and/or granitic gneiss or 100% crushed limestone and/or crushed shell rock without interblending the aggregate types.

Table 2-4. FC-5 Gradation Design Range (Source: FDOT, 2022)

19 mm	12.5 mm	9.5 mm	4.75 mm	2.36 mm	1.18 mm	0.6 mm	0.075 mm
100	85-100	55-75	15-25	5-10	-	-	2-5

2.2.3 Determination of Optimum Binder Content

Mix design methods identify a range of trial asphalt binder contents, normally in 0.5% increments, from which optimum can be selected. Kline (2010) categorized the optimum binder content (OBC) determination methods for OGFC into three approaches:

1. Property and performance specification where samples of various binder contents are tested for certain characteristics and samples prepared of the OBC should meet a set of criteria,
2. Oil absorption method where the oil absorption of the aggregate is used in a series of empirical calculations to determine the optimum binder content (Smith et al., 1974), and
3. Visual determination method where binder draindown is visually analyzed to determine the optimum binder content.

The design criteria suggested by different standards are summarized in Table 2-5. Bennert and Cooley (2014) proposed a new design method with a combination of draindown and Cantabro loss for selecting the optimum asphalt content. The concept allows selecting the optimum binder content based on an acceptable range instead of one value. FDOT follows the visual determination method using a pie plate in accordance with FM5-588. The asphalt content that produces sufficient bonding between the mixture and the bottom of the plate without evidence of excessive asphalt draindown is considered the OBC. Based on the aggregate type, the allowable range of binder content for FC-5 mixtures is given in Table 2-6.

Table 2-5. Optimum Asphalt Content Properties for OGFC Mixtures

Mix Property	NCHRP 640	ASTM D7064	NAPA Series 115
Air Voids, percent	18 – 22	≥ 18	≥ 18
Unaged Cantabro Loss, percent	≤ 15.0	≤ 20.0	≤ 20.0
VCA _{MIX} , percent	$< VCA_{DRC}$	$\leq VCA_{DRC}$	$\leq VCA_{DRC}$
Tensile Strength Ratio	≥ 0.70	≥ 0.80	≥ 0.80
Draindown at Production Temperature, percent	≤ 0.30	≤ 0.30	≤ 0.30
Permeability, m/day	100	100	100

Table 2-6. Range of FDOT Design Binder Contents

Aggregate Type	Binder Content
Crushed Granite and/or Granitic Gneiss	5.5 - 7.5
Crushed Limestone and/or Shell Rock	6.0 - 8.0

2.2.4 Performance Testing

A successful mixture design method for OGFC should be capable of producing a functional and durable pavement during its service life. The design practice followed by all agencies measure mixture functionality but do not directly address durability (Qureshi et al., 2015). Watson et al. (2018) developed a balanced mix design approach where the optimum binder content was determined based on the air void, Cantabro loss, and permeability criteria for the selected gradation. Next, performance testing was conducted on the mix design that met the functional requirements. The tests recommended were the draindown test with the wire basket method, HWTT, the Illinois flexibility index test (I-FIT), the indirect tensile strength test, and the shear strength test. Table 2-7 presents the OGFC mixture specification requirements of the balanced mix design procedure by Watson et al. (2018). The study found that the air voids content of OGFC mixtures was directly related to their permeability. The Cantabro test proved to be a good indicator of mixture durability and resistance to raveling. The indirect tensile strength test, based on a modified version of AASHTO T 283, was identified as a good indicator of mixture cohesiveness. The peak load of the I-FIT test was shown to be a good measure of resistance to cracking, while the Hamburg wheel tracking test provided an accurate prediction of rutting resistance. They also observed that the higher percentage of contents passing the No. 200 sieve improved the durability of OGFC mixtures with high air voids, high Cantabro loss, and low tensile strength.

Table 2-7. Proposed OFGC Mixture Specification Requirements (Source: Watson et al., 2018)

Property	Requirement
Air Voids, percent	15 to 20 (CoreLok method); 17 to 22 (Dimensional)
Cantabro Mass Loss, percent	20 max.
Permeability, m/day	Meet agency criteria (50 min. recommended)
Shear Strength, psi (optional)	125
Conditioned Tensile Strength, psi	50 min.
Tensile Strength Ratio	0.70 min.
Draindown, percent	0.30 max
Hamburg Wheel Tracker, Cycles before reaching 12.5 mm rut depth (Optional)	PG 64 or higher, $\geq 10,000$ passes PG 70, $\geq 15,000$ passes PG 76 or higher, $\geq 20,000$ passes
Cracking, I-FIT FI (Optional)	25 min.

Another cracking test that could possibly be used to evaluate the intermediate-temperature load-related cracking resistance of OGFC mixtures is the Indirect Tensile Asphalt Cracking Test (Ideal-CT). The test was developed by Zhou et al. (2017) and has gained quick popularity among several state highway agencies and the asphalt industry due to its simplicity, practicality, and ease of implementation. Nevertheless, Arambula-Mercado et al. (2019) observed that the OGFC specimens with the HP binder endured large deformations during the IDEAL-CT testing, which caused the sample to touch the edges of the loading frame, inducing small error in the acquired data. Further, large variations in the cracking tolerance index (CT_{Index}) were reported for all the mix designs evaluated. The test was also highly sensitive to the air void content.

For OGFC mix design approval, FDOT currently requires mixtures with unaged Cantabro loss of 20%, retained tensile strength ratio of at least 0.80, and a minimum tensile strength (unconditioned) of 100 psi. Although several improvements were made for the OGFC mix design over the years,

there is still a need to investigate the suitable mix designs specific to the binder type. This thesis attempts to develop a mix design procedure for OGFC mixtures with epoxy-modified asphalt. The different trials performed, issues encountered, and the proposed design procedures for mixtures with two epoxy materials are documented in later chapters.

2.3 Approaches to Improve OGFC Durability

The two main factors that influence the high quality of OGFC are the binder modification and gradation of the mixture, which also influences the total air void content. Binder modification has a significant impact on the performance and durability of OGFC mixtures. And the gradation strongly impacts the quality of the stone-on-stone skeleton within the microstructure of the mixture and, consequently, its resistance to raveling. This section reviews a few previous studies that addressed these factors to improve the durability of OGFC mixtures without additional maintenance operations.

Polymers are commonly used additives that enhance the properties of asphalt binders (Zhu et al., 2014, Polacco et al., 2015; Watson et al., 2018). Two phases develop when a polymer is introduced into the binder, which influences the durability and mechanical response of the binder. They are the polymer-rich phase and the asphaltene-rich phase. The amount of polymer determines the final modification network and, consequently, the mechanical response of the binder. Binders containing 6% to 8% of a polymer by weight of binder are called HP asphalt. The most common polymer used for the production of HP binders is SBS, although other polymers such as styrene-butadiene rubber and styrene-butadiene could also be used (Kuennen, 2012).

Based on the enhanced durability, improved rutting resistance, and reduced thermal cracking susceptibility observed in dense-graded hot mix asphalt (Timm et al., 2012; NCAT, 2015), Arámbula-Mercado et al. (2019) performed an extensive study investigating the mechanical

performance and durability of OGFC (FC-5) mixtures containing HP binder versus PMA binder. A series of tests were performed, including linear viscoelasticity (LVE), surface free energy (SFE), fatigue cracking, and creep recovery tests on both HP and PMA binders under different aging conditions. Furthermore, IDEAL-CT and the semicircular bending (SCB) test were used to assess the fracture properties of the OGFC mixtures containing HP and PMA binders. Moisture damage was evaluated using the IDT strength test. Finally, the Cantabro abrasion loss test was performed to determine the durability of OGFC mixtures. The LVE properties and the SFE were determined for mastics fabricated with both binders and two aggregate types (i.e., limestone and granite). For fracture and durability tests, mixtures were prepared with a combination of two binders and two aggregates and subjected to different aging conditions prior to testing. The results showed that the PMA binder and PMA mastics had better LVE properties than the HP binder and mastics. However, the HP binder and HP mastics had superior fatigue cracking and creep recovery at all aging conditions. Based on the IDEAL-CT and SCB test results, binder type was found to be the most influential factor in the cracking resistance of the mixtures. The OGFC mixtures fabricated with the HP binder were less prone to fracture. The Cantabro test also demonstrated that the OGFC mixtures with HP binder were significantly more durable than those with PMA binder. Moisture susceptibility tests did not provide consistent results to determine the influence of binder, aggregate type, or aging state on the propensity of the mixtures to moisture damage. Additional analysis using numerical finite element simulations conducted at a long-term aging state indicated that the FC-5 mixtures with HP binder were less prone to raveling under field conditions. Finally, the life cycle cost analysis showed that the extended service life of the FC-5 mixtures with HP binder offered a cost-effective alternative. Based on thesis results, the authors concluded that using an HP binder could be a viable option to improve the raveling resistance of OGFC in Florida.

Dating back, Plug et al. (2012) manufactured seventeen laboratory-aged open-graded asphalt mixtures using SBS modification with or without recycled asphalt granulate. The Cantabro test was performed at 5°C to assess the effect of SBS concentration on the raveling resistance of these mixtures. The results showed that the loss of mass was mainly dependent on the SBS concentration (2-7%). Specifically, the mass loss decreased with an increase in SBS concentration.

Daines (1986) and Daines and Colwill (1989) performed an extensive field study on porous asphalt. In this study, fifteen road sections on the A38 in the UK with different modifications (fibers, polymers, etc.) were tested for durability for several years, as well as for permeability, spray intensity, texture depth, skid resistance, and void retention. The researchers concluded that three sections performed better than average in terms of overall field performance: one section with epoxy asphalt and two sections with soft asphalt binder and SBS modified asphalt. A further noticeable observation was that the improved durability resulted from increased binder content, which was obtained at the expense of hydraulic conductivity.

Wu et al. (2019) measured the long-term durability of epoxy-modified open-graded porous asphalt (EMOGPA) against mixtures using conventional unmodified 80–100 penetration grade base binder as well as a modified binder with 4% SBS polymer. Oxidative aging, Cantabro test, indirect tensile modulus (ITM), indirect tensile fatigue, and surface abrasion test were conducted to verify the durability of EMOGPA aged up to 194 days at 85°C using an open-graded porous asphalt (OGPA) mix design with 20% air voids. Six asphalt binders were evaluated: control unmodified binder, 25% epoxy asphalt binder, 50% epoxy asphalt binder, 75% epoxy asphalt binder, 100% epoxy asphalt binder, and 4% SBS modified asphalt binder. All test results showed that the epoxy-modified mixtures, especially with high EDR, outperformed the 4% SBS mixture as well as the unmodified OGPA using 80–100 penetration grade asphalt binder. The SBS mixture still

performed better than the 80–100 penetration grade control mixture. The normalized graph of indirect tensile modulus over the initial modulus indicated that the curing of the epoxy had contributed greatly to the relatively faster rate of increase in indirect tensile modulus when compared to the 80–100 control and the PMA OGPA mixtures, which oxidized at the same rate. The Cantabro mass loss decreased with the increase of epoxy content for epoxy-modified OGPA mixtures.

Another polymer that could improve the performance of OGFC mixtures is polyethylene. Aiming to minimize the costs and maximize the lifespan of OGFC mixtures, Al-Busaltan et al. (2020) investigated the effect of using a recycled stabilizing asphalt modifier, Recycled Low-Density Polyethylene (R-LDPE), on the performance of OGFC asphalt mixtures. OGFC mixtures were prepared with crushed limestone aggregate, hydrated lime anti-stripping additive, and 40/60 penetration grade asphalt binder. Six dosages of R-LDPE ranging from 1% to 6% by weight of binder were added to the neat binder. Initially, mixtures were prepared with asphalt binder contents ranging between 5% and 7% with 0.5% increments (without R-LDPE additive) to determine the optimum binder content. According to ASTM D7064, 6.2% was selected as the asphalt content for all the OGFC mixtures. Later, the performance of OGFC mixtures containing R-LDPE additive was compared with the performance of the control mixture in terms of volumetrics, porosity, draindown, permeability, rutting, tensile cracking, moisture sensitivity, and Cantabro loss. For the aged Cantabro loss test, the compacted samples were conditioned at 60°C using a forced draft oven for seven days (168 hours) to simulate the long-term aging. The mixture test results showed that R-LDPE modification increased mixture air void, porosity, and permeability by 15%, 10%, and at least 40%, respectively, compared with unmodified asphalt samples. It also contributed to reducing rut depth, moisture damage, and abrasion loss (both unaged and aged) by 31%, 20%, and at least

40%, respectively. Further, the asphalt draindown was almost eliminated when the R-LDPE modified binder was used.

Tian et al. (2011) investigated the effect of mixture gradation and aging on the durability of the OGFC mixture. Three gradations were selected with basalt crushed stone aggregates, and the optimum asphalt content for the three gradations was determined as 4.8%, 4.9%, and 5% using draindown and Cantabro test results. Further, 12% to 20% of high viscosity asphalt modifier, SinoTPS, was used in the study. The modifier was specially developed with thermoplastic rubber, together with adhesive resin, plasticizers, and other components of synthetic anti-aging agent. The optimum dosage was determined as 17% by the weight of the total asphalt binder. The loose OGFC mixtures were aged in the oven for up to 8 hours at 135°C, and Marshall specimens were prepared to conduct the Cantabro test. The results showed that the passing percentage of the 9.5 mm sieve had a vital effect on the durability of the OGFC mixture. The bigger the passing percent, the smaller was the Cantabro mass loss, and the better the durability. The mass loss increased rapidly with the increase of aging time. The mass loss still met the maximum limit of 30% after 8 hours of aging at 135°C. Thus, the authors concluded that the high viscosity asphalt modified with SinoTPS could ensure the adequate long-term durability of the OGFC mixture.

A review of OGFC performance at the NCAT Test Track showed that a 2.5 thickness/nominal maximum aggregate size (NMAS) ratio was needed to develop sufficient internal cohesion for good performance (Watson, 2014). However, the Alabama Department of Transportation's (ALDOT) OGFC mix gradation and placement thickness corresponded to a thickness/NMAS ratio of 1.4. Hence, to make an informed decision for adjusting the design parameters, Qureshi et al. (2015) studied the effect of aggregate gradation and layer thickness through laboratory performance testing. Two mix designs were selected, one with a coarser gradation and the other

with a finer gradation. The mixture with the coarser aggregate gradation had sandstone aggregates and 6.3% of PG 76-22 binder modified with SBS. The finer gradation mixture was made up of granite aggregate and PG 76-22 binder with cellulose fibers. Slabs specimens were prepared with different thicknesses between 19 mm to 38 mm, and the permeability, Cantabro, HWTT, and IDT tests were performed on the cores taken out of the slab. The results indicated that both aggregate gradation and layer thickness significantly affected the durability of the OGFC surfaces, with layer thickness showing more significant influence. The HWTT results indicated a 50% to 60% higher resistance to moisture damage of OGFC with an increase in specimen thickness from 19 mm to 38 mm. Comparatively, the coarser aggregate gradation had higher moisture susceptibility than the finer aggregate mixture based on the HWTT results. The Cantabro mass loss was reduced by 10% to 50%, with an increase in specimen thickness from 19 mm to 38 mm. However, the mixture with coarser aggregate gradation was more durable, especially for 38 mm layer thickness, compared to the mixture with finer aggregate gradation. The permeability tests results indicated a 12% to 100% increase in permeability with the increase in layer thickness from 19 mm to 38 mm. Again, the OGFC mixtures with coarser aggregate gradation were more permeable as compared to the finer gradation mixture. The indirect tensile strength tests indicated a 50% to 300% increase in strength with an increase in layer thickness from 19 mm to 38 mm. In this case, the IDT strength of the OGFC mixture with coarser aggregate gradation was lower than that of the finer graded mixture. Based on thesis results, the study recommended an increase in layer thickness to achieve a higher thickness/NMAS ratio. The study also concluded that a robust mixture design with optimum gradation and layer thickness could produce a successful functional and durable OGFC pavement. Additionally, Xie et al. (2019) identified three possible changes to the typical OGFC mix design in Alabama that could improve the field performance of OGFC mixtures. They included: 1) use of

a finer gradation with a 9.5 mm NMAS instead of the 12.5 mm NMAS currently specified, 2) utilizing 0.3% synthetic fiber instead of cellulose fiber, and 3) using asphalt binder modified with 12% ground-tire rubber (GTR) by weight of asphalt binder in place of polymer without cellulose fiber. These three experimental OGFC mixtures were paved on the NCAT Pavement Test Track, and measurements of rut depth, ride quality, surface texture, and visual inspection for cracking were collected on a weekly basis. Furthermore, the permeability of the three test sections was measured immediately after construction and every quarter thereafter. It was observed that after 20 million ESALs, none of the test sections showed cracking, and rutting in all sections was very low at approximately 1.5 mm. The mean International Roughness Index and mean texture depth of the three test sections did not change over two research cycles from 2012 through 2017, indicating that raveling did not occur in the three test sections. In terms of permeability, the 9.5 mm mixture performed better than the modified 12.5 mm mixtures, as the highest permeability was always noted for the 9.5 mm mixture. The slope of the permeability degradation curve for the 9.5 mm mixture was flatter than those for the other two mixtures, indicating the 9.5 mm mixture had a lower rate of permeability degradation over traffic loading. For example, after the application of 10 million ESALs, the 12.5 mm mixtures with synthetic fibers and GTR had a permeability of 0.002 cm/sec and 0.0008 cm/sec, respectively, while 0.04cm/sec permeability was recorded for the 9.5 mm mixture. Further, bulk specific gravity, Cantabro, and TSR tests were performed on the laboratory specimen of the three mixtures to determine their air void content, Cantabro loss, and splitting tensile strengths. The results indicated that the three OGFC mixtures selected for evaluation on the Test Track had higher air voids than the mixtures designed based on the existing ALDOT procedure. Based on the IDT strength, TSR, and Cantabro loss results, the changes in

ALDOT's OGFC mix design procedure improved the moisture susceptibility and raveling resistance of the mixtures, especially for 9.5 mm OGFC mixtures with cellulose fiber.

FDOT uses 1% hydrated lime by weight of aggregate to address the stripping of asphalt binder. However, the premature raveling was still affecting the FDOT pavements, making it necessary to develop better solutions to reduce the moisture susceptibility and improve the durability of these mixtures. Gu et al. (2021) examined whether using the LAS, additional hydrated lime, or both could produce longer-lasting FC-5 mixtures and whether the increased life span of the FC-5 mixture would offset the increased cost of the additional additives using cost-benefit analysis. Laboratory OGFC mixtures were prepared with two granite-based FC-5 mixtures containing 1% hydrated lime by weight of aggregate, 1% hydrated lime plus 0.5% LAS additive by weight of asphalt binder, 1.5% hydrated lime, and 1.5% hydrated lime plus 0.5% LAS additive. Further, a combination of two sources of granite aggregates and four types of LAS additives were studied. All the mixtures had 6.8% SBS binder and 0.3 to 0.4% cellulose or mineral fiber. The long-term water infiltration, vapor diffusion, and thermal and ultraviolet oxidation were simulated using the Asphalt Pavement Weathering System (APWS). The Binder Bond Strength test was used to screen the suitable LAS agents. Mixture performance tests, including the Cantabro test, tensile strength ratio test, and Hamburg wheel tracking test, were used to evaluate the durability and moisture susceptibility of the mixtures. The study showed that the Cantabro mass loss increased with longer APWS conditioning time. The modified TSR results indicated that the addition of LAS significantly enhanced the moisture resistance of asphalt mixtures after APWS conditioning. All mixtures exhibited minimal rutting and no stripping issues. Overall, based on the Cantabro test and the cost analysis results, the combination of 1% hydrated lime and 0.5% LAS additive significantly improved the cost-effectiveness of one granite mix design, and the combination of

1.5% hydrated lime and 0.5% LAS additive maximized the cost-effectiveness of the other granite mix design.

Shuler and Hanson (1990) also evaluated the durability of OGFC mixtures based on stripping assessment. The Texas Boiling test was used to measure the stripping in mixtures containing three asphalts with and without both LAS agents (0.5%, 1.5%) and hydrated lime (1.5%). The effect of polymer modification was also studied by using a 3% (by weight) block copolymer that is processed by using the Styrelf procedure. The underlying concept for using stripping potential was that open-graded mixtures provide high permeability such that rainwater can drain away from the pavement by flowing through the mixture. However, during service, the aggregates within the mixture can migrate together under traffic loading reducing the permeability of OGFC mixtures. This reduction in permeability causes clogging of water within the OGFC for extended periods. Eventually, with the decrease in permeable voids in the mixture, water attempts to fill voids in the mixture or aggregate particles. As the water gets in contact with the aggregates, asphalt is displaced or removed entirely from the aggregate surface. This stripping of the asphalt film by water causes aggregates to become dislodged from the mixture, ultimately leading to the failure of OGFC. The results showed that all treatments provided significant improvement to stripping potential in comparison to the control mixture. The mixture containing a 1.5% LAS agent performed the best, followed by the polymer-modified asphalt plus lime slurry. The polymer-modified asphalt mixture without lime still performed better than control mixtures and those treated only with hydrated lime slurry. The optimum binder content of the mixtures varied among the treatments used but generally decreased when a LAS agent was added to the binder. The mixtures treated with hydrated lime slurry did not necessarily require increased binder content.

2.4 Epoxy-Modified Asphalt Binders and Mixtures

2.4.1 Epoxy Asphalt Binders

Epoxy asphalt is a two-phase system in which the continuous phase is a thermosetting epoxy resin, and the discontinuous phase is asphalt and curing agent. The two components are mixed prior to use, and curing takes place over time. The process of curing an epoxy resin converts the initially low molecular weight resin into its thermoset form, which is a space network or three-dimensional chemical structure. When completely cured, the epoxy asphalt turns into a thermoset polymer with the flexibility of asphalt concrete and the strength of Portland cement concrete (Seim, 1974). The concept of epoxy-modified asphalt binder was originally developed to resist jet fuels and heat blasts (Wu et al., 2019). The thermosetting properties of epoxy asphalt surfaces also provide the basis for high skid resistance when epoxy asphalt is used with a selected, tough, abrasion-resistant, and polish-resistant aggregate. The epoxy asphalt binder does not flush to the surface or migrate within the pavement. Further, it holds the aggregate in a strong thermosetting grip that is durable under heavy traffic conditions (Seim, 1973). One additional advantage of epoxy asphalt is the absence of solvent, which makes the EMA binder 100% non-volatile.

In the term thermosetting, the prefix "thermo" implies that the cross-linking proceeds through the influence of heat energy input, and "setting" indicates that an irreversible reaction has occurred on a macro scale (Peng and Riedl, 1995). Depending on the manufacturer, the epoxy materials for asphalt modification are supplied either as two separate components (Part A - epoxy resin and Part B - curing agent) or an epoxy resin (Part A) and a blend of asphalt binder with an epoxy curing agent (Part B). But regardless of the manufacturer selected, when the Part A and Part B of epoxy materials are fully blended with asphalt binder, the EMA binder will behave more like a modified thermosetting polymer rather than asphalt (Dinnen, 1991). Usually, the liquid epoxy resin is

prepared by combining either bisphenol-A or bisphenol-F and epichlorohydrin with each other in a chemical reaction producing diglycidyl ether of bisphenol. As for curing agents, polyamides and polyamines are often used. When added to the binder, the epoxide rings in the asphalt binder system react with long-chain hardener components to form dense, flexible cross-links that block nucleophilic sites where asphalt oxidation occurs (McGraw, 2018). In terms of the mechanisms of interaction between EMA binders and mineral aggregates, the epoxy resin can form covalent bonds with silicon monoxide Si-O molecules on the surface of silicon oxide-containing aggregates during the polymerization reaction, which are highly resistant to ultraviolet (UV) exposure and stripping. A list of commonly used tests on the epoxy asphalt binders is presented in Table 2-8.

Table 2-8. Testing Procedures to Investigate Chemistry and Rheology of Epoxy Asphalt Binders (Source: Yin et al., 2021)

Property	Test Type	Research Parameter
Curing Behavior	Rotational Viscometer	Viscosity
	Softening Point	Melting temperature
Compatibility	Storage Stability	Polymer separation
Morphology	Fluorescence Microscopy	Network formation
	Atomic Force Microscopy	Microstructure characteristics
Cohesive and Adhesive Properties	Binder Bond Strength	Pull-off tensile strength
Chemical Characterization	Differential Scanning Calorimetry	Glass-transition temperature
	FTIR Spectroscopy	Structural functions
Rheological Characterization	Dynamic Shear Rheometer Dynamic Mechanical Analysis	$ G^* $, δ , J_{nr} , N_f , Yield Energy Storage modulus (E') and loss factor ($\tan \delta$)
Oxidative Aging	Rolling Thin Film Oven Pressure Aging Vessel	Rheological performance after aging

To broaden the application of epoxy asphalt binders and determine the most cost-effective epoxy dosage rate, called “epoxy resin content” by the authors of the study, the relationship between the epoxy resin content and the properties of the epoxy asphalt was investigated by Tian et al. (2021). In the study, the mechanical properties were evaluated by the tensile and viscosity tests. The micromorphological characteristics were observed using fluorescence microscopy, and the chemical compositions were obtained by a Fourier transform infrared spectroscopy test. A 70# asphalt was used as the base binder, and it was mixed with the epoxy resin at nine mixing ratios, which are 1:9, 2:8, 3:7, 4:6, 5:5, 6:4, 7:3, 8:2, and 9:1. The epoxy resin was designed by mixing two components, the main epoxy resin and an epoxy hardener. The mixing mass ratio of components was 56:44. Epoxy asphalt was prepared by mixing the epoxy resin blend and base binder at 160°C using a high-speed shearing mixer with a speed of 2,000 rpm for 6 minutes. For preparing the cured samples, the uncured epoxy asphalt was kept at 60°C for four days. The specimens were then cooled to the ambient temperature at 23°C for further testing. The tensile strength test results confirmed that the presence of the epoxy resin increased the strength of the base binder. The tensile strength of the epoxy asphalt improved from 0.2 MPa to 2.3 MPa when increasing the epoxy resin content from 30% to 40% by weight of the total binder. The tensile strength of epoxy asphalt reached the highest at 3.6 MPa with 50% epoxy resin. Only mixtures with 40% or above epoxy resin passed the minimum tensile strength requirement according to the Specifications for the Design of Highway Asphalt Pavement in China. The average elongation of the epoxy asphalt decreased with the increase in the epoxy resin. The elongation was 862% at 10% epoxy resin, which was reduced to 383% at 50% epoxy resin. The original viscosity of the epoxy asphalt increased as the epoxy resin content increased and decreased as the mixing temperature increased. Considering the workability of epoxy asphalt, the growth rate of the asphalt viscosity

was restricted to 1000 mPa·s. Further, to ensure sufficient compaction of the epoxy asphalt mixture in road projects, the construction time, which refers to the duration between the completion of the asphalt mixture mixing and the time when the epoxy asphalt reaches a viscosity of 1000 mPa·s was required to be greater than 60 minutes. Based on the maximum viscosity limit and 60-minute minimum duration, the authors suggest curing temperatures in the range of 140°C to 200°C for asphalt with up to 20% epoxy resin. For asphalt with 30% and 40% and above epoxy resin, the curing temperature was recommended not to exceed 160°C and 180°C, respectively.

The epoxy asphalt system consisted of neat asphalt, component A (bisphenol A-type epoxy resin), and component B (a kind of amine blends curing agent). Once components A and B were mixed, the chemical reaction initiated, presenting consecutive-step addition esterification and simultaneous addition etherification. As a result, the formation of a highly cross-linked three-dimensional network occurred (Figure 2-3). The Fourier-transform infrared spectroscopy (FTIR) spectra analyzed in the study showed that all the peaks appearing in the infrared spectrum of epoxy asphalt had corresponding peaks in the spectra of the epoxy resin or base asphalt. Hence, after mixing the asphalt with epoxy resin, no new functional groups were formed in the blending process. Further, the absorption ratio drastically decreased between zero days to two days, revealing that the epoxy groups of the epoxy resin were consumed, and the three-dimensional cross-linked network of the epoxy resin was formed. Based on the variation in the absorbance ratio, the area of 1085, 1108, and 1118 cm^{-1} peaks of the infrared spectra of the epoxy asphalt (after curing at room temperature for four days) increased with the increase in the epoxy resin content. Finally, on comparing the fluorescence micrographs before and after epoxy curing, it was observed that the curing reaction changed the shape of epoxy resin particles from spherical to irregular. The irregularity of the epoxy resin particles was more obvious when the epoxy resin

(Seim, 1974). In 1997, the Japanese Asphalt Association published a construction manual for porous epoxy asphalt for roadways based on the enhanced durability and functionality of EMA OGFC pavements (Lu and Bors, 2015). The performance was observed through multiple studies conducted in the laboratory and field sections between 1992 to 1996. Later on, several research studies were conducted all over the world to characterize the engineering properties of EMA mixtures. A few of these studies are described in the following sections.

The Joint Organization for Economic Co-operation and Development (OECD)/European Conference of Ministers of Transport (ECMT) Transport Research Centre carried out a project in two phases to economically evaluate long-life pavements and investigate materials suitable as a long-life surfacing for heavily trafficked roads (OECD, 2008). Herrington and Alabaster (2008) discussed the Phase II study undertaken to determine the effect of epoxy-modified asphalt binder on the cohesive properties of oxidized OGPA. They also performed an accelerated loading trial and a field trial to assess the potential difficulties with full-scale manufacture and construction of epoxy-modified asphalt mixtures, as well as evaluate the performance of the pavement. An epoxy-modified mixture was prepared with the epoxy asphalt supplied by ChemCo Systems Ltd and standard aggregate grading conforming to the Transit New Zealand (TNZ) P/11 OGPA specification. Part A (used at 14.6% by weight) consisted of an epoxy resin formed from epichlorohydrin and bisphenol-A, and Part B (85.4%) consisted of a fatty acid curing agent in an approximately 70 penetration grade binder. The mixtures were cured for 120 hours at 85°C before testing. The control mixture was prepared with the same aggregates as the epoxy-modified mixture but with a standard 80/100 penetration grade binder. The strength and cohesion of the mixtures were evaluated using the ITM and Cantabro tests, respectively. The measurements on uncured or unoxidized specimens were made within 24 to 48 hours of fabrication. The results showed that the

ITM of the epoxy-modified open-graded mixture increased over seven times from 570 MPa initial value to 4300 MPa after curing. In contrast, the ITM of the control specimens increased from 840 MPa to only 2500 MPa after a comparable period at 85°C. Equivalent Cantabro mass loss of ~16% was observed for both control mixtures and epoxy-modified mixtures cured for 120 to 310 hours. However, upon laboratory aging at 85°C for thirty-eight days, the mass loss of the control specimens almost doubled, whereas that of the epoxy asphalt specimens decreased slightly. The superior oxidation resistance of the epoxy material was more evident in the Cantabro test conducted at 10°C. The accelerated pavement testing trial demonstrated that full-scale manufacture and surfacing construction with epoxy OGPA could be undertaken without significant modification to plant, machinery, or operating procedures. Trafficking of the test sections with 198000-wheel passes, including a skewed tire, resulted in early signs of surface abrasion in the control section but not in the epoxy-modified section. However, the skid resistance of the epoxy-modified section measured using the British Pendulum Tester reduced after the 198,000-wheel passes, indicating polishing of epoxy binder on the aggregate surface. The authors explained that the decrease in skid resistance of the epoxy section could also be due to a build-up of tire rubber, whereas in the control section, this effect was masked by the surface disruption and abrasion damage on the surface. Finally, early life rutting was observed in the epoxy-modified mixtures, but it was not significantly greater than that of the corresponding control mixtures.

An extensive laboratory study was performed by Youtcheff et al. (2006) in the U.S. as a part of the same international project under the OECD Road Transport Research program. The objectives of their study were to: 1) Characterize an epoxy asphalt binder in comparison with different polymer-modified binders, and 2) Evaluate asphalt mixes prepared with each binder type through performance testing. The broader purpose was to determine the economic viability of surface

pavement with radically extended and maintenance-free service life, in contrast to costs associated with user delays due to road maintenance and rehabilitation. ChemCo Systems of California supplied the epoxy asphalt used in this study. The control mixture was an unmodified PG 70-22 asphalt binder with a diabase aggregate of 12.5 mm NMAS. The optimum asphalt binder content was 5.3% by the total mass. The intermediate and high-temperature characteristics of epoxy asphalt were evaluated using a dynamic shear rheometer, and the low-temperature properties were measured on the bending beam rheometer. The cured beams were conditioned in a Q-Panel Xenon test chamber for 24 hours to 16 weeks to assess the effect of ultraviolet oxidation. The study observed that, apart from hairline cracks, there was no prominent penetration due to the cross-linking nature of the epoxy system. Shear test, moisture susceptibility tests using Pine Wheel Tester and HWT device, thermal stress restrained specimen test, direct axial test, reversed tension-compression test, cyclic loading compact tension test, semicircular bending test, and simple performance test were performed on the mixtures. Collectively, the tests showed that the epoxy-modified mixtures exhibited negligible amounts of rutting and moisture damage and significantly better resistance to crack initiation and fracture propagation than the control mixtures.

As discussed earlier, Wu et al. (2019) also observed that the EMA OGFC mixtures, especially those containing undiluted EMA binder and diluted EMA binder, had significantly better resistance to fatigue cracking and raveling than the SBS modified and unmodified 80–100 penetration grade OGFC mixtures. Despite the multiple performance benefits of EMA OGFC mixtures, there are still limitations to be addressed. Luo et al. (2015) identified two limitations for the use of EMA for roadway applications. They are: 1) requirement of curing period of EMA binder before gaining adequate strength to open to traffic, and 2) five to ten folds higher cost of epoxy asphalt compared to conventional modified and unmodified asphalt binders. Whether or not

the high material cost of epoxy asphalt can be justified by improved mixture performance remains unknown and needs further investigation.

CHAPTER 3. SELECTION OF CHEMICALLY COMPATIBLE EPOXY ASPHALT BINDERS

This chapter presents the experimental plan, test results, and findings of Experiment 1 of the study. The experiment sought to investigate if two epoxy materials (one from a domestic source and the other from a foreign source) were chemically compatible with four PG 67-22 base asphalt binders with different chemical compositions (i.e., crude oil source) for epoxy modification. The ultimate purpose of this experiment was to select the most suitable base asphalt binder for each epoxy material. This was achieved by: 1) investigating the compatibility between the epoxy materials and the base asphalt binders by the storage stability test and Soxhlet asphalt extraction, 2) evaluating the morphology of EMA binders by fluorescence microscopy, and 3) analyzing the SARA fractions [i.e., saturates (S), aromatics (A), resins (R), and asphaltenes (A)] of the base asphalt binders used for epoxy modification. However, the following section is limited to the microscopy analysis because the compatibility test and SARA fraction analysis are beyond the scope of this thesis, but detailed discussions of the test results and research findings can be found elsewhere (Yin et al., 2021).

3.1 Experimental Plan

3.1.1 Materials

Two epoxy materials were employed in this study. They were acquired from a domestic and a foreign source. The manufacturer of the domestic source (U) materials provided an epoxy resin (Part A) and a blend of acid-based epoxy curing agent and asphalt binder (Part B) (Figure 3-1). After combining Part A and Part B, the domestic epoxy materials had an EDR of approximately 40%, as defined in Equation 3-1. Whereas for foreign (J) epoxy materials, the manufacturer provided an epoxy resin (Part A) and an amine-based curing agent (Part B) by itself (Figure 3-1).

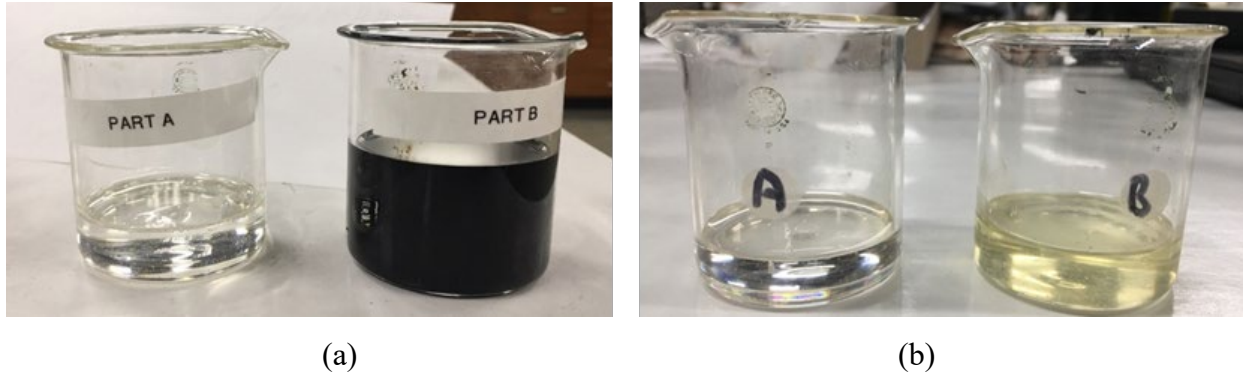


Figure 3-1. Epoxy Material Samples from Two Different Sources: (a) Domestic Source – Part A: Liquid Epoxy Resin, Part B: Blend of Asphalt Binder and Curing Agent, and (b) Foreign Source – Part A: Liquid Epoxy Resin, Part B: Curing Agent

$$Epoxy\ Dosage\ Rate = \frac{Epoxy\ Resin + Curing\ Agent}{Epoxy\ Resin + Curing\ Agent + Asphalt\ Binder} \quad \text{Equation 3-1}$$

Four unmodified asphalt binders from FDOT approved product list were selected for modification with the two epoxy materials. The four base binders were classified in terms of PG as 67-22 and are indicated in this thesis as binders A, C, G, and Z. Table 3-1 presents the testing matrix for Experiment 1. As listed, a total of 16 EMA binders, encompassing four unmodified asphalt binders from different crude sources, curing agents of two different sources, and two EDRs were screened for morphology evaluation. The 15% and 25% epoxy dosages were chosen based on the results of a preliminary proof-of-concept study conducted at NCAT (Moraes and Yin, 2020). The study showed that an EMA binder with an EDR of 8% did not perform as well as a PG 76-22 PMA binder in terms of creep compliance, fatigue resistance, and aging resistance. Further, the thermosetting behavior of epoxy materials was anticipated in EMA binders at an EDR of 30% and above. Hence, the testing was limited to low EDRs. The nomenclature of "(epoxy source, U or J) (EDR, 15%, and 25%) (base binder source, A, C, G, and Z)" was followed in the entire thesis to name EMA binders prepared with different sources of epoxy materials, EDRs, and base binders.

For example, "U15C" denotes an EMA binder prepared with the domestic (U) epoxy materials, 15% EDR, and a PG 67-22 base binder C.

Table 3-1. Proposed Testing Matrix for Experiment 1

Factor Name	Factor No.	Description
Asphalt Binder	4	Four unmodified asphalt binders (PG 67-22) from FDOT approved product list
Epoxy Resin and Curing Agent	2	One domestic source, one foreign source
Epoxy Dosage Rate	2	15%, 25%
Laboratory Binder Test	1	Fluorescence microscopy

3.1.2 Preparation of EMA Binders

The preparation of J-EMA binders started with preheating the PG 67-22 base binder for two hours at 130°C, and epoxy resin (Part A) and curing agent (Part B) for one hour at 60°C. The epoxy resin and curing agent were first blended for two minutes using a low shear mixer, placed on a hot plate to maintain a constant blending temperature of approximately 130°C. Then, the PG 67-22 base binder was added and blended for another 15 minutes. Table 3-2 gives the blending proportions of the component materials for J-EMA binders at the two selected EDRs.

Table 3-2. Blending Proportions of Component Materials for J-EMA Binders

EDR	Proportions (Percent by Weight)		
	PG 67-22 Base Binder	Part A: Epoxy Resin	Part B: Curing Agent
15%	85.00	8.80	6.20
25%	75.00	14.60	10.40

The preparation of U-EMA binders included preheating the base asphalt binder and Part B of the epoxy asphalt material for two hours at 130°C, followed by blending for 15 minutes using a low shear mixer. The epoxy resin (Part A) was preheated for 15 minutes at the same temperature (i.e., 130°C) and manually blended with the diluted Part B of the epoxy asphalt material for approximately 30 to 40 seconds using a stirring rod. After the epoxy resin was added, it started to react with the acid-based curing agent and base asphalt binder, which significantly increased the viscosity of the resultant U-EMA binders and sometimes adversely triggered a thermosetting behavior when considering the EDR of 25%. Table 3-3 presents the blending proportions of the component materials for U-EMA binders at the two EDRs.

Table 3-3. Blending Proportions of Component Materials for U-EMA Binders

EDR	Proportions (Percent by Weight)		
	PG 67-22 Base Binder	Part A: Epoxy Resin	Part B: Blend of Curing Agent and Soft Asphalt Binder
15%	62.50	7.30	30.20
25%	37.50	12.10	50.40

3.1.3 Fluorescence Microscopy Testing and Analysis

Fluorescence microscopy is an imaging technique that allows the excitation of fluorophores and subsequent detection of the fluorescence signal. It has been widely used to investigate heterogeneous surfaces where components have different UV light excitation responses. When light excites or moves an electron to a higher energy state, light of a longer wavelength, lower energy, and different color to the original light absorbed is generated, causing fluorescence (ONI, 2021). In asphalt binders, only aromatics and resins produce strong fluorescence signals, while

polymers do not fluoresce. Thus, due to the presence of fluorescing aromatics and resins trapped in the polymer structure, UV microscopy helps visualize polymer-rich regions.

The above method was employed in this experiment to evaluate the morphology of the EMA binders by observing the distribution and network formation of the epoxy materials within the base asphalt binders. A Zeiss Axiovert 200 Inverted Fluorescence Microscope was used for the testing, as shown in Figure 3-2. The samples were prepared by placing a small drop of heated EMA binder on a microscopic glass slide, loading a cover glass on top of the asphalt sample, and pressing firmly to spread the EMA binder into a uniform thin film. The microscopic slides containing the EMA binder sample were then allowed to cool down to room temperature before testing. The microscope was supported by Nis-Elements BR 4.6 software, through which the images were visually assessed in 10x magnification and captured on a 100 μ m scale. Three replicate images were obtained, and each image was analyzed for its particle size distributions using the ImageJ program.

ImageJ is an open-source image processing program designed for multidimensional scientific images. One of the many useful features of ImageJ is that it can calculate the area and pixel value statistics of user-defined selections and intensity-specified objects. This feature was used in this study to determine the area of each epoxy polymer particle in a fluorescence micrograph image and then quantify its overall particle size distribution in the EMA binders. During the image analysis, a significant challenge was deciding a suitable threshold value, as the outlines of the particles detected by the program showed high dependency on the threshold applied. Hence, the final threshold value for each EMA binder sample was selected cautiously based on two criteria: 1) visually all the particles were captured and 2) the particles were spread enough for the program to avoid accidentally combining or erasing multiple particles. Figure 3-3 presents the major steps of analyzing the fluorescence micrographs in ImageJ.

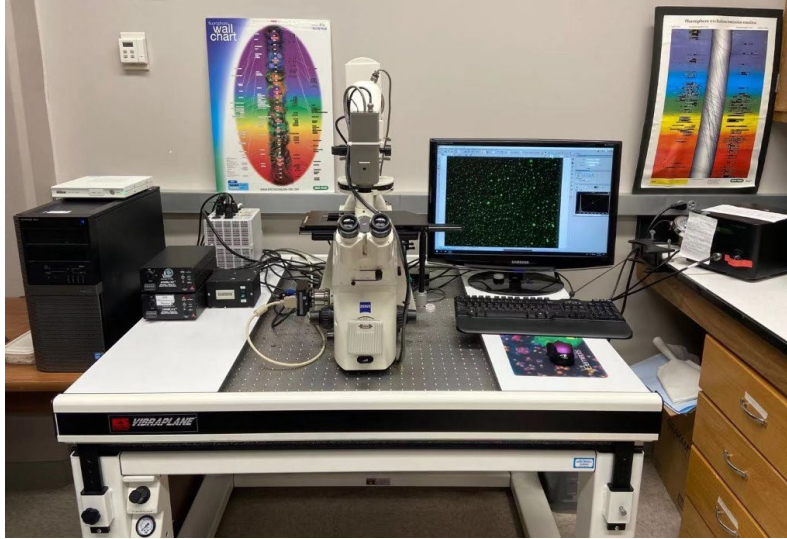


Figure 3-2. Zeiss Axiovert 200 Inverted Fluorescence Microscope

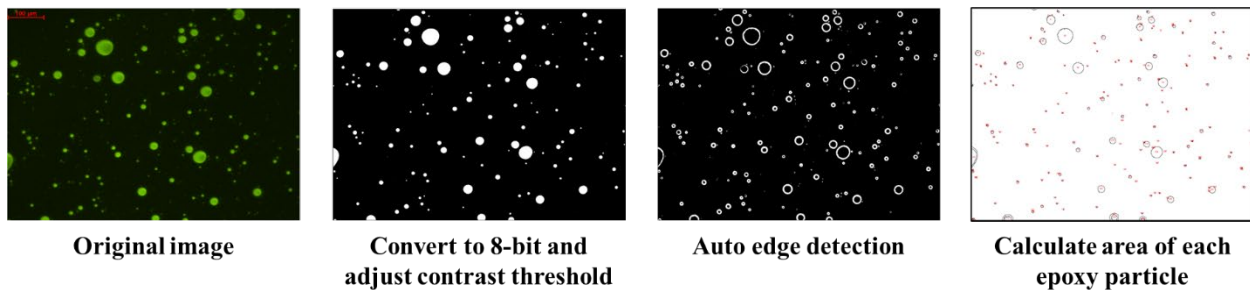


Figure 3-3. Major Steps of Analyzing Fluorescence Micrographs in ImageJ (Source: Yin et al., 2021)

3.2 Test Results and Discussion

Figure 3-4 presents the fluorescence micrographs of the J-EMA binders at 15% EDR, while Figure 3-5 presents those of the J-EMA binders at 25% EDR. The fluorescent and dark phases in both the figures correspond to the epoxy-rich and asphalt-rich phases, respectively. Overall, the compatibility between the base asphalt binders and the epoxy materials from a foreign source before curing was observed as fair since the distribution of the epoxy resin in the asphalt phase was not homogeneous. Moreover, as the EDR increased from 15% to 25%, the distribution of the epoxy resin became less uniform, indicating a decrease in compatibility. Based on visual

assessment of the fluorescence micrographs in Figure 3-4 and Figure 3-5, the base asphalt binder Z appeared to have the best compatibility with the epoxy materials from a foreign source (J) at both evaluated EDRs.

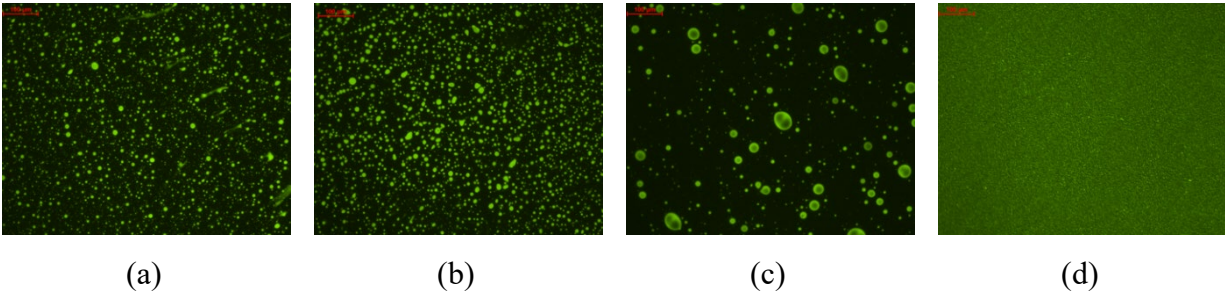


Figure 3-4. Fluorescence Micrographs of J-EMA Binders at 15% EDR: (a) Base Binder A, (b) Base Binder C, (c) Base Binder G, (d) Base Binder Z

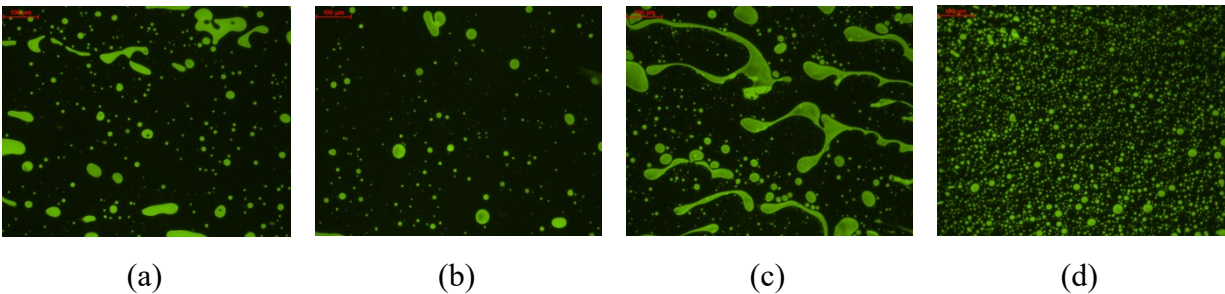


Figure 3-5. Fluorescence Micrographs of J-EMA Binders at 25% EDR: (a) Base Binder A, (b) Base Binder C, (c) Base Binder G, (d) Base Binder Z

The fluorescence micrographs of the U-EMA binders at 15% EDR are given in Figure 3-6, and the micrographs of the U-EMA binders at 25% EDR are given in Figure 3-7. Similar to J-EMA binders, the compatibility between the base asphalt binders and epoxy materials from a domestic source was observed as fair before curing, which decreased as the EDR increased from 15% to 25%. As seen in Figure 3-6 and Figure 3-7, the base asphalt binder C appeared to exhibit the best compatibility with the epoxy materials from a domestic source (U) at both evaluated EDRs. This observation was confirmed by the ImageJ analysis results discussed below.

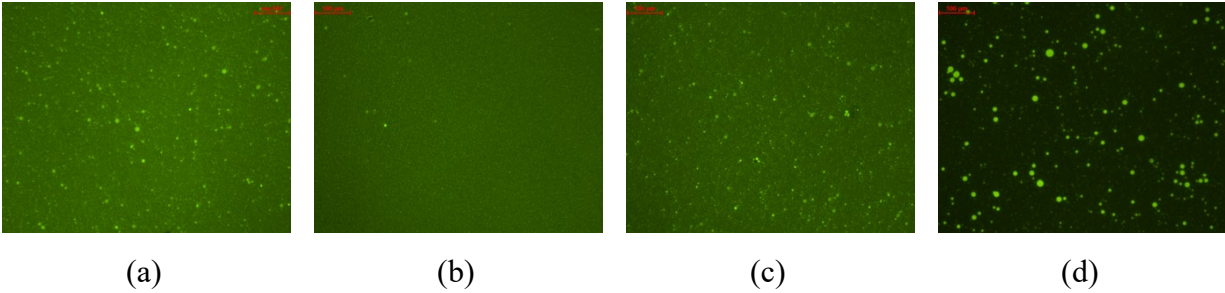


Figure 3-6. Fluorescence Micrographs of U-EMA Binders at 15% EDR: (a) Base Binder A, (b) Base Binder C, (c) Base Binder G, (d) Base Binder Z

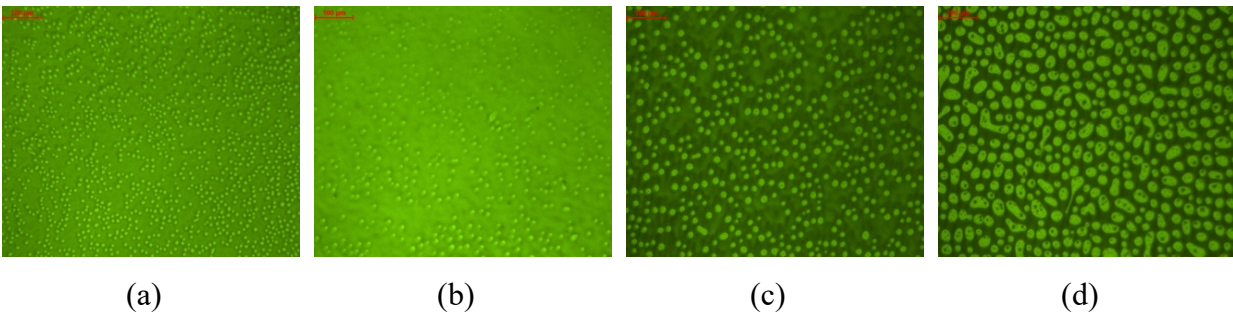


Figure 3-7. Fluorescence Micrographs of U-EMA Binders at 25% EDR: (a) Base Binder A, (b) Base Binder C, (c) Base Binder G, (d) Base Binder Z

Table 3-4 summarizes the epoxy particle sizes for each EMA binder obtained from the image analysis using ImageJ. The cumulative distribution curves of the epoxy particle sizes are graphically illustrated in Figure 3-8 through Figure 3-11 for J-EMA binders at 15% EDR, J-EMA binders at 25% EDR, U-EMA binders at 15%, and U-EMA binders at 25%, respectively. Using the lowest average and median particle sizes as well as the lowest standard deviation as criteria, the J15Z, J25Z, U15G, and U25A binders were found to have the best morphology in their corresponding categories (i.e., combinations of the source of epoxy materials and EDR). Nevertheless, the U15C and U15G binders, as well as the U25A and U25C binders, also had very similar particle size distribution curves, as shown in Figure 3-10 and Figure 3-11, respectively. Comparatively, EMA binders at 15% EDR were considered to be more compatible than those at

25% EDR because they did not exhibit large-size agglomerated epoxy resin particles. Furthermore, epoxy materials from a domestic source (U) were more uniformly dispersed within the base binders than those from a foreign source (J).

Table 3-4. Summary of Epoxy Particle Sizes of EMA Binders at 15% and 25% EDRs

Source of Epoxy Materials	EDR	Average Particle Size (μm^2)	Median Particle Size (μm^2)	Standard Deviation (μm^2)
Foreign Source (J)	15%	22.08	17.70	19.98
		20.92	15.00	21.51
		46.12	31.00	50.69
		12.01	7.09	15.52
	25%	45.86	35.40	79.06
		42.10	28.30	61.30
		34.64	22.60	239.20
		31.55	23.00	34.10
Domestic Source (U)	15%	17.99	8.80	34.43
		12.14	7.09	18.30
		11.71	6.64	17.22
		26.22	12.80	35.23
	25%	15.73	6.20	22.62
		17.07	3.54	33.86
		42.05	7.09	44.21
		24.37	7.97	80.87

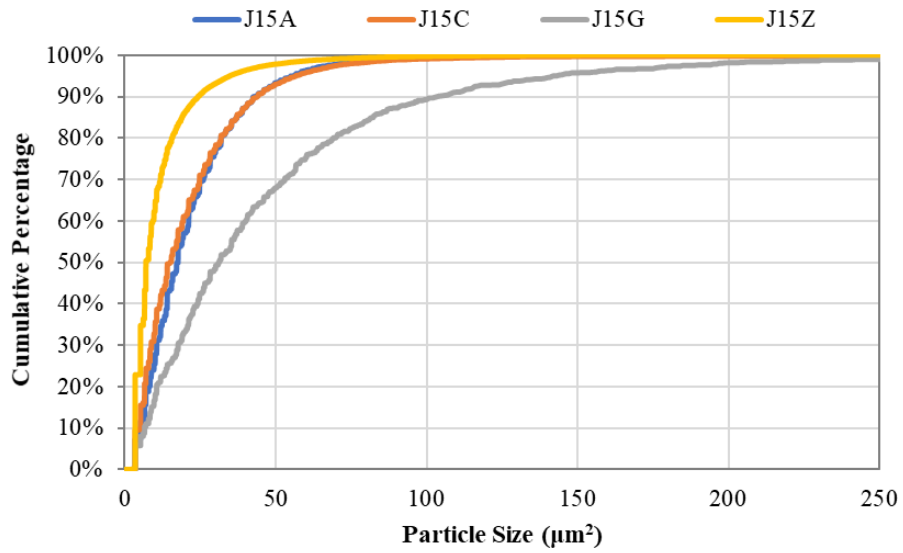


Figure 3-8. Cumulative Distribution Curves of Epoxy Particle Sizes for J-EMA Binders at 15% EDR

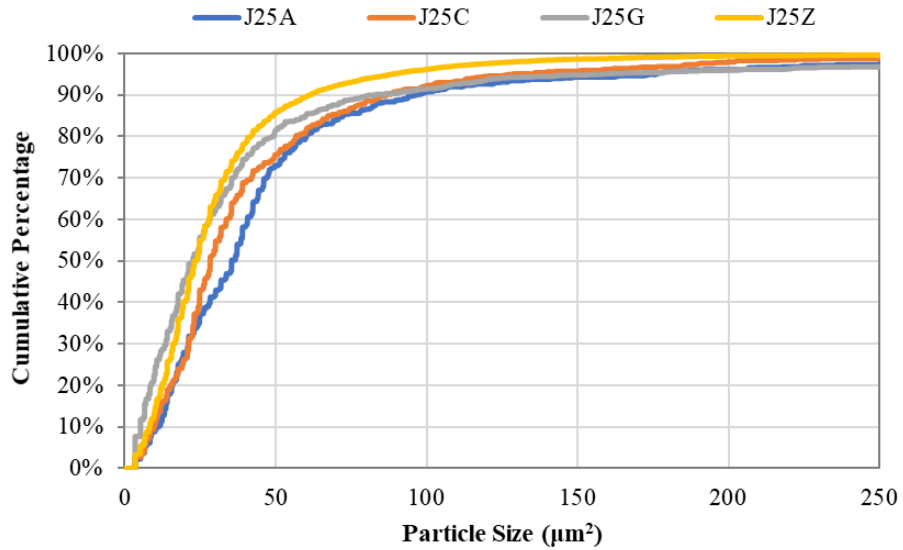


Figure 3-9. Cumulative Distribution Curves of Epoxy Particle Sizes for J-EMA Binders at 25% EDR

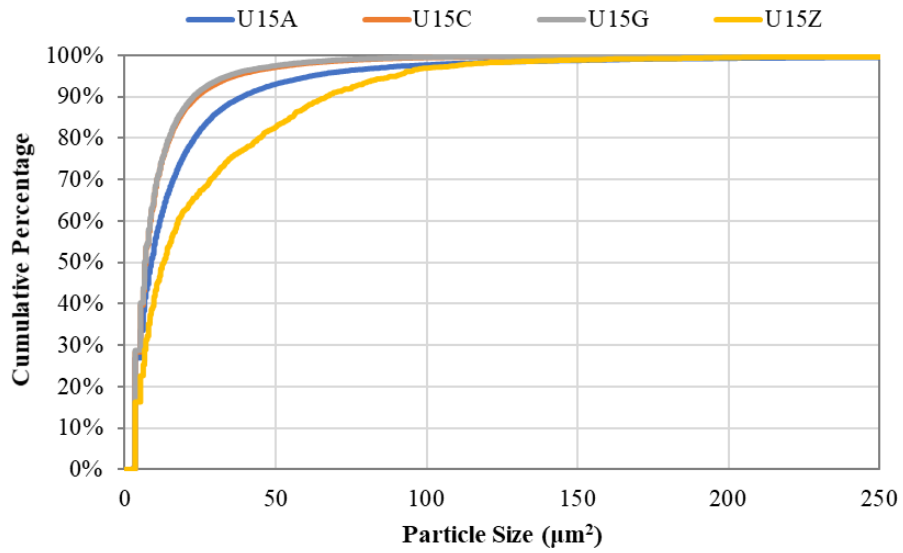


Figure 3-10. Cumulative Distribution Curves of Epoxy Particle Sizes for U-EMA Binders at 15% EDR

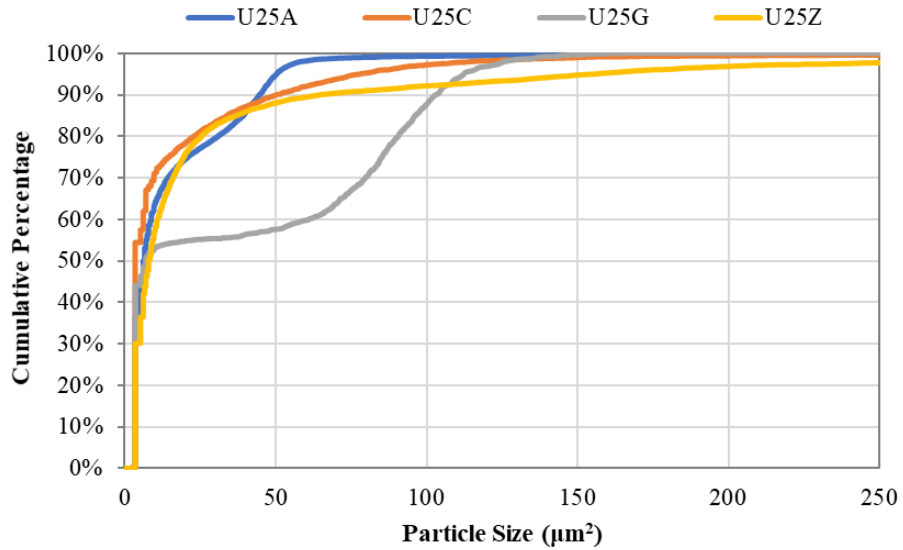
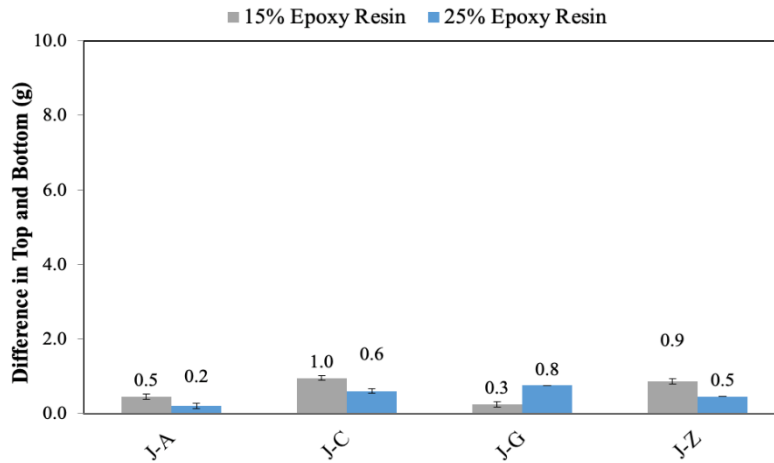


Figure 3-11. Cumulative Distribution Curves of Epoxy Particle Sizes for U-EMA Binders at 25% EDR

Yin et al. (2021) investigated the compatibility between the epoxy materials and the base asphalt binders by a modified storage stability test and Soxhlet asphalt extraction (Figure 3-12). The study

concluded that the base asphalt binders A and Z showed the best compatibility with the epoxy materials from the foreign source (J). On the other hand, the base asphalt binders A and C were most compatible with the epoxy materials from the domestic source (U). Further, according to the SARA (saturates, aromatics, resins, and asphaltenes) fractions of the base asphalt binders detailed in Yin et al. (2021), the four base asphalt binders showed different chemical compositions (Figure 3-13). Based on the Colloidal Instability Index (CII) calculated using the SARA fractions, the authors ranked the four base asphalt binders from least stable to most stable as Binder A < Binder C \approx Binder Z < Binder G. Furthermore, it was observed that the base asphalt binders with the lowest resin content (i.e., binders A and Z) allowed lower precipitation of the epoxy resin from a foreign source; while the base asphalt binders with the highest saturate content (i.e., binders C and A) allowed lower precipitation of the epoxy resin from a domestic source (Yin et al., 2021).



(a)

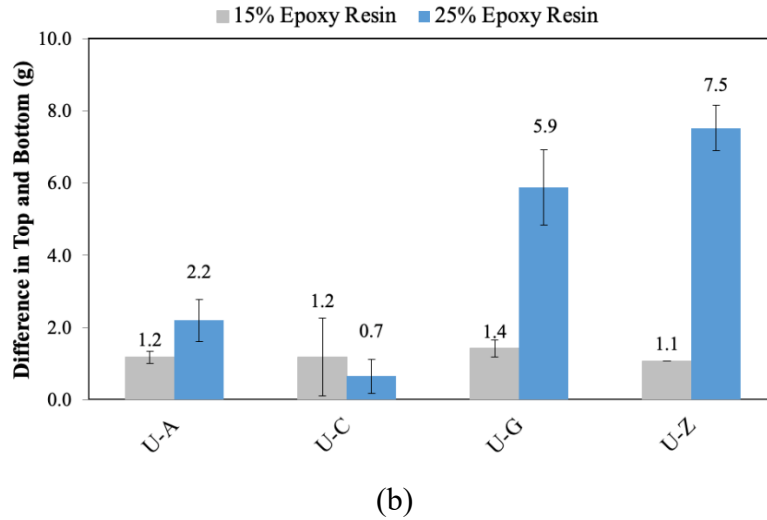


Figure 3-12. Difference in the Residue of Top and Bottom Portions after Storage Stability Test Followed by Soxhlet Asphalt Extraction: (a) J-EMA Binders, (b) U-EMA Binders (Source: Yin et al., 2021)

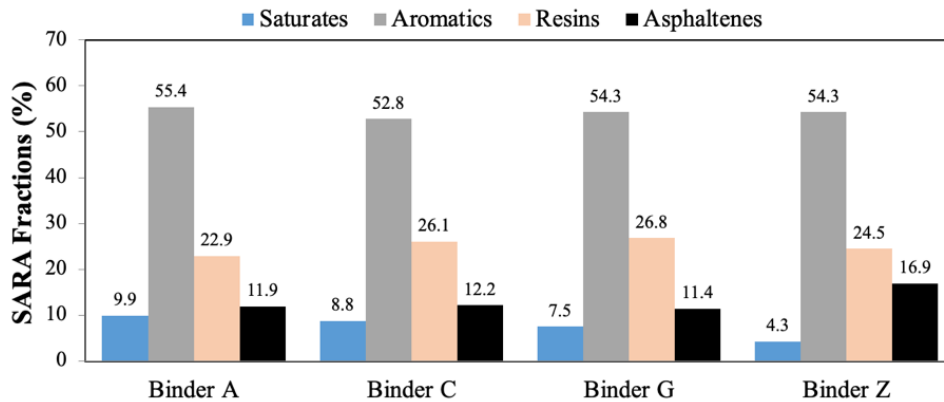


Figure 3-13. SARA Fractions of the Base Asphalt Binders (Source: Yin et al., 2021)

3.3 Summary of Findings

Fluorescence microscopy showed that the compatibility between the four base asphalt binders and the two epoxy materials was fair (i.e., not homogeneous) in general, although distinctions existed among the various resultant EMA binders. Based on the uniformity of the epoxy resin distribution, the compatibility decreased as the EDR increased from 15% to 25%. J-EMA binders prepared with base asphalt binder Z and U-EMA binders prepared with base asphalt binder C, which exhibited

the best morphology through visual observation and image analysis of the fluorescence micrographs, were considered to be most chemically compatible. It was assumed that these base binders would be compatible even for higher dosages. Overall, binders Z and C were collectively selected as chemically suitable base binders for modification with the epoxy materials from foreign (J) and domestic (U) sources, respectively.

CHAPTER 4. DETERMINATION OF OPTIMUM EPOXY DOSAGE RATE

This chapter presents the experimental plan, test results, and findings of Experiment 2 of the study. The aim of this experiment was to determine the optimum (i.e., the most cost-effective) EDR with respect to mixture performance properties and material costs. It is hypothesized that the selected cost-effective EDR would consistently provide EMA OGFC mixtures with better performance properties than the control PMA mixtures, thus having the potential of increasing the life span of OGFC.

The experiment consisted of two sub-experiments: binder testing experiment and mixture testing experiment. The binder testing experiment focused on evaluating the curing behavior, aging characteristics, rheological properties, cohesive and adhesive properties, and moisture susceptibility of EMA binders at 15% and 25% EDRs *versus* a PG 76-22 PMA binder and an HP binder. The mixture testing experiment was to evaluate the raveling resistance, tensile strength, and fracture resistance of OGFC mixtures prepared with EMA binders at different EDRs ranging from 15% to 40% *versus* a control PG 76-22 PMA binder. Since the focus of this thesis was on mixtures, the information on binder testing was not included. However, a detailed discussion of the tests and observations can be found elsewhere (Yin et al., 2021). All the EMA mixtures were prepared with a "drop-in" approach following two existing mix designs provided by FDOT, and thus, they had the same aggregate gradations and asphalt binder contents as the control PMA mixtures. Further, three mix aging conditions were included to account for the impact of asphalt aging on the performance properties of OGFC mixtures. The experimental plan and the results are detailed in the following sections of the chapter.

4.1 Experimental Plan

4.1.1 Materials and Mix Designs

As with Experiment 1 discussed in chapter 3, two different sources of epoxy materials were used (i.e., domestic source (U) and foreign source (J)). Based on the findings of Experiment 1, a PG 67-22 base binder from source C was used for modification with the epoxy materials from a domestic source, while a PG 67-22 base binder from source Z was used to prepare EMA binders with the epoxy materials from a foreign source.

Table 4-1 presents the proposed mixture testing matrix for Experiment 2. A total of eight EMA binders were prepared by blending two base binders (i.e., C and Z) with their respective epoxy materials at four EDRs ranging from 15% to 40%. These eight EMA binders, along with a PG 76-22 PMA binder (as control), were used to prepare OGFC mixtures based on two FC-5 mix designs approved by the FDOT. The job mix formula (JMF) of these two mixtures: one with granite aggregates (GRN1) and the other with limestone aggregates (LMS), are presented in Table 4-2.

Table 4-1. Proposed Mixture Testing Matrix for Experiment 2

Factor Name	Factor No.	Description
Epoxy Materials and Base Binder	2	Domestic source epoxy materials + base binder C Foreign source epoxy materials + base binder Z
Epoxy Dosage Rates	4	15%, 25%, 30%, 40%
EMA Binders	8	U15C, U25C, U30C, U40C J15Z, J25Z, J30Z, J40Z
PMA Control Binder	1	Selected from FDOT's approved product list
Mix Design, Aggregate Source	2	Granite (GRN1), limestone (LMS)

Table 4-2. Job Mix Formula Summary of GRN1 and LMS Mixtures

Mix Design ID		GRN1	LMS
Aggregate Gradation, Percent Passing	3/4"	100	100
	1/2"	99	94
	3/8"	71	74
	No. 4	24	23
	No. 8	9	10
	No. 16	5	8
	No. 30	4	6
	No. 50	3	5
	No. 100	3	4
	No. 200	2.5	3.3
Combined G_{sb}		2.769	2.417
JMF OBC, percent		6.8	6.9
Additives		0.3% Cellulose Fiber, 1.0% Hydrated Lime	0.3% Cellulose Fiber

4.1.2 Preparation of EMA Binders and Mixtures

4.1.2.1 J-EMA Binders and Mixtures

The same procedure was followed to prepare J-EMA as described in chapter 3 with PG 67-22 base binder from source Z for all EDRs. It was found extremely important to follow the order of the procedure by mixing the epoxy resin (Part A) and curing agent (Part B) initially and then adding PG 67-22 to the blend for preparing J-EMA binders. A different blending procedure was previously attempted in which the PG 67-22 base binder was first blended with epoxy resin before adding the curing agent. Because the curing agent was added later in the process, it did not fully react with the epoxy resin, consequently creating a significant amount of fumes when the J-EMA

binder was mixed with hot aggregates. Table 4-3 presents the blending proportions of the component materials for J-EMA binders at various EDRs.

Table 4-3. Blending Proportions of Component Materials for J-EMA Binders

EDR	Proportions (Percent by Weight)		
	PG 67-22 Base Binder Z	Part A: Epoxy Resin	Part B: Curing Agent
15%	85.00	8.80	6.20
25%	75.00	14.60	10.40
30%	70.00	17.55	12.45
40%	60.00	23.40	16.60

For the preparation of J-EMA mixtures, the aggregates were preheated at 188°C overnight. Immediately after the J-EMA binder was prepared, the aggregates, lime, and fiber (if used) were added into the mixing bucket and mixed for 30 seconds. Then the J-EMA binder was added into the mixer and mixed for one minute. The final mixing temperature of the mixture was around 157°C to 160°C. After mixing, the loose mixture was conditioned in an oven for two hours at 157°C and then compacted in a Superpave Gyration Compactor (SGC) for 50 gyrations with a final height of approximately 110 to 120 mm. The compacted sample was allowed to cool in the SGC mold for five minutes and then extruded for further cooling in front of a fan.

4.1.2.2 U-EMA Binders and Mixtures

The procedure established in chapter 3 worked for blending U-EMA binders. However, the addition of epoxy resin increased the viscosity of the U-EMA binder and sometimes triggered thermosetting behavior for those at an EDR of 25% or higher. Therefore, high EDR U-EMA binders had a limited time window to remain workable before they could be mixed with the aggregates for mixture production. The duration of this time window varied greatly depending on

the base binder used for epoxy modification, EDR, temperature, and other factors. Beyond the workable time window, the U-EMA binders reached the final stage of polymerization, wherein the cross-linking reaction took place. As a result, the U-EMA binders could not be reheated for additional testing or mixing with the aggregates. The blending proportions of the component materials for U-EMA binders at various EDRs are presented in Table 4-4.

Table 4-4. Blending Proportions of Component Materials for U-EMA Binders

EDR	Proportions (Percent by Weight)		
	PG 67-22 Base Binder	Part A: Epoxy Resin	Part B: Blend of Curing Agent and Soft Asphalt Binder
15%	62.50	7.30	30.20
25%	37.50	12.10	50.40
30%	25.00	14.50	60.50
40%	0.00	19.40	80.60

The U-EMA mixtures were prepared in a similar manner as the J-EMA mixtures, with three exceptions. The first exception was that the aggregates were preheated at a lower temperature of 143°C instead of 188°C to achieve a final mixing temperature of approximately 121°C per epoxy asphalt manufacturer recommendations. The second one was that hydrated lime was not used in U-EMA mixtures per recommendations of the epoxy asphalt manufacturer because of the concern that hydrated lime could trigger an undesired reaction with the acid-based epoxy curing agent. The last exception was that after mixing, the loose mixture was conditioned for 30 minutes to 50 minutes at 121°C instead of two hours at 157°C prior to compaction. This reduced conditioning time and temperature were selected based on the viscosity curing data of the U-EMA binders provided by the epoxy asphalt manufacturer.

4.1.3 Mixture Testing Plan

Cantabro and IDT tests were used to evaluate the raveling resistance, tensile strength, and fracture resistance of OGFC mixtures containing a control PMA binder and EMA binders at different EDRs. Both tests were conducted at three mix aging conditions to account for the impact of asphalt oxidative aging. The first aging condition corresponded to a short-term aging (STA) condition per AASHTO R 30. The second aging condition was a long-term aging (LTA1) condition where the mixture samples were aged in an environmental chamber for ten days at 85°C prior to being tested (Figure 4-1). The last aging condition was an extended long-term aging (LTA2) where the mixture samples were aged in an environmental chamber for 20 days at 85°C prior to testing. These two LTA protocols were selected for this study above the loose mixture aging protocols to avoid the EMA binders from becoming polymerized entirely, which makes it impossible to compact the loose mixtures. However, it is uncertain how these two LTA protocols correlate to the field aging of OGFC, which is a limitation of this study and warrants further investigation.



Figure 4-1. Aging of Compacted OGFC Mixture Samples in the Environmental Chamber

The Cantabro test was performed in accordance with AASHTO TP 108-14. The OGFC sample was placed inside the Los Angeles abrasion machine without the steel charges and allowed to

freely rotate within the drum at a rate of 30 to 33 revolutions per minute for 300 revolutions. The sample was then removed from the abrasion machine and weighed after discarding the loose mixture particles (Figure 4-2). Three replicate samples were tested for each mixture. The Cantabro mass loss was calculated as the relative change between the final weight and the initial weight of the sample. It is indicative of the overall durability of OGFC mixtures, where a lower value is desired for better durability and raveling resistance.

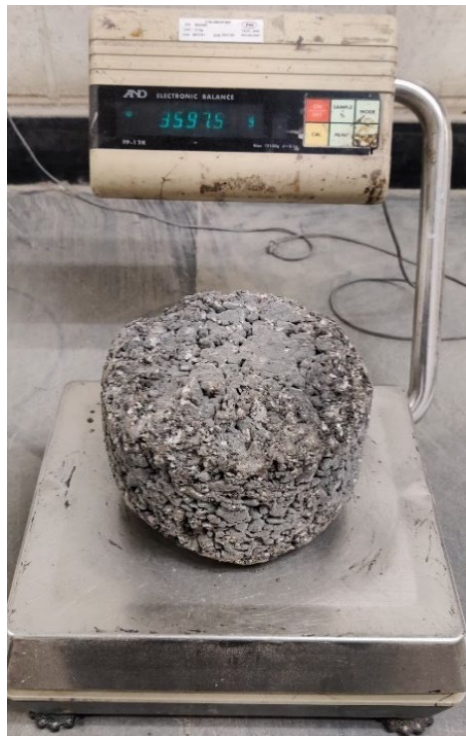


Figure 4-2. Weighing an OGFC Mixture Sample after the Cantabro Test

The IDT test was conducted in the same manner as the IDEAL-CT per ASTM D8225-19. The OGFC samples were compacted to 50 gyrations and then cut into two halves with a height of appropriately 56 mm. During the test, a monotonic load was applied along the sample at a constant displacement rate of 50 mm/min (Figure 4-3). Six replicate samples were tested for each mixture. In this study, the IDT test results were analyzed based on the tensile strength and fracture energy parameters instead of the CT_{Index} . Although CT_{Index} has proved to be an effective index parameter

for evaluating the cracking resistance of dense-graded and gap-graded asphalt mixtures, its calculation requires the determination of the post-peak slope of the load-displacement curve to indicate the relative brittleness of the mixture, which, however, may not be applicable to OGFC mixtures because of the significantly high air voids associated with the open-graded aggregate structure. Furthermore, the CT_{Index} results of OGFC mixtures were found to have abnormally high variability among the replicates. The coefficient of variation (COV) (out of six replicates) of different mixtures tested in this experiment varied greatly from 6% to 107%.



Figure 4-3. IDEAL CT Equipment and Sample after Testing

Figure 4-4 presents an example of the load-displacement curve from the test. Tensile strength (σ) was calculated based on the peak load and dimensions of the sample, as shown in Equation 4-1. Fracture energy (G_f) was calculated as the area under the entire load-displacement curve divided by the area of the cracking face using Equation 4-2. G_f indicates the amount of energy required to

create a unit surface area of a crack within the mixture. Higher σ and G_f values are desired for OGFC mixtures with better strength and fracture resistance characteristics.

$$\sigma = \frac{2 * P_{max}}{\pi * T * D} \quad \text{Equation 4-1}$$

Where,

- σ = tensile strength, psi;
- P_{max} = peak load, lbf;
- T = sample thickness, inch; and
- D = sample diameter, inch.

$$G_f = \frac{W}{A} \quad \text{Equation 4-2}$$

Where,

- G_f = fracture energy, J/m²;
- W = work of failure, J; and
- A = area of cracking face, m².

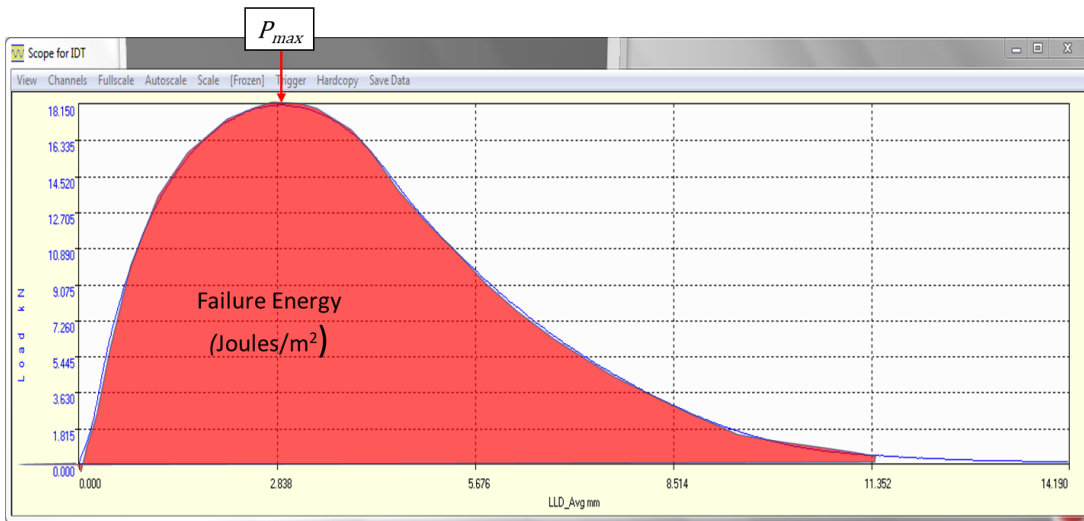


Figure 4-4. Example of Load-Displacement Curve from the IDT Test

4.2 Test Results and Discussion

4.2.1 Mixture Testing Experiment Results

4.2.1.1 Cantabro Loss Results

GRN1 Mix Design

The Cantabro loss results of GRN1 mixtures containing the PMA and J-EMA binders at various EDRs are presented in Figure 4-5. In all cases except one, the Cantabro loss of the J-EMA mixtures decreased as the EDR increased, which indicated improved raveling resistance. The exception was the J30Z mixture, as it had a slightly higher average Cantabro loss value than the J25Z mixture at the STA condition. However, this difference was not statistically significant. The comparison of the PMA and J-EMA mixtures was highly dependent on the EDR and mix aging condition (i.e., aging time). At the STA condition, the PMA mixture had a similar or lower average Cantabro loss value than the J-EMA mixtures at all EDRs. At the LTA1 and LTA2 conditions, most EMA mixtures, especially those at higher EDRs, outperformed the PMA mixture in the Cantabro test. Thus, they are expected to have better raveling resistance after long-term aging.

Statistical analysis was conducted to discriminate better the raveling resistance of PMA *versus* EMA mixtures at each mix aging condition to consider the variability of the Cantabro test results. Specifically, the ANOVA and Tukey's HSD tests were used to determine whether the PMA and EMA mixtures have significantly different Cantabro loss results at a 95% confidence level. According to Tukey's rankings in Figure 4-5, the statistical comparisons for the Cantabro loss results of PMA *versus* J-EMA mixtures are summarized in Table 4-5.

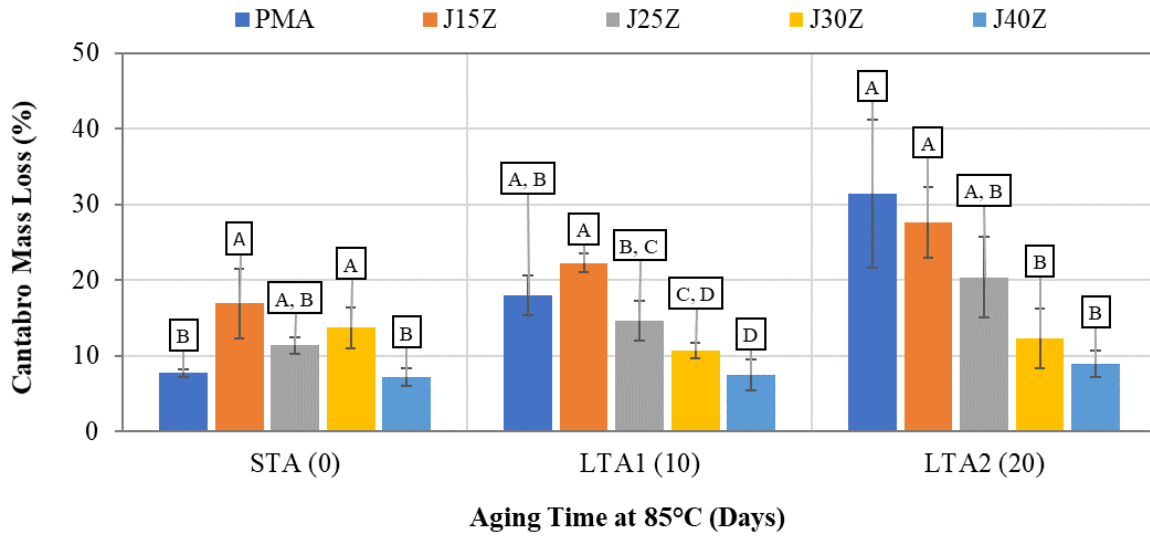


Figure 4-5. Cantabro Mass Loss Results of GRN1 Mixtures with PMA and J-EMA Binders at Different Mix Aging Conditions

Table 4-5. Statistical Comparison for Cantabro Loss Results of GRN1 Mixtures with PMA and J-EMA Binders

Aging Condition	Statistically Lower than PMA	Statistically Equivalent to PMA	Statistically Higher than PMA
STA	-	J25Z, J40Z	J15Z, J30Z
LTA1	J30Z, J40Z	J15Z, J25Z	-
LTA2	J30Z, J40Z	J15Z, J25Z	-

Cantabro test results for GRN1 mixtures containing PMA and U-EMA binders at varying EDRs are shown in Figure 4-6. An unexpected trend was observed for the results at STA condition, where the Cantabro loss of U-EMA mixtures increased with an increase in EDR up to 30%. Furthermore, the PMA mixture had a lower average Cantabro loss value than all the U-EMA mixtures. Different trends were observed for the comparison of PMA and U-EMA mixtures after long-term aging. At both the LTA1 and LTA2 conditions, the Cantabro loss of the U-EMA mixtures consistently increased with an increase in EDR, which indicated that U-EMA mixtures at a higher EDR are

expected to have better raveling resistance than those at a lower EDR. At the LTA1 condition, the PMA mixture had an average Cantabro loss of 17.9%, which was lower than those of the U15C and U25C mixtures but higher than the U30C and U40C mixtures. At the LTA2 condition, the average Cantabro loss of the PMA mixture was higher than those of the U-EMA mixtures at all EDRs. These results indicated that the U-EMA mixtures are expected to have better raveling resistance than the PMA mixture after long-term aging. The statistical comparisons for the Cantabro loss results of PMA against U-EMA combinations are summarized in Table 4-6, according to Tukey's groupings (Figure 4-6) for the Cantabro loss results.

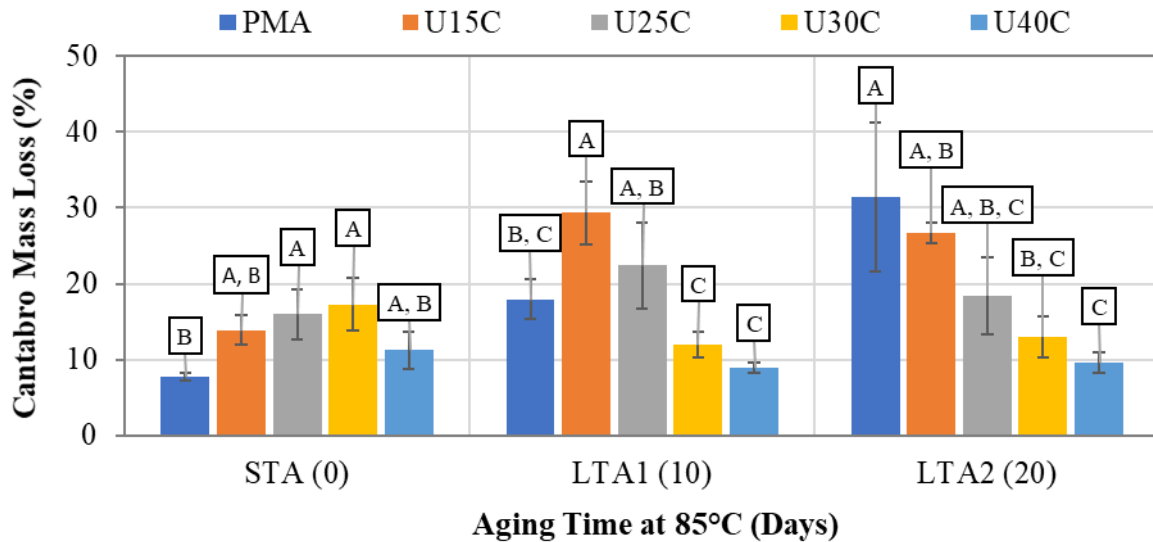


Figure 4-6. Cantabro Mass Loss Results of GRN1 Mixtures with PMA and U-EMA Binders at Different Mix Aging Conditions

Table 4-6. Statistical Comparison for Cantabro Loss Results of GRN1 Mixtures with PMA and U-EMA Binders

Aging Condition	Statistically Lower than PMA	Statistically Equivalent to PMA	Statistically Higher than PMA
STA	-	U15C, U40C	U25C, U30C
LTA1	-	U25C, U30C, U40C	U15C
LTA2	U30C, U40C	U15C, U25C	-

LMS Mix Design

Figure 4-7 shows the Cantabro loss results of LMS mixtures containing the PMA and J-EMA binders at different EDRs. There was a general trend that the Cantabro loss values decreased with an increase in EDR for the J-EMA mixtures for all the aging conditions. At the STA condition, the PMA and J-EMA mixtures at various EDRs had similar Cantabro loss results, indicating equivalent raveling resistance before long-term aging. At the LTA1 and LTA2 conditions, most of the J-EMA mixtures, especially those at high EDRs, performed better in the Cantabro test and thus, are expected to have better raveling resistance than the PMA mixture. These results were affirmed with the statistical analysis results. According to Tukey's groupings shown in Figure 4-7, the statistical comparisons for the Cantabro loss results of PMA *versus* J-EMA mixtures are summarized in Table 4-7.

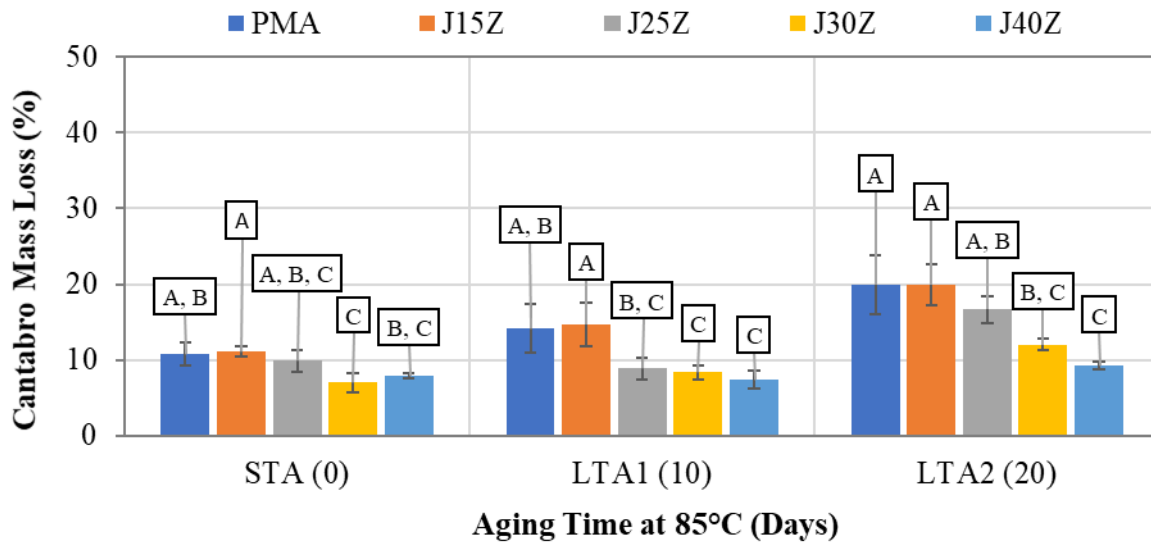


Figure 4-7. Cantabro Mass Loss Results of LMS Mixtures with PMA and J-EMA Binders at Different Mix Aging Conditions

Table 4-7. Statistical Comparison for Cantabro Loss Results of LMS Mixtures with PMA and J-EMA Binders

Aging Condition	Statistically Lower than PMA	Statistically Equivalent to PMA	Statistically Higher than PMA
STA	J30Z	J15Z, J25Z, J40Z	-
LTA1	J30Z, J40Z	J15Z, J25Z	-
LTA2	J30Z, J40Z	J15Z, J25Z	-

The Cantabro loss results of LMS mixtures containing the PMA and U-EMA binders at different EDRs are shown in Figure 4-8. At the STA condition, the average Cantabro loss of the PMA mixture was nearly identical to those of the U-EMA mixtures except for the U40C mixture, which had a slightly lower average Cantabro loss than the other mixtures. At the LTA1 and LTA2 conditions, the average Cantabro loss of U-EMA mixtures decreased with an increase in the EDR, which indicated improved raveling resistance due to epoxy modification of the asphalt binder. Furthermore, most of the U-EMA mixtures, particularly those with high EDRs, outperformed the PMA mixture in the Cantabro test; thus, they are expected to have better raveling resistance than the PMA mixture after long-term aging. Based on Tukey's rankings presented in Figure 4-8, the statistical comparisons for the Cantabro loss results of PMA *versus* U-EMA mixtures are summarized in Table 4-8.

Table 4-8. Statistical Comparison for Cantabro Loss Results of LMS Mixtures with PMA and U-EMA Binders

Aging Condition	Statistically Lower than PMA	Statistically Equivalent to PMA	Statistically Higher than PMA
STA	-	U15C, U25C, U30C, U40C	-
LTA1	U40C	U15C, U25C, U30C	-
LTA2	U25C, U30C, U40C	U15C	-

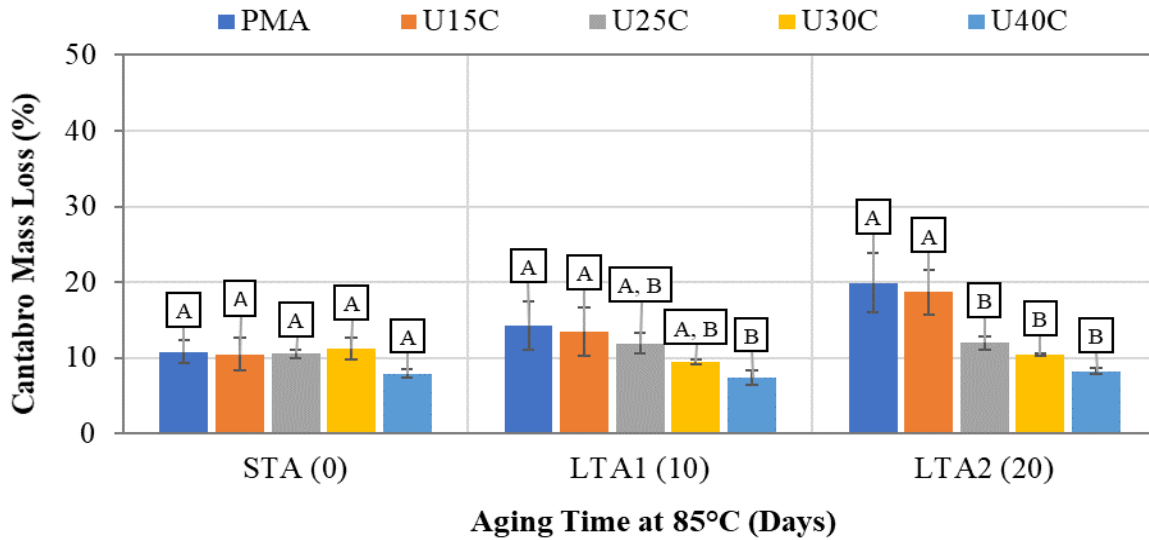


Figure 4-8. Cantabro Mass Loss Results of LMS Mixtures with PMA and U-EMA Binders at Different Mix Aging Conditions

4.2.1.2 Aging Resistance Evaluation

An aging index parameter called Cantabro Aging Index (CAI) was proposed based on the Cantabro test results at different mix aging conditions to quantitatively evaluate the aging resistance of OGFC mixtures, including EMA and PMA binders. CAI is defined as the percentage change in the Cantabro loss of the mixture at the STA condition to the LTA condition (Equation 4-3). A lower (i.e., less positive or higher negative) CAI value indicates that the mixture is more resistant to aging in terms of raveling resistance.

$$CAI = \frac{CL_{LTA} - CL_{STA}}{CL_{STA}} * 100 \quad \text{Equation 4-3}$$

Where,

CL_{STA} = Cantabro loss at the STA condition; and

CL_{LTA} = Cantabro loss at the LTA condition.

The CAI results of GRN1 and LMS mixtures containing the PMA, J-EMA, and U-EMA binders for the LTA1 and LTA2 conditions are presented in Figure 4-9 and Figure 4-10. For both mix designs, the PMA mixture has the highest CAI value, which indicates that it is most susceptible to aging in terms of raveling resistance. A general trend was observed among the EMA mixtures with a few exceptions that the CAI values decreased as the EDR increased. These results indicate that EMA mixtures at higher EDRs are expected to have better aging resistance than those at lower EDRs. In some cases, the EMA mixture had a negative CAI value. This improvement is mainly attributed to the post-compaction curing of the EMA binder during aging, which is expected to increase the cohesive strength of the mixture significantly. Therefore, the negative CAI values of certain EMA mixtures were caused by the combined effects of asphalt aging and curing on the Cantabro test results. For both the GRN1 and LMS mix designs, the two lowest CAI values correspond to the U30C and U40C mixtures at both long-term aging conditions. Overall, the CAI results indicate that the U-EMA mixtures have the greatest aging resistance, followed by the J-EMA mixtures and the PMA mixtures, respectively.

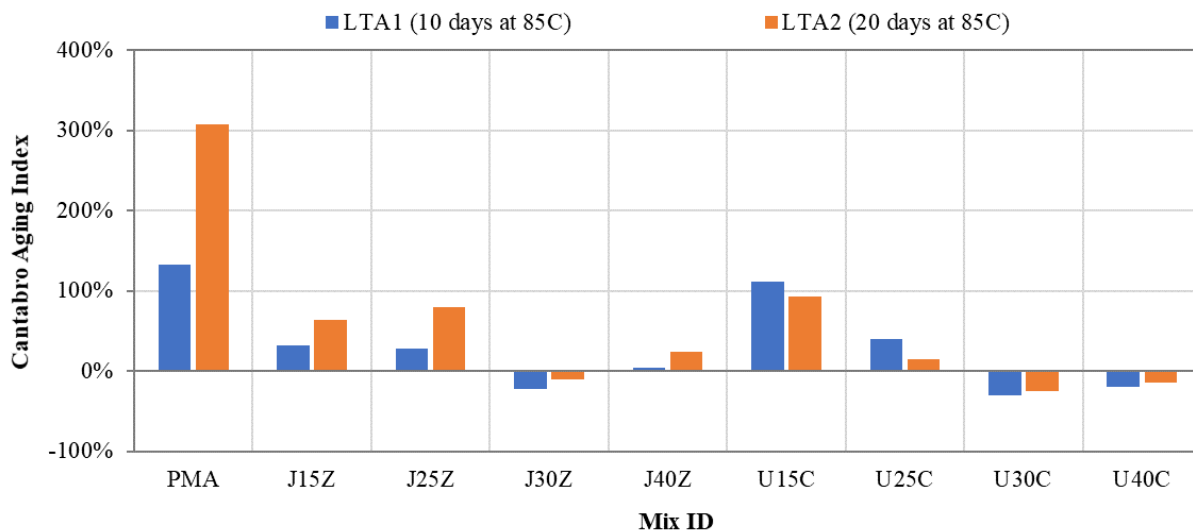


Figure 4-9. Cantabro Aging Index Results of GRN1 Mixtures

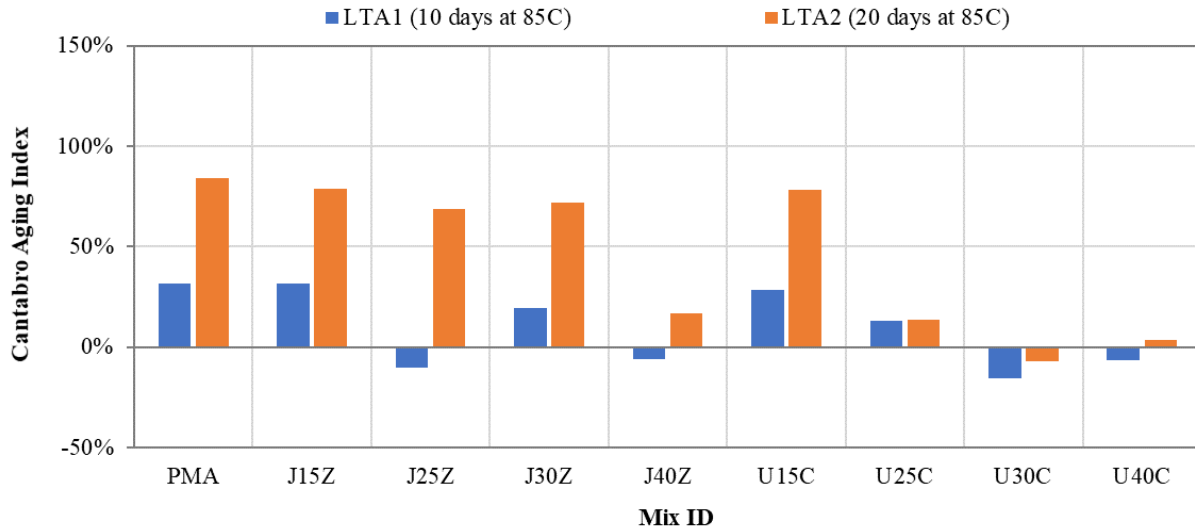


Figure 4-10. Cantabro Aging Index Results of LMS Mixtures

4.2.1.3 IDT Strength Results

GRN1 Mix Design

Figure 4-11 presents the IDT strength results of GRN1 mixtures containing the PMA and J-EMA binders at various EDRs. In all the cases except two, the IDT strength of the J-EMA mixtures increased as the EDR increased. The two exceptions were the J30Z mixture at the STA and LTA2 conditions. Although the J30Z mixture had a slightly lower average IDT strength than the J25Z mixture at the STA condition, it had considerably higher variability than the other mixtures, which made the comparison inconclusive. At the LTA2 condition, the J25Z and J30Z mixtures had almost identical average IDT strength results. For all the mix aging conditions, the PMA mixture had consistently lower average IDT strength results than the EMA mixtures regardless of the EDR. The differences were more pronounced compared to the EMA mixtures at higher EDRs. Based on Tukey's rankings in Figure 4-11, the statistical comparisons for the IDT strength results of GRN1 mixtures containing the PMA *versus* J-EMA binders are summarized as follows (Table 4-9).

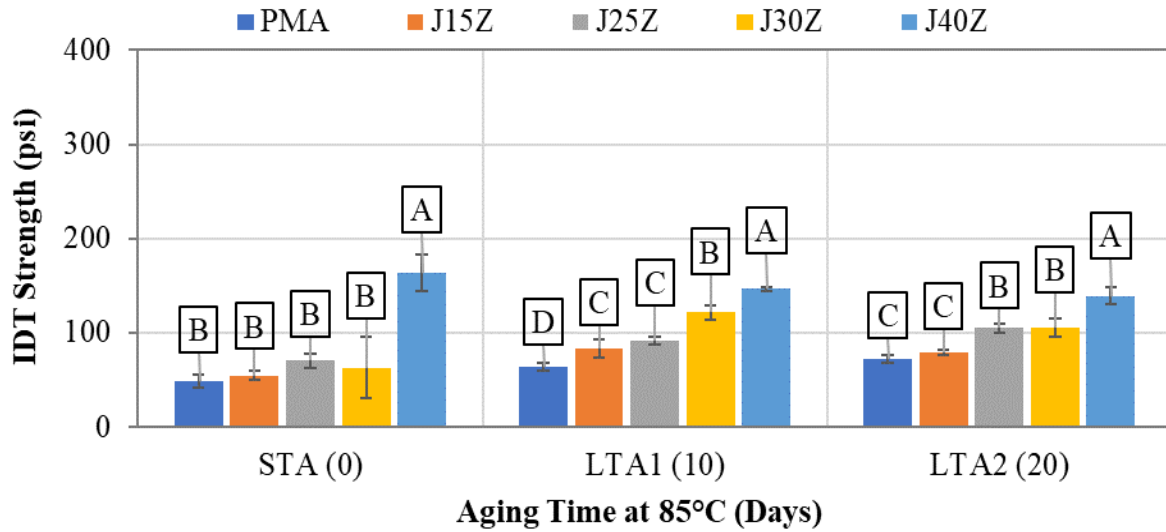


Figure 4-11. IDT Strength Results of GRN1 Mixtures with PMA and J-EMA Binders at Different Mix Aging Conditions

Table 4-9. Statistical Comparison for IDT Strength Results of GRN1 Mixtures with PMA and J-EMA Binders

Aging Condition	Statistically Lower than PMA	Statistically Equivalent to PMA	Statistically Higher than PMA
STA	-	J15Z, J25Z, J30Z	J40Z
LTA1	-	-	J15Z, J25Z, J30Z, J40Z
LTA2	-	J15Z	J25Z, J30Z, J40Z

Figure 4-12 presents the IDT strength results of GRN1 mixtures containing the PMA and U-EMA binders at various EDRs. In all cases, the IDT strength of the U-EMA mixtures increased with an increase in EDR, which indicated that epoxy modification of the asphalt binder has a positive impact on the strength properties of OGFC mixtures. The comparison between the PMA and U-EMA mixtures was dependent on the EDR. At all the mix aging conditions, the PMA and U25C mixtures had similar IDT strength results, which were consistently higher than those of the U15C mixture. On the other hand, the U30C and U40C mixtures had considerably higher IDT strength

results than the PMA mixture. Based on Tukey's rankings shown in Figure 4-12, the statistical comparisons for the IDT strength results of GRN1 mixtures containing the PMA *versus* U-EMA binders are summarized in Table 4-10.

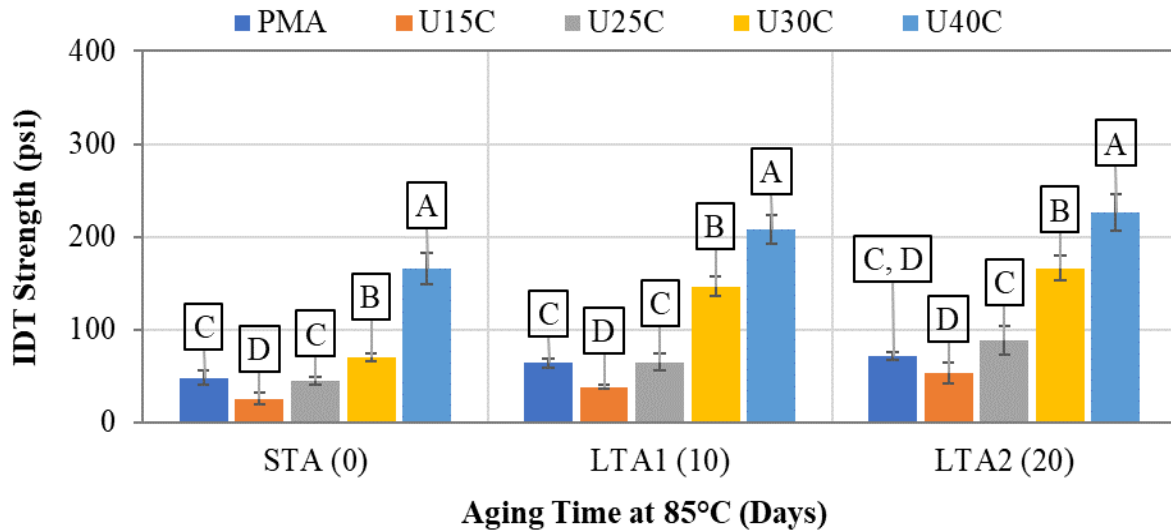


Figure 4-12. IDT Strength Results of GRN1 Mixtures with PMA and U-EMA Binders at Different Mix Aging Conditions

Table 4-10. Statistical Comparison for IDT Strength Results of GRN1 Mixtures with PMA and U-EMA Binders

Aging Condition	Statistically Lower than PMA	Statistically Equivalent to PMA	Statistically Higher than PMA
STA	U15C	U25C	U30C, U40C
LTA1	U15C	U25C	U30C, U40C
LTA2	-	U15C, U25C	U30C, U40C

LMS Mix Design

The IDT strength results of LMS mixtures containing the PMA and J-EMA binders at various EDRs are presented in Figure 4-13. As can be seen, the IDT strength of the J-EMA mixtures increased with an increase in EDR for all three mix aging conditions. At the STA and LTA1

conditions, the PMA mixture had lower average IDT strength results compared to the J-EMA mixtures. At the LTA2 condition, the PMA mixtures had the second-lowest average IDT strength after the J15Z mixture, but the difference was not practically significant. Overall, the J-EMA mixtures had similar or higher IDT strength than the PMA mixture. Based on Tukey's rankings given in Figure 4-13, the statistical comparisons for the IDT strength results of LMS mixtures with PMA *versus* J-EMA binders are summarized in Table 4-11.

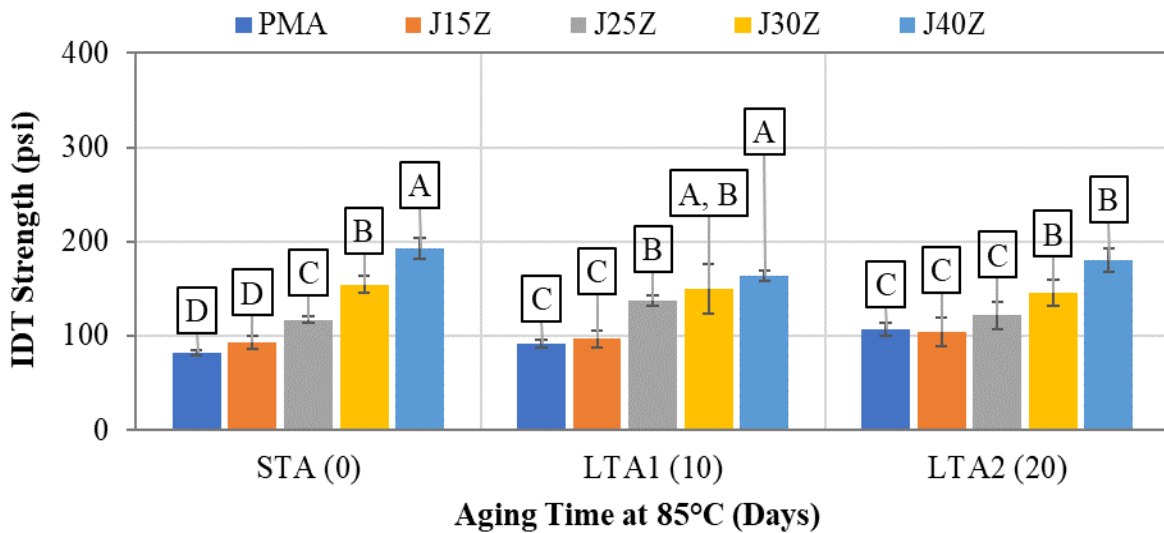


Figure 4-13. IDT Strength Results of LMS Mixtures with PMA and J-EMA Binders at Different Mix Aging Conditions

Table 4-11. Statistical Comparison for IDT Strength Results of LMS Mixtures with PMA and J-EMA Binders

Aging Condition	Statistically Lower than PMA	Statistically Equivalent to PMA	Statistically Higher than PMA
STA	-	J15Z	J25Z, J30Z, J40Z
LTA1	-	J15Z	J25Z, J30Z, J40Z
LTA2	-	J15Z, J25Z	J30Z, J40Z

Figure 4-14 shows the IDT strength results of LMS mixtures containing the PMA and U-EMA binders at various EDRs. The IDT strength of the U-EMA mixtures increased with an increase in EDR for the three mix aging conditions. All the EMA mixtures except U15C had similar or higher IDT strength results than the PMA mixture, regardless of the mix aging condition. These results were confirmed by the statistical comparisons presented in Table 4-12, based on Tukey's rankings shown in Figure 4-14.

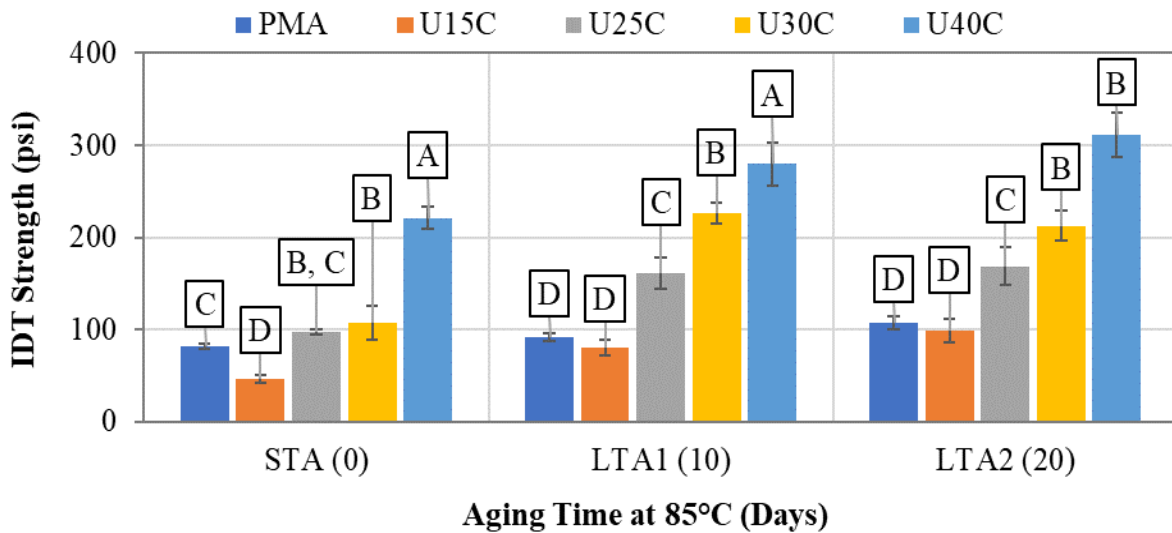


Figure 4-14. IDT Strength Results of LMS Mixtures with PMA and U-EMA Binders at Different Mix Aging Conditions

Table 4-12. Statistical Comparison for IDT Strength Results of LMS Mixtures with PMA and U-EMA Binders

Aging Condition	Statistically Lower than PMA	Statistically Equivalent to PMA	Statistically Higher than PMA
STA	U15C	U25C	U30C, U40C
LTA1	-	U15C	U25C, U30C, U40C
LTA2	-	U15C	U25C, U30C, U40C

4.2.1.4 IDT Fracture Energy (G_f) Results

GRN1 Mix Design

The IDT G_f results of GRN1 mixtures containing the PMA and J-EMA binders at different EDRs are plotted in Figure 4-15. In all cases except two, the IDT G_f of J-EMA mixtures increased with an increase in EDR, which indicated improved fracture resistance. The two exceptions were the J30Z mixture at the STA condition and the J25Z mixture at the LTA1 mixture. The comparison between the PMA and J-EMA mixtures was dependent on the EDR and mixing aging condition. At the STA condition, the PMA mixture had a similar or slightly higher average IDT G_f value than the J15Z and J30Z mixtures, while the opposite trend was observed for the comparison with the J25Z and J40Z mixtures. The J30Z mixture had considerably higher variability than the other mixtures, which made the comparison inconclusive. At the LTA1 condition, the J30Z and J40Z mixtures outperformed the PMA mixture in mixture resistance, but the PMA mixture had slightly higher average G_f results than the J15Z and J25Z mixtures. At the LTA2 condition, the J-EMA mixtures at 25%, 30%, and 40% EDRs showed higher average G_f results than the PMA mixture, while the J15Z mixture had a marginally lower G_f value. Overall, the EMA mixtures at high EDRs had higher IDT G_f results and, thus, better fracture resistance than the PMA mixture at all the mixing aging conditions. According to Tukey's rankings given in Figure 4-15, the statistical comparisons for the IDT G_f results of GRN1 mixtures with PMA *versus* J-EMA binders are summarized in Table 4-13.

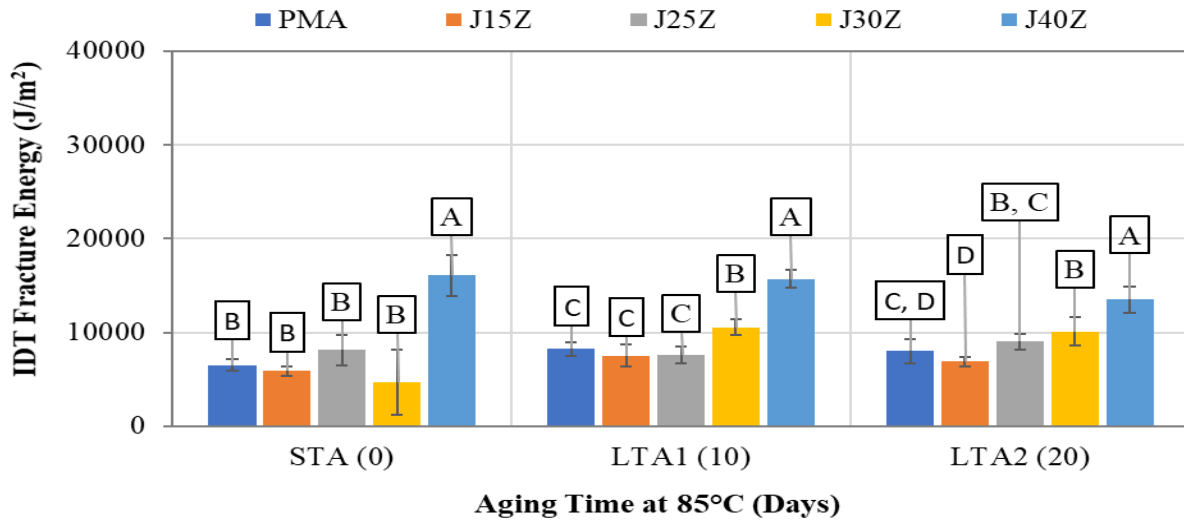


Figure 4-15. IDT G_f Results of GRN1 Mixtures with PMA and J-EMA Binders at Different Mix Aging Conditions

Table 4-13. Statistical Comparison for IDT Fracture Energy Results of GRN1 Mixtures with PMA and J-EMA Binders

Aging Condition	Statistically Lower than PMA	Statistically Equivalent to PMA	Statistically Higher than PMA
STA	-	J15Z, J25Z, J30Z	J40Z
LTA1	-	J15Z, J25Z	J30Z, J40Z
LTA2	-	J15Z, J25Z	J30Z, J40Z

The IDT G_f results of GRN1 mixtures containing the PMA and U-EMA binders are presented in Figure 4-16. The results show that the IDT G_f of the U-EMA mixtures increased with an increase in EDR at all three mix aging conditions. The comparison between the PMA and U-EMA mixtures was highly dependent on the EDR. At all three mix aging conditions, the U30C and U40C mixtures had consistently higher IDT G_f results and thus, are expected to have better fracture resistance than the PMA mixture, while the U15C and U20C mixtures had similar or lower IDT G_f results than the PMA mixture. According to Tukey's rankings shown in Figure 4-16, the statistical comparisons

for the IDT G_f results of GRN1 mixtures with PMA versus U-EMA binders are given in Table 4-14.

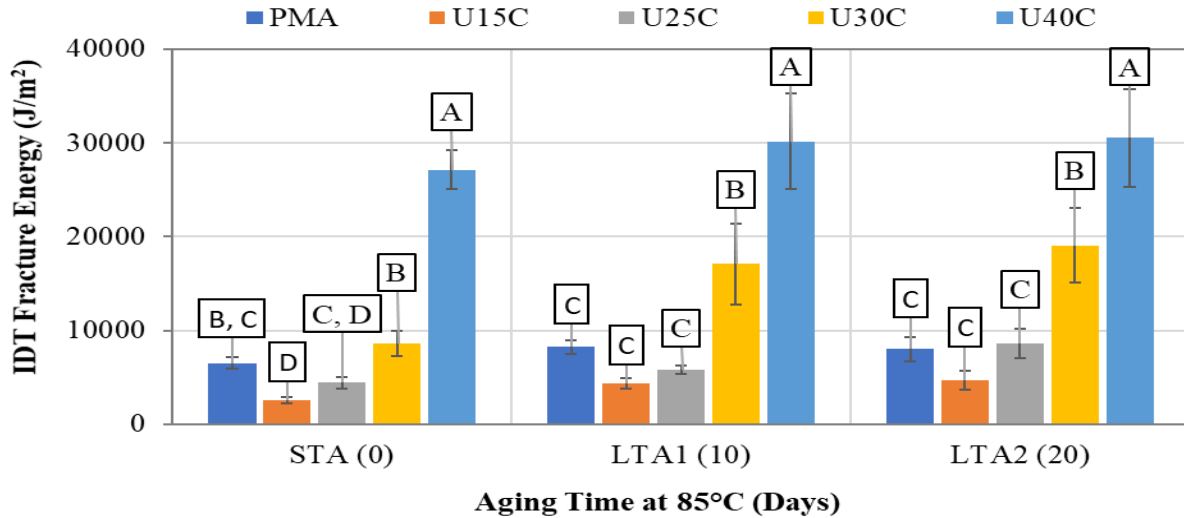


Figure 4-16. IDT G_f Results of GRN1 Mixtures with PMA and U-EMA Binders at Different Mix Aging Conditions

Table 4-14. Statistical Comparison for IDT Fracture Energy Results of GRN1 Mixtures with PMA and U-EMA Binders

Aging Condition	Statistically Lower than PMA	Statistically Equivalent to PMA	Statistically Higher than PMA
STA	U15C	U25C, U30C	U40C
LTA1	-	U15C, U25C	U30C, U40C
LTA2	-	U15C, U25C	U30C, U40C

LMS Mix Design

Figure 4-17 presents the IDT G_f results of LMS mixtures containing the PMA and J-EMA binders at three mix aging conditions. For all the J-EMA mixtures except one, the IDT G_f increased as the EDR increased. The only exception was the J40Z mixture, which had a slightly lower average IDT

G_f value than the J30Z mixture at the STA condition. However, this difference may not be practically significant if considering the variability of the results (as indicated by the error bars). At all three mix aging conditions, the J25Z, J30Z, and J40Z mixtures had higher average IDT G_f results and, thus, are expected to have better fracture resistance than the PMA mixture. The opposite trend was observed for the comparison between the J15Z and PMA mixtures. According to Tukey's rankings presented in Figure 4-17, the statistical comparisons for the IDT G_f results of LMS mixtures with PMA *versus* J-EMA binders are summarized as follows (Table 4-15).

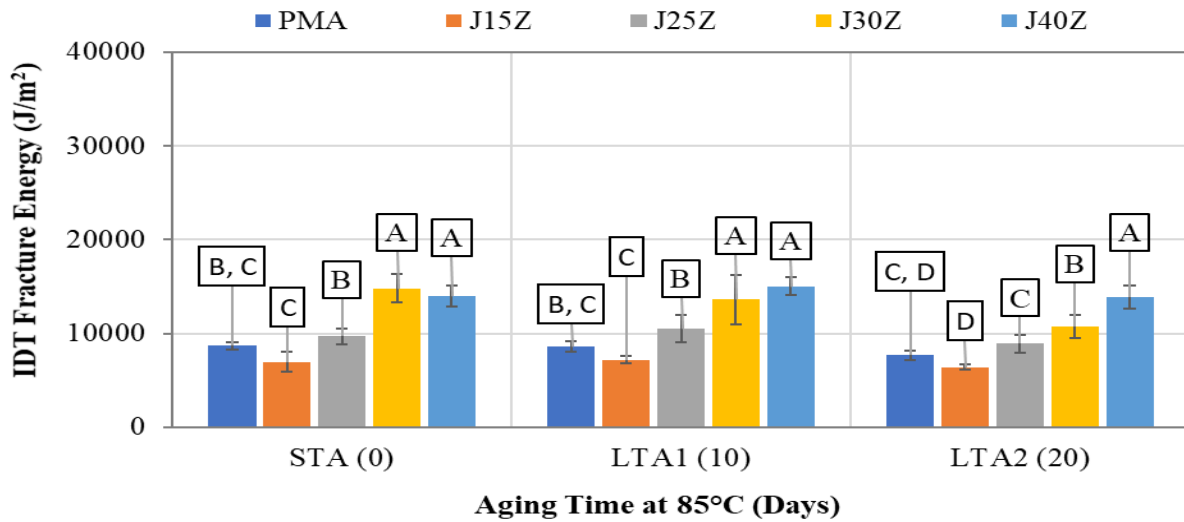


Figure 4-17. IDT G_f Results of LMS Mixtures with PMA and J-EMA Binders at Different Mix Aging Conditions

Table 4-15. Statistical Comparison for IDT Fracture Energy Results of LMS Mixtures with PMA and J-EMA Binders

Aging Condition	Statistically Lower than PMA	Statistically Equivalent to PMA	Statistically Higher than PMA
STA	-	J15Z, J25Z	J30Z, J40Z
LTA1	-	J15Z, J25Z	J30Z, J40Z
LTA2	-	J15Z, J25Z	J30Z, J40Z

The IDT G_f results of LMS mixtures containing the PMA and U-EMA binders at different EDRs are shown in Figure 4-18. For all three mix aging conditions, the IDT G_f of the U-EMA mixtures increased with an increase in EDR. The comparison between the PMA and U-EMA mixtures was dependent on the EDR and mix aging condition. Only the U40C mixture had consistently higher IDT G_f results than the PMA mixture at the three mix aging conditions. The opposite trend was observed for the comparison between the U15C and PMA mixtures. The U30C and PMA mixtures had similar IDT G_f results at the STA condition, but the U30C mixture showed significantly higher IDT G_f results after long-term aging. The statistical comparisons for the IDT G_f results of LMS mixtures with PMA *versus* U-EMA binders are given in Table 4-16, according to Tukey's rankings shown in Figure 4-18.

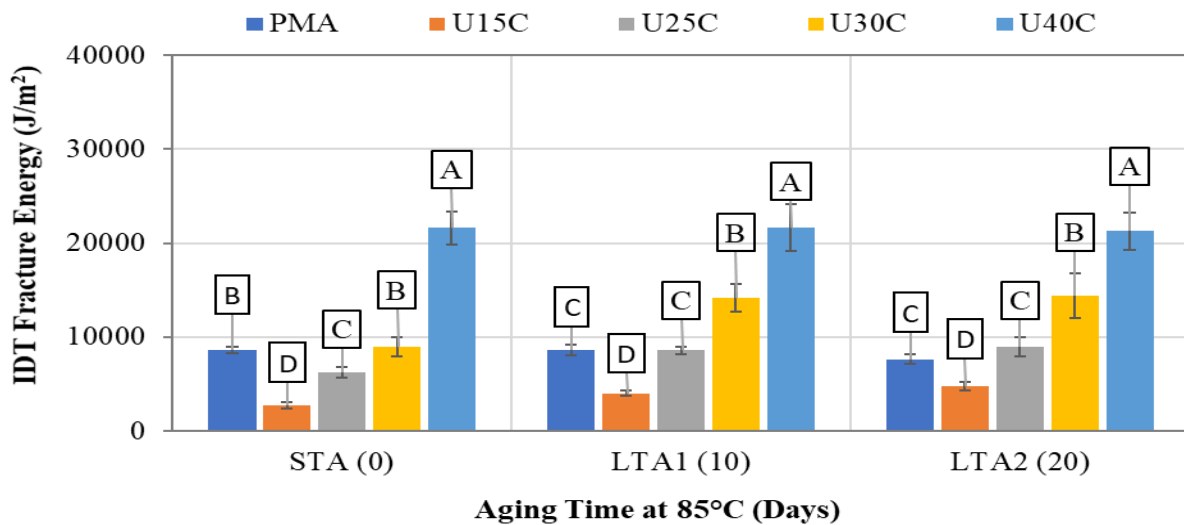


Figure 4-18. IDT G_f Results of LMS Mixtures with PMA and U-EMA Binders at Different Mix Aging Conditions

Table 4-16. Statistical Comparison for IDT Fracture Energy Results of LMS Mixtures with PMA and U-EMA Binders

Aging Condition	Statistically Lower than PMA	Statistically Equivalent to PMA	Statistically Higher than PMA
STA	U15C, U25C	U30C	U40C
LTA1	U15C	U25C	U30C, U40C
LTA2	U15C	U25C	U30C, U40C

4.2.2 Selection of Optimum EDR

The optimum EDR of EMA binders was selected based on the following three criteria applicable to the Cantabro and IDT test results determined at three mix aging conditions:

1. At the STA condition, the EMA mixture at the optimum EDR should have an average Cantabro loss of less than 20%. This criterion was selected based on recommendations from the NCHRP project 1-55, which also matches FDOT's current Cantabro test criterion for mix design approval of FC-5 mixtures with a PMA or HP binder. Criterion 1 is primarily to ensure that the EMA mixture has adequate raveling resistance before long-term aging.

2. At the LTA1 condition, the EMA mixture at the optimum EDR should have *statistically* lower Cantabro loss results but *statistically* higher IDT strength and G_f results than the corresponding PMA mixture. This evaluation requires statistical comparisons (i.e., ANOVA and Tukey's HSD tests) to account for the variability of the test results and, thus, is considered a more conservative approach than using the numerical comparisons of the average test results. Criterion 2 is to ensure that the EMA mixture has significantly better raveling resistance, tensile strength, and fracture resistance than the PMA mixture after long-term aging.

3. At the LTA2 condition, the EMA mixture at the optimum EDR should have *statistically* lower Cantabro loss but *statistically* higher IDT strength and G_f results than the corresponding PMA mixture. This criterion is fundamentally the same as Criterion 2 but requires statistical comparisons of the Cantabro and IDT test results after extended long-term aging. Criterion 3 evaluates if the EMA mixture has greater potential for extending the life span of OGFC through better performance properties than the PMA mixture after extended long-term aging.

Table 4-17 summarizes statistical comparisons of the Cantabro and IDT test results *versus* the proposed criteria for selecting optimum EDR for J-EMA mixtures. The comparison results are denoted as "Pass" or "Fail," where "Pass" indicates that the test results meet the proposed criterion and "Fail" indicates that the results fail the criterion. As shown, all the J-EMA mixtures had acceptable Cantabro loss results at the STA condition and thus, passed Criterion 1 regardless of the EDR. At the LTA1 and LTA2 conditions, most of the J-EMA mixtures at 15% and 25% EDRs did not statistically outperform the PMA mixtures in the Cantabro and IDT tests, and thus, failed Criterion 2 and Criterion 3. The J-EMA mixtures at 30% and 40% EDR, on the other hand, passed both criteria corresponding to the Cantabro and IDT test results after long-term aging for both mix designs.

Similar trends were observed for the comparison results of U-EMA mixtures in Table 4-18. For both mix designs, the U-EMA mixtures at 15% to 40% EDRs passed Criterion 1 with an average Cantabro loss of less than 20% at the STA condition. Most of the U-EMA mixtures at 15% and 25% EDRs failed Criterion 2 and Criterion 3 based on comparisons of the long-term aged Cantabro and IDT test results against the PMA mixtures. However, the U-EMA mixtures at 30% EDR passed both criteria for most of the test result comparisons. The only two exceptions were a mixture

with the GRN1 mix design and a mixture with the LMS mix design. In both cases, the U-EMA mixtures at 30% EDR had lower average Cantabro loss results than the corresponding PMA mixtures at the LTA condition, but the differences were not statistically significant according to Tukey's groupings. Finally, the U-EMA mixtures at 40% EDR passed both Criterion 2 and Criterion 3 for all the test result comparisons except one. The exception was a mixture with the GRN1 mix design, which had a lower average Cantabro loss than the corresponding PMA mixture at the LTA1 condition. However, the results were considered statistically equivalent based on Tukey's HSD test.

Table 4-17. Selection of Optimum EDR for J-EMA Binders

EDR	FC-5 Mix Design	Criterion 1	Criterion 2			Criterion 3		
		Cantabro Loss	Cantabro Loss	IDT Strength	IDT G_f	Cantabro Loss	IDT Strength	IDT G_f
15%	GRN1	<u>Pass</u>	Fail	<u>Pass</u>	Fail	Fail	Fail	Fail
	LMS	<u>Pass</u>	Fail	Fail	Fail	Fail	Fail	Fail
25%	GRN1	<u>Pass</u>	Fail	<u>Pass</u>	Fail	Fail	<u>Pass</u>	Fail
	LMS	<u>Pass</u>	Fail	<u>Pass</u>	Fail	Fail	Fail	Fail
30%	GRN1	<u>Pass</u>	<u>Pass</u>	<u>Pass</u>	<u>Pass</u>	<u>Pass</u>	<u>Pass</u>	<u>Pass</u>
	LMS	<u>Pass</u>	<u>Pass</u>	<u>Pass</u>	<u>Pass</u>	<u>Pass</u>	<u>Pass</u>	<u>Pass</u>
40%	GRN1	<u>Pass</u>	<u>Pass</u>	<u>Pass</u>	<u>Pass</u>	<u>Pass</u>	<u>Pass</u>	<u>Pass</u>
	LMS	<u>Pass</u>	<u>Pass</u>	<u>Pass</u>	<u>Pass</u>	<u>Pass</u>	<u>Pass</u>	<u>Pass</u>

Table 4-18. Selection of Optimum EDR for U-EMA Binders

EDR	FC-5 Mix Design	Criterion 1	Criterion 2		Criterion 3			
		Cantabro Loss	Cantabro Loss	IDT Strength	IDT G_f	Cantabro Loss	IDT Strength	IDT G_f
15%	GRN1	<u>Pass</u>	Fail	Fail	Fail	Fail	Fail	Fail
	LMS	<u>Pass</u>	Fail	Fail	Fail	Fail	Fail	Fail
25%	GRN1	<u>Pass</u>	Fail	Fail	Fail	Fail	Fail	Fail
	LMS	<u>Pass</u>	Fail	<u>Pass</u>	Fail	<u>Pass</u>	<u>Pass</u>	Fail
30%	GRN1	<u>Pass</u>	Fail	<u>Pass</u>	<u>Pass</u>	<u>Pass</u>	<u>Pass</u>	<u>Pass</u>
	LMS	<u>Pass</u>	Fail	<u>Pass</u>	<u>Pass</u>	<u>Pass</u>	<u>Pass</u>	<u>Pass</u>
40%	GRN1	<u>Pass</u>	Fail	<u>Pass</u>	<u>Pass</u>	<u>Pass</u>	<u>Pass</u>	<u>Pass</u>
	LMS	<u>Pass</u>	<u>Pass</u>	<u>Pass</u>	<u>Pass</u>	<u>Pass</u>	<u>Pass</u>	<u>Pass</u>

Based on the comparison results in Table 4-17 and Table 4-18, both 30% and 40% EDR pass all the proposed criteria for J-EMA mixtures and most of the criteria for U-EMA mixtures; therefore, either of the two could be selected as the optimum EDR from a mixture performance evaluation perspective. However, OGFC mixtures at these two EDRs would have considerably different material costs. Based on the limited available cost information of epoxy materials, it was estimated that U-EMA binders at 30% and 40% EDR cost approximately \$5,000/ton and \$6,500/ton, respectively, and that J-EMA binders at 30% and 40% EDR would cost approximately \$3,300/ton and \$4,200/ton, respectively. Using these estimated binder costs, OGFC mixtures with U-EMA binders at 30% and 40% EDR were estimated to cost approximately \$380/ton and \$480/ton, respectively, while those containing J-EMA binders at 30% and 40% EDR were costing approximately \$260/ton and \$330/ton, respectively. Because of the significantly high costs of epoxy materials, the lower EDR of 30% was selected as the final optimum (i.e., most cost-effective) EDR for both U-EMA and J-EMA binders for further evaluation in the study. At this

EDR, the overall material costs of OGFC mixtures with an EMA binder were approximately 3.5 to 5 times higher than that of the traditional PMA mixtures, with an estimated material cost of \$75/ton.

4.3 Summary of Findings

Based on the mixture testing experiment, the epoxy modification of the asphalt binder had a positive impact on improving the raveling resistance, tensile strength, and fracture resistance of OGFC mixtures since the Cantabro loss gradually decreased while the IDT strength and G_f results increased with an increase in the EDR range between 15% and 40%. The comparison in the Cantabro and IDT test results between the PMA and EMA mixtures was highly dependent on the EDR and mix aging condition. In general, the EMA mixtures at high EDRs (i.e., 30% and 40%) outperformed the PMA mixtures in the Cantabro and IDT tests, and the differences were more pronounced after long-term aging. According to the CAI results, the U-EMA mixtures were expected to have the best aging resistance, followed by the J-EMA mixtures and PMA mixtures, respectively. Finally, three criteria based on statistical comparisons of the Cantabro and IDT test results at various mix aging conditions were proposed for the selection of optimum EDR of EMA binders. The comparison results showed that EMA mixtures at 30% and 40% EDR had consistently better performance properties than the PMA mixtures and thus, have the potential of extending the life span of OGFC. Because of the high costs of epoxy materials, the EDR of 30% was selected as the final optimum (i.e., most cost-effective) EDR of EMA binders prepared with both the domestic source and foreign source epoxy materials. At this EDR, OGFC mixtures with an EMA binder were estimated to be approximately 3.5 to 5 times more expensive than those containing a PMA binder from the materials cost perspective.

CHAPTER 5. MIX DESIGN OF EMA OGFC MIXTURES

The aim of Experiment 3 was to determine an effective method to design OGFC mixtures containing EMA binders. This chapter presents the experimental plan, test results, and findings of the experiment. Currently, FDOT uses the pie plate method to select the OBC of FC-5 mixtures per FM 5-588. In this method, pie plate samples of OGFC mixtures containing a PG 67-22 binder at different binder contents are prepared and examined to visually assess the degree of bonding between the mixture and the bottom of the pie plate as well as asphalt draindown on the pie plate. Based on visual observation of the pie plates, the OBC is selected as the binder content of which the corresponding pie plate exhibits sufficient bonding without excessive asphalt draindown. In 2018/2019, FDOT added an additional step in the FC-5 mix design approval process, which requires the Cantabro testing, per AASHTO TP 108-14, of the OGFC mixture prepared with a PMA or HP binder at the OBC to evaluate its raveling resistance. The mix design will only be accepted if the PMA or HP mixture has a Cantabro loss of less than 20% when tested at the unaged condition (i.e., without additional long-term aging after compaction). This experiment sought to develop a similar mix design procedure for OGFC mixtures containing EMA binders.

5.1 Experimental Plan

5.1.1 *Materials and Mix Design*

Four FDOT approved FC-5 mix designs were evaluated, which corresponded to three granite (GRN1, GRN2, and GRN3) mixes and one limestone (LMS) mix. The JMF of these mix designs is summarized in Table 5-1. Two EMA binders prepared with two sources of epoxy materials at 30% EDR were included. Based on a partial factorial design, four combinations of mix design and EMA binder were evaluated with the proposed procedure of designing OGFC mixtures containing EMA binders. Table 5-2 presents the proposed testing matrix of Experiment 3.

Table 5-1. Job Mix Formula Summary of GRN1, GRN2, GRN3, and LMS Mixes

Mix Design ID		GRN1	GRN2	GRN3	LMS
Aggregate Gradation, Percent Passing	3/4"	100	100	100	100
	1/2"	99	95	95	94
	3/8"	71	75	69	74
	No. 4	24	23	24	23
	No. 8	9	10	10	10
	No. 16	5	6	4	8
	No. 30	4	4	3	6
	No. 50	3	3	3	5
	No. 100	3	3	3	4
	No. 200	2.5	2.1	3.0	3.3
Combined G _{sb}		2.769	2.625	2.633	2.417
JMF OBC, Percent		6.8	6.6	6.5	6.9
Additives		0.3% Cellulose Fiber, 1.0% Hydrated Lime	0.4% Mineral Fiber, 1.0% Hydrated Lime	0.3% Cellulose Fiber, 1.0% Hydrated Lime	0.3% Cellulose Fiber

Table 5-2. Testing Matrix of Experiment 3

Factor Name	Factor No.	Description
Binder Source and Epoxy Resin Source	2	Two combinations selected in Experiment 1
Epoxy Dosage Rate	1	Optimum EDR selected in Experiment 2
Mix Design	4	GRN1, GRN2, GRN3, LMS
Combination	4	GRN1 + U30C EMA binder GRN2 + J30Z EMA binder GRN3 + J30Z EMA binder LMS + U30C EMA binder

5.1.2 Proposed Mix Design Procedure for EMA OGFC Mixtures

The proposed mix design procedure for OGFC mixtures containing EMA binders is graphically illustrated in Figure 5-1. The procedure is similar to the current FDOT mix design procedure for OGFC mixtures with PMA or HP binders with additional pie plate testing of mixtures containing an EMA binder.

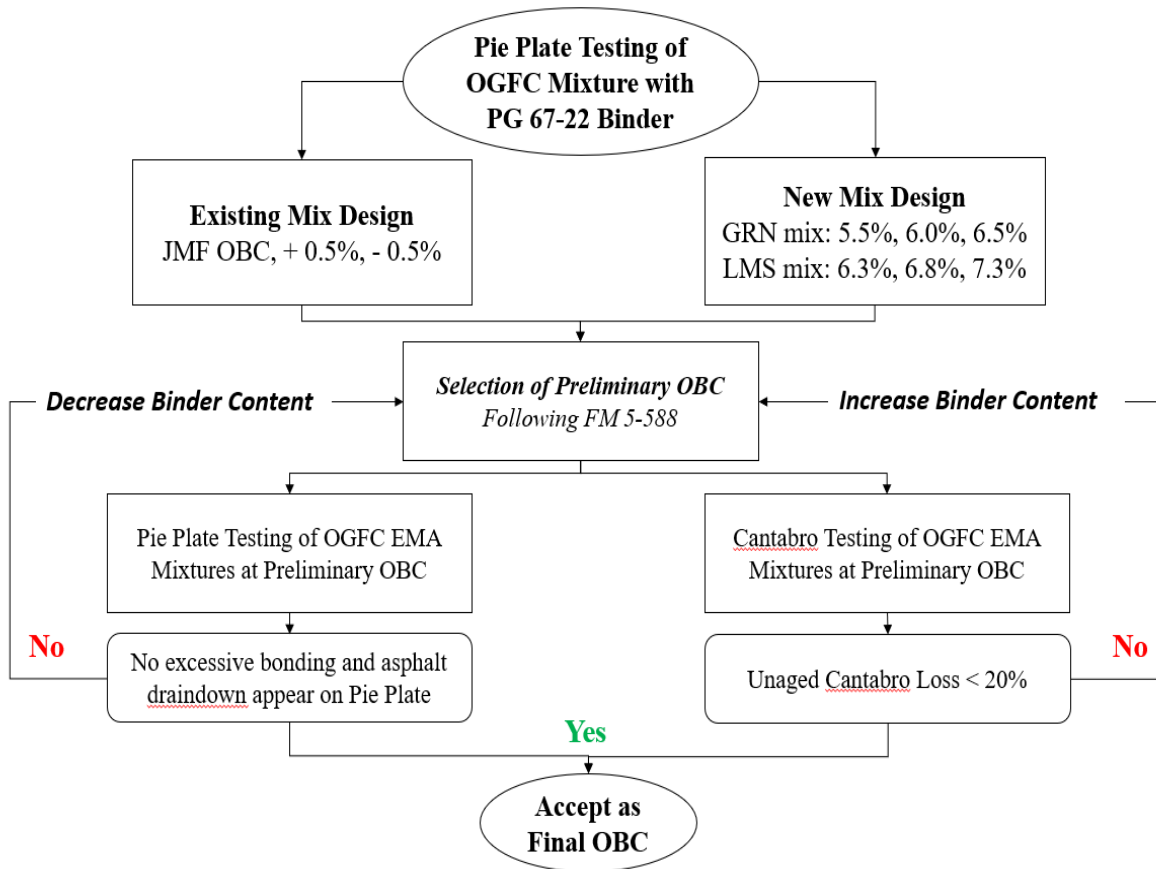


Figure 5-1. Proposed Mix Design Procedure for EMA OGFC Mixtures

The first step of the proposed procedure was the pie plate testing of OGFC mixtures prepared with a PG 67-22 unmodified binder at three binder contents, as shown in Figure 5-2. For existing mix designs, the three binder contents recommended were the JMF optimum binder content (OBC), JMF OBC plus 0.5%, and JMF OBC minus 0.5%. The FM 5-588 method suggests using 5.5%,

6.0%, and 6.5% for mixtures with granite aggregate, and 6.8%, 7.3%, and 7.8% for mixtures with limestone aggregate. For all the pie plates prepared, the asphalt draindown was visually assessed in comparison with the reference pie plate pictures in FM 5-588 (Figure 5-2). The preliminary OBC was selected as the binder content of which the corresponding pie plate displayed sufficient bonding between the mixture and the bottom of the pie plate without evidence of excessive asphalt draindown, as shown in Figure 5-2(b). After the preliminary OBC was selected, another pie plate was prepared for the OGFC mixture with an EMA binder (instead of a PG 67-22 unmodified binder) at the preliminary OBC using a modified pie plate test procedure. The pie plate was then examined to visually assess the degree of bonding between the mixture and the pie plate as well as asphalt draindown.

Furthermore, a set of unaged EMA OGFC mixture samples was prepared and tested with the Cantabro test to evaluate the raveling resistance. The preliminary OBC was accepted as the final OBC if the mixture did not exhibit bonding and asphalt draindown in the pie plate test and had a Cantabro loss of less than 20%. Otherwise, the preliminary OBC was needed to be adjusted, and the mixture retested until acceptable results were obtained in both pie plate and Cantabro tests.

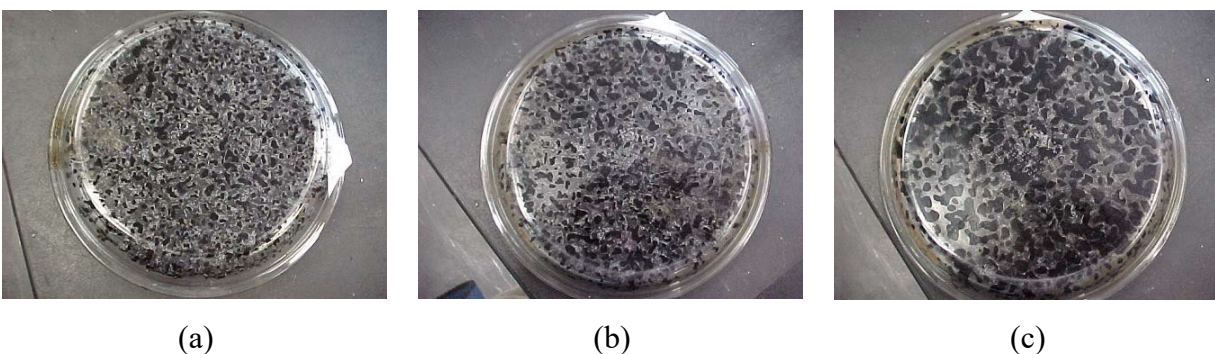


Figure 5-2. Reference Pie Plate Pictures of OGFC mixtures with PG 67-22 Unmodified Binder at Different Binder Contents: (a) 5.5%, (b) 6.0%, (c) 6.5% (FDOT, 2020)

5.1.3 Modified Pie Plate Test Procedure for OGFC Mixtures with EMA Binders

Several trial-and-error attempts were made to prepare pie plate samples for OGFC mixtures containing U30C and J30Z EMA binders following the test procedure in FM 5-588. The developed procedure depended highly on the binder type. The modifications performed are explained below. In general, the existing test procedure worked well for the J30Z EMA binder. Therefore, no major modifications to the pie plate test procedure were needed for the J30Z EMA binder except for revising Sections 5.5 and 5.6 to as follows:

- Heat aggregate batches for a minimum of two hours in an oven at $370 \pm 5^{\circ}\text{F}$ ($188 \pm 3^{\circ}\text{C}$) instead of $320 \pm 5^{\circ}\text{F}$ ($160 \pm 3^{\circ}\text{C}$). Further, heat the PG 67-22 base binder for two hours at $266 \pm 5^{\circ}\text{F}$ ($130 \pm 3^{\circ}\text{C}$). Heat the epoxy resin (Part A) and epoxy curing agent (Part B) for 1 hour at $140 \pm 5^{\circ}\text{F}$ ($60 \pm 3^{\circ}\text{C}$).
- Mix the epoxy resin (Part A) and epoxy curing agent (Part B) and blend for 2 minutes using a low shear mixer. Then add the PG 67-22 base binder and continue to blend with a low shear mixer for 15 minutes at $266 \pm 5^{\circ}\text{F}$ ($130 \pm 3^{\circ}\text{C}$). Add the preheated aggregate and J-EMA binder into the mixing bowl. Using the spatula, gently mix the aggregate batch and J-EMA binder in the mixing bowl at the following three prescribed asphalt binder contents (by weight of total mix): 5.5%, 6.0%, and 6.5% for granite aggregate or 6.8%, 7.3%, and 7.8% for limestone aggregate. Continue mixing until all of the aggregate particles are thoroughly coated, ensuring that there are no large conglomerates of fine particles. The final mixing temperature of the J30Z EMA mixture was around $160 \pm 3^{\circ}\text{C}$.

While in the case of the U30C EMA binder, the initial attempts using the existing pie plate test procedure were not successful because of its fast rate curing behavior after mixing the epoxy resin (Part A) with the curing agent in Part B of the epoxy materials. Using the recommended mixing

temperature (i.e., 160°C) and post-mixing conditioning temperature (i.e., one hour at 160°C) in FM 5-588, the U30C EMA mixture became thermoset in the pie plate. This made the visual assessment of the asphalt draindown and the degree of bonding between the mixture and the pie plate difficult. Therefore, to address this limitation, essential modifications were proposed to Sections 5.5, 5.6, and 5.7 of the pie plate test procedure in FM 5-588, which are described as follows:

- Heat aggregate batches for a minimum of two hours in an oven at a lower temperature of $290 \pm 5^\circ\text{F}$ ($143 \pm 3^\circ\text{C}$). Heat the PG 67-22 base binder and Part B of the epoxy materials for two hours at $266 \pm 5^\circ\text{F}$ ($130 \pm 3^\circ\text{C}$). Heat the epoxy resin (Part A) for 15 minutes at $266 \pm 5^\circ\text{F}$ ($130 \pm 3^\circ\text{C}$).
- Mix the PG 67-22 base binder and Part B of the epoxy materials and blend for 15 minutes using a low shear mixer. Then add the epoxy resin (Part A) and manually blend for 30 to 40 seconds using a stirring rod. Add the preheated aggregate and U-EMA binder into the mixing bowl. Using the spatula, gently mix the aggregate batch and U-EMA binder in the mixing bowl at the following three prescribed asphalt binder contents (by weight of total mix): 5.5%, 6.0%, and 6.5% for granite aggregate or 6.8%, 7.3%, and 7.8% for limestone aggregate. Continue mixing until all of the aggregate particles are thoroughly coated, ensuring that there are no large conglomerates of fine particles." The final mixing temperature of the U30C EMA mixture was around $121 \pm 3^\circ\text{C}$.
- Immediately after mixing, carefully transfer the mixture from the mixing bowl into a pie plate using a method that will evenly distribute the mixture over the entire bottom surface of the pie plate without causing segregation. Care should be taken to ensure that the mixture is not disturbed once it has contacted the pie plate. After placing the mixture in the pie plate,

place the pie plate on a level surface in an oven and heat for 40 minutes at $250 \pm 5^\circ\text{F}$ ($121 \pm 3^\circ\text{C}$). Repeat this step for each of the remaining samples. This modified post-mixing conditioning procedure was selected based on the viscosity curing data of the U30C binder provided by the epoxy asphalt manufacturer.

5.2 Test Results and Discussion

Following the proposed mix design procedure in Figure 5-1, for each mix design, pie plate samples were prepared for OGFC mixtures with a PG 67-22 unmodified binder at three binder contents (i.e., JMF OBC, JMF OBC+0.5%, and JMF OBC-0.5%). In this report, the pie plate pictures are presented in two ways. Initially, photos were taken with the loose mixture inside the pie plate per FM 5-588. Though this process allowed for visual assessment of the pie plate samples with different binder contents, the glare of the glass combined with the concentration of black-colored asphalt mixture made it challenging to differentiate the pie plate samples in the photos. Hence, after conditioning, the pie plate was rested on an insulating surface until the sample inside cooled. Once the system reached near room temperature, the pie plate was overturned. At this point, the loose mixture was not fully set but was hard enough to fall off the plate at once on overturning without sliding and creating smudge. If large-size aggregate particles were stuck to the plate, they were removed carefully by hand. Finally, another set of pictures were taken by placing the empty pie plate on a white background, which allowed for better discrimination of the pie plate samples based on visual observation of the pictures. However, the second set of pie plate pictures were used for documentation purposes only.

5.2.1 GRN1 Mix Design

Figure 5-3 and Figure 5-4 present the pie plate pictures of GRN1 mixtures containing a PG 67-22 binder with and without the loose mixture, respectively. As shown, the pie plate at the JMF OBC-0.5% (6.3%) had the least asphalt draindown and bonding between the mixture and the bottom of the pie plate, while that of the JMF OBC+0.5% (7.3%) had the most asphalt draindown. Compared with the reference pictures in FM 5-588 (Figure 5-2), the pie plate at the JMF OBC (6.8%) seemed to have more asphalt draindown than it should be at the OBC. Hence, in this case, the preliminary OBC would have been selected between the 6.3% and 6.8% based on visual observation of the pie plates. However, given this was an existing mix design provided by FDOT, it was decided to proceed with 6.8% as the preliminary OBC to evaluate the EMA mixture.

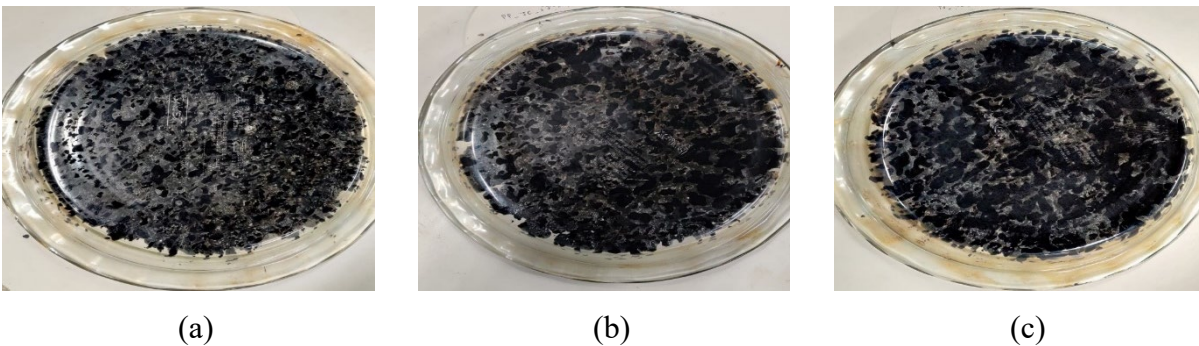


Figure 5-3. Pie Plate Pictures (with loose mixture) of GRN1 Mixtures with PG 67-22 Binder at: (a) JMF OBC-0.5% (6.3%), (b) JMF OBC (6.8%), (c) JMF OBC+0.5% (7.3%)

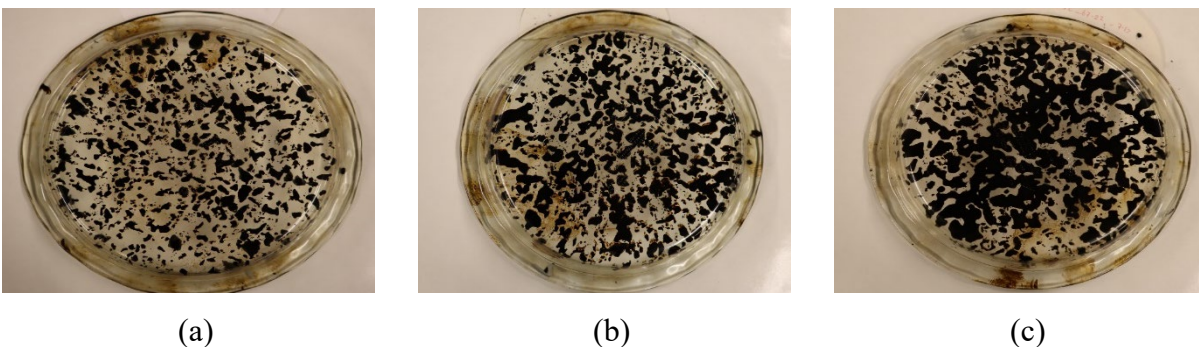


Figure 5-4. Pie Plate Pictures (without loose mixture) of GRN1 Mixtures with PG 67-22 Binder at: (a) JMF OBC-0.5% (6.3%), (b) JMF OBC (6.8%), (c) JMF OBC+0.5% (7.3%)

Figure 5-5 presents the pie plate pictures of the GRN1 mixture prepared with the U30C EMA binder at the preliminary OBC of 6.8%. Compared to the PG 67-22 binder at the same binder content (Figure 5-3(b)), the U30C EMA binder significantly reduced the amount of asphalt draindown in the pie plate. Based on visual observation, the degree of bonding and asphalt draindown in Figure 5-5(a) was similar to the reference picture at the OBC in FM 5-588 (Figure 5-2(b)). When tested at the unaged condition, the U30C EMA mixture had an average Cantabro loss of 17%, which met the proposed maximum 20% criterion. Therefore, the JMF OBC of 6.8% was accepted as the final OBC for the U30C EMA mixture.



Figure 5-5. Pie Plate Pictures of GRN1 Mixture with U30C EMA Binder at JMF OBC (6.8%): (a) with Loose Mixture, (b) without Loose Mixture

5.2.2 GRN2 Mix Design

The pie plate pictures with and without the loose mixture of GRN2 mixtures containing a PG 67-22 binder at different binder contents are presented in Figure 5-6 and Figure 5-7, respectively. The degree of bonding between the mixture and the pie plate and the asphalt draindown consistently increased as the binder content increased from 6.1% to 6.6% and then to 7.1%. As compared to the reference picture at the OBC in FM 5-588 (Figure 5-2(b)), the pie plate at the JMF OBC-0.5% (6.1%) seemed to have insufficient bonding and asphalt draindown while those at the JMF OBC (6.6%) and JMF OBC+0.5% (7.1%) exhibited excessive draindown. Therefore, based on Figure

5-6, the preliminary OBC would have been between 6.1% and 6.6% instead of 6.6%, as provided in the JMF.

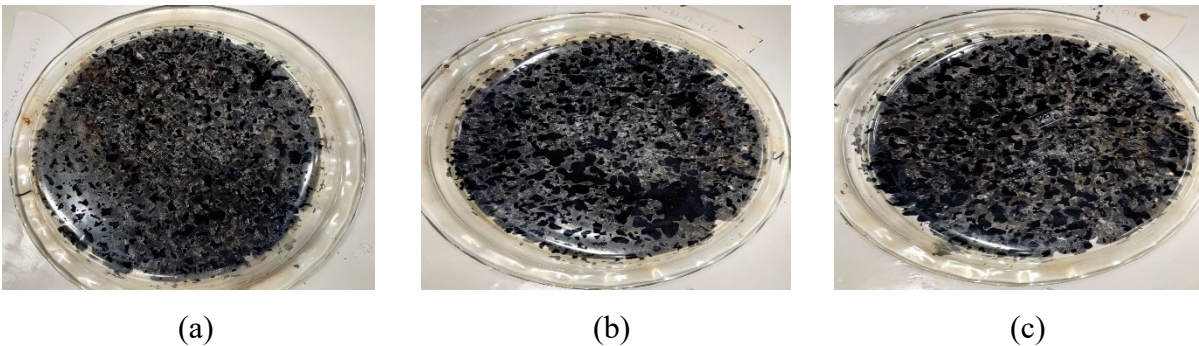


Figure 5-6. Pie Plate Pictures (with loose mixture) of GRN2 Mixtures with PG 67-22 Binder at: (a) JMF OBC-0.5% (6.1%), (b) JMF OBC (6.6%), (c) JMF OBC+0.5% (7.1%)

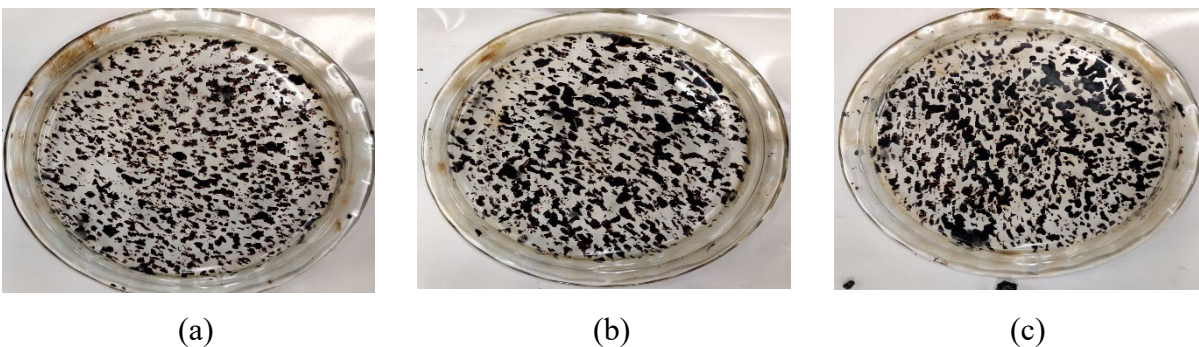


Figure 5-7. Pie Plate Pictures of GRN2 Mixtures with PG 67-22 Binder at: (a) JMF OBC-0.5% (6.1%), (b) JMF OBC (6.6%), (c) JMF OBC+0.5% (7.1%)

Figure 5-8 presents the pie plate pictures of the GRN2 mixture prepared with the J30Z EMA binder at the JMF OBC of 6.6%. The J30Z EMA binder reduced the amount of asphalt draindown in the pie plate compared to the PG 67-22 binder at the same binder content (Figure 5-6(b)). Based on visual observation, the degree of bonding and asphalt draindown in Figure 5-8(a) was similar to the reference picture at the OBC in FM 5-588 (Figure 5-2(b)). The J30Z EMA mixture had an average Cantabro loss of 17% at the unaged condition (less than 20%). Therefore, the JMF OBC of 6.6% was accepted as the final OBC for the J30Z EMA mixture.



Figure 5-8. Pie Plate Pictures of GRN2 Mixture with J30Z EMA Binder at JMF OBC (6.6%): (a) with Loose Mixture, (b) without Loose Mixture

5.2.3 GRN3 Mix Design

Figure 5-9 and Figure 5-10 present the pie plate pictures with and without the loose mixture, respectively, of GRN3 mixtures containing a PG 67-22 binder at different binder contents. The pie plates at the JMF OBC-0.5% (6.0%) and JMF OBC (6.5%) exhibited a similar degree of bonding and asphalt draindown as the reference picture at the OBC in FM 5-588 (Figure 5-2(b)), while that at the JMF OBC+0.5% (7.0%) showed excessive bonding and asphalt draindown. Upon visual observation of the pie plates in Figure 5-9, the preliminary OBC would have been selected as 6.5%, which matched the JMF OBC.

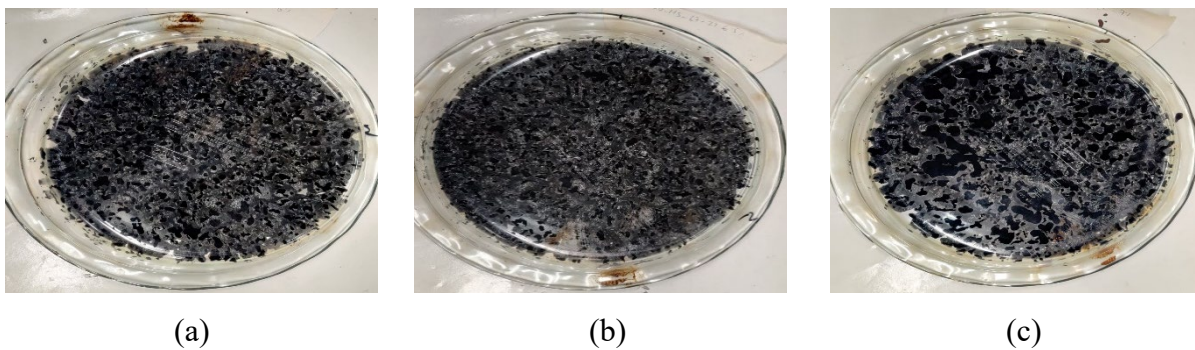


Figure 5-9. Pie Plate Pictures (with loose mixture) of GRN3 Mixtures with PG 67-22 Binder at: (a) JMF OBC-0.5% (6.0%), (b) JMF OBC (6.5%), (c) JMF OBC+0.5% (7.0%)

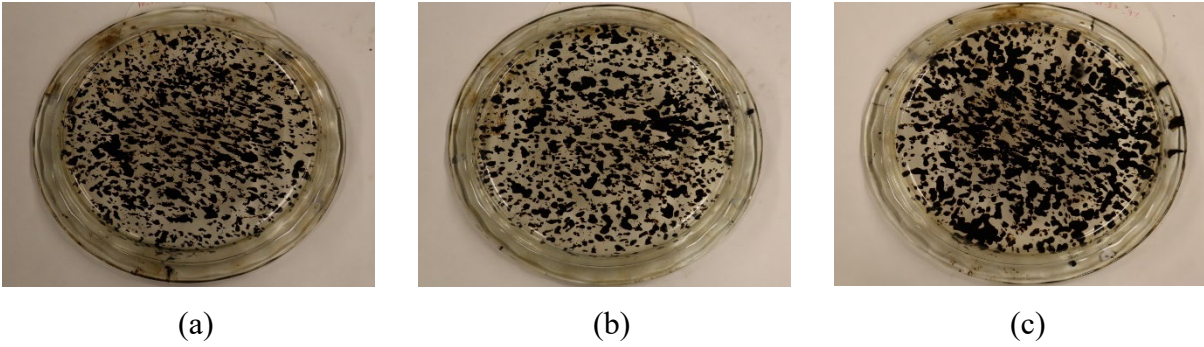


Figure 5-10. Pie Plate Pictures (without loose mixture) of GRN3 Mixtures with PG 67-22 Binder at: (a) JMF OBC-0.5% (6.0%), (b) JMF OBC (6.5%), (c) JMF OBC+0.5% (7.0%)

Figure 5-11 presents the pie plate pictures of the GRN3 mixture prepared with the J30Z EMA binder at the JMF OBC of 6.5%. The J30Z EMA binder showed a reduced degree of asphalt draindown in the pie plate than the PG 67-22 binder at the same binder content (Figure 5-9(b)).

According to visual observation, the degree of bonding and asphalt draindown in Figure 5-11(a) was less than the reference picture at the OBC in FM 5-588 (Figure 5-2(b)). When tested at the unaged condition, the J30Z EMA mixture had an average Cantabro loss of 11%, which met the proposed criterion of a maximum of 20%. Therefore, the JMF OBC of 6.5% was accepted as the final OBC for the J30Z EMA mixture.



Figure 5-11. Pie Plate Pictures of GRN3 Mixture with J30Z EMA Binder at JMF OBC (6.5%): (a) with Loose Mixture, (b) without Loose Mixture

5.2.4 LMS Mix Design

Figure 5-12 and Figure 5-13 present the pie plate pictures with and without the loose mixture, respectively, of LMS mixtures containing a PG 67-22 binder. Based on visual observation, the pie plate at the JMF OBC-0.5% (6.4%) had insufficient bonding, and that at the JMF OBC+0.5% (7.4%) showed excessive asphalt draindown. No considerable difference was observed between the pie plates at 6.4% and 6.9%. As compared to the reference pie plate picture at the OBC in Figure 5-2(b), the mixture prepared at 6.9% exhibited a slightly lower degree of asphalt draindown. Therefore, the preliminary OBC would have been selected between the 6.9% and 7.4% based on the pie plates in Figure 5-12. However, the JMF OBC of 6.9% was used to evaluate the EMA mixture further using the pie plate and Cantabro tests for the same reasons mentioned previously.

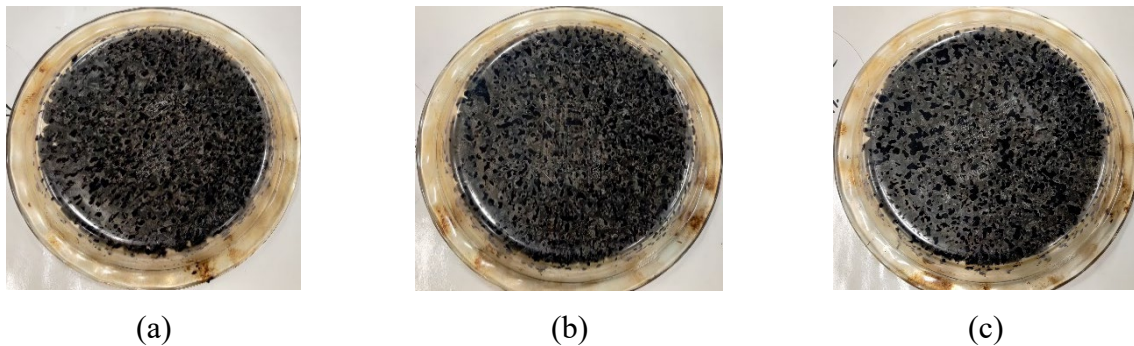


Figure 5-12. Pie Plate Pictures (with loose mixture) of LMS Mixtures with PG 67-22 Binder at: (a) JMF OBC-0.5% (6.4%), (b) JMF OBC (6.9%), (c) JMF OBC+0.5% (7.4%)

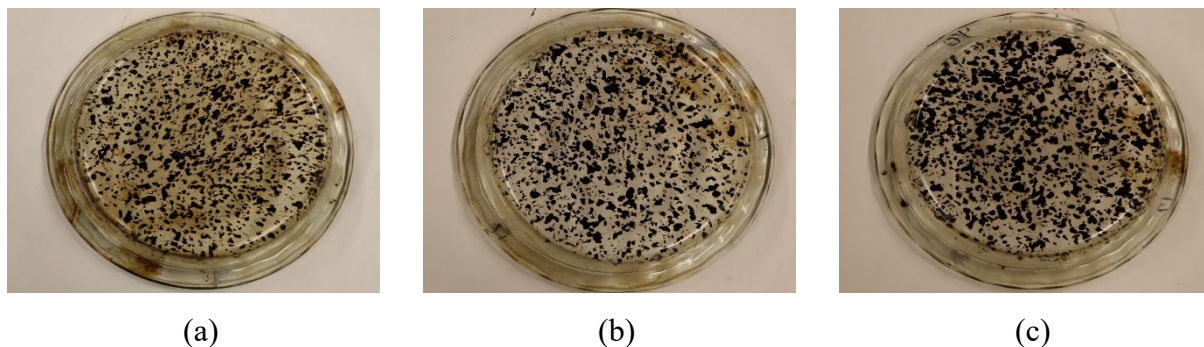


Figure 5-13. Pie Plate Pictures (without loose mixture) of LMS Mixtures with PG 67-22 Binder at: (a) JMF OBC-0.5% (6.4%), (b) JMF OBC (6.9%), (c) JMF OBC+0.5% (7.4%)

Figure 5-14 presents the pie plate pictures of the LMS mixture prepared with the U30C EMA binder at the JMF OBC of 6.9%. As compared to the PG 67-22 binder at the same binder content (Figure 5-12(b)), the U30C EMA binder yielded a significantly lower amount of asphalt draindown in the pie plate. Furthermore, the degree of bonding and asphalt draindown in Figure 5-14(a) was less than that of the reference pie plate picture at the OBC in FM 5-588 (Figure 5-2(b)). Finally, the U30C EMA mixture had an average Cantabro loss of 11% when tested at the unaged condition, which met the proposed criterion of a maximum of 20%. Therefore, the JMF OBC of 6.9% was accepted as the final OBC for the U30C EMA mixture.



Figure 5-14. Pie Plate Pictures of LMS Mixture with U30C EMA Binder at JMF OBC (6.9%): (a) with Loose Mixture, (b) without Loose Mixture

5.3 Summary of Findings

For the four FC-5 mix designs evaluated in this experiment, OGFC mixtures prepared with U30C and J30Z EMA binders at the JMF OBC had less asphalt draindown in the pie plate test than those containing the PG 67-22 unmodified binder. This trend was consistent with FDOT's experience with the pie plate testing of OGFC mixtures with PMA and HP binders. All the EMA mixtures at their corresponding JMF OBC had an average Cantabro loss of less than 20% at the unaged condition, which indicated adequate raveling resistance before long-term aging. In summary, the proposed mix design procedure for OGFC mixtures containing EMA binders was successfully

validated with four FDOT approved mix designs. The modified pie plate and Cantabro test results in this experiment indicate that the proposed procedure has the potential of designing EMA OGFC mixtures with minimal asphalt draindown during production and adequate raveling resistance before aging.

CHAPTER 6. PERFORMANCE CHARACTERIZATION OF EMA OGFC MIXTURES

Experiment 4 was conducted to characterize the performance properties of OGFC mixtures with EMA, PMA, and HP binders. The experimental plan, results, and findings of the tests adopted are presented in this chapter. Four FDOT approved FC-5 mix designs were included, which corresponded to three sources of granite aggregates and one source of limestone aggregate. Four sets of OGFC mixtures for each mix design were prepared with two EMA binders, one PMA binder, and one HP binder. The Cantabro, IDT, TSR, and HWTT tests were used to characterize the raveling resistance, tensile strength, fracture resistance, moisture susceptibility, and rutting resistance of OGFC mixtures containing different types of asphalt binders. Specifically, this experiment sought to determine if the use of EMA binders at the optimum EDR (determined in Experiment 3) would yield OGFC mixtures with better performance properties than those containing a PMA or HP binder, and thus, have the potential of increasing the current life span of OGFC mixtures in Florida.

6.1 Experimental Plan

6.1.1 Materials and Mix Design

This experiment used the same four FC-5 mixes (i.e., GRN1, GRN2, GRN3, and LMS) designed in Experiment 3. For each mix design, four sets of OGFC mixtures were prepared, which corresponded to two EMA binders at the 30% EDR (i.e., J30Z and U30C binders), one PMA binder, and one HP binder. The same procedure used to prepare EMA binders and mixtures in Experiment 2 was followed.

6.1.2 Laboratory Testing

6.1.2.1 Cantabro Test

The Cantabro test was performed following AASHTO TP 108-14 on OGFC mixtures subjected to two mix aging conditions: STA and LTA2 (i.e., aging compacted samples for 20 days at 85°C prior to testing). The Cantabro loss was used to evaluate the raveling resistance of OGFC mixtures before and after extended long-term aging.

6.1.2.2 Indirect Tensile Test

The test procedure of the IDEAL-CT test per ASTM D8225-19 was used for the IDT test in this experiment. Data analysis of the IDT test results was based on the tensile strength and G_f parameters. As with the Cantabro test, the IDT test was conducted after two mix aging conditions (STA and LTA2) to consider the impact of asphalt aging on the tensile strength and fracture resistance of OGFC mixtures prepared with different asphalt binders.

6.1.2.3 Tensile Strength Ratio Test

The TSR test was performed in accordance with AASHTO T 283, with a few modifications made to accommodate OGFC mixtures. These modifications include: 1) samples were compacted to N_{design} , 2) moisture conditioned samples were saturated at 26 inches Hg below atmospheric pressure for 10 minutes regardless of the level of saturation, and 3) moisture conditioned samples were kept submerged in water during the freeze conditioning cycle. Both the unconditioned and moisture conditioned samples were tested to determine their IDT strengths using a Marshall Stability press with a loading rate of 2 inches per minute. TSR was calculated as the average wet (i.e., moisture conditioned) strength ratio over the average dry (i.e., unconditioned) strength. A higher TSR value is desired for OGFC mixtures with better moisture resistance.

6.1.2.4 Hamburg Wheel Tracking Test

The HWTT test was used to evaluate the moisture susceptibility and rutting resistance of OGFC mixtures containing different types of asphalt binders and aggregates. The test was performed per AASHTO T 324. During the test, four cylindrical samples were placed in a water bath at 50°C and subjected to running steel wheel load at a speed of 52 passes per minute. The HWTT samples were prepared by compacting a large SGC sample at N_{design} with a final height of approximately 115 mm, then cut into two halves of approximately 50 mm each. A 12 mm thick plastic plate was placed at the bottom of the HWTT mold to align the surface of the sample with the surface of the mold for testing. Rut depths were recorded at various positions along the samples with each wheel pass. Typical HWT test parameters include SIP and rut depth at a critical number of wheel passes (e.g., 10,000 and 20,000 passes).

6.2 Test Results and Discussion

6.2.1 Cantabro Loss Results

Table 6-1 summarizes the Cantabro loss results of sixteen OGFC mixtures corresponding to a combination of four FDOT approved FC-5 mix designs and four types of asphalt binders. In addition, the CAI results were calculated for the LTA2 protocol. According to the CAI results, the U30C mixtures seemed to have the best aging resistance, followed by the J30Z mixtures and then the HP and PMA mixtures. Overall, the HP mixtures had lower Cantabro loss results and, thus, were expected to have better raveling resistance than the PMA and EMA mixtures at both the STA and LTA2 conditions. The PMA mixture performed similarly or better than the EMA mixtures in the Cantabro test at the STA condition. However, upon extended long-term aging, the PMA mixtures showed significantly higher Cantabro loss results than the EMA mixtures, indicating increased susceptibility to raveling. In most cases, the two EMA mixtures had similar Cantabro

loss results as the HP mixtures at the LTA2 condition, which indicated comparable raveling resistance after extended long-term aging. Considering the impact of asphalt aging on mix embrittlement, the Cantabro test results obtained after long-term aging were believed to provide more meaningful evaluation for the long-term raveling resistance and durability of OGFC mixtures than those at the short-term aging (or unaged) condition. Detailed discussions of the Cantabro loss results for each mix design are provided as follows.

Table 6-1. Summary of Cantabro Loss and Cantabro Aging Index (CAI) Results

Mix Design ID	Binder Type	Cantabro Loss (%)						CAI
		STA			LTA2			
		Avg.	Std Dev.	COV	Avg.	Std Dev.	COV	
GRN1	PMA	7.7	0.5	6.8%	31.4	9.9	31.4%	307%
	HP	3.3	1.2	36.7%	11.2	4.0	35.6%	238%
	J30Z	14.7	2.5	17.3%	13.6	3.0	21.9%	-7%
	U30C	17.3	3.4	19.8%	13.1	2.7	20.9%	-24%
GRN2	PMA	21.7	5.0	23.1%	43.1	1.5	3.4%	84%
	HP	2.6	0.9	36.4%	12.3	2.1	16.8%	85%
	J30Z	16.6	3.0	18.4%	21.6	0.6	2.7%	72%
	U30C	26.1	1.6	6.2%	29.9	0.8	2.7%	-7%
GRN3	PMA	12.9	0.7	5.6%	26.8	1.9	7.2%	98%
	HP	6.2	1.7	27.6%	11.5	2.2	19.4%	376%
	J30Z	11.0	1.6	14.9%	13.9	0.6	4.6%	30%
	U30C	12.5	3.3	26.0%	10.8	1.4	12.5%	15%
LMS	PMA	10.8	1.5	14.0%	19.9	3.9	19.6%	108%
	HP	3.6	0.3	7.7%	6.8	0.2	3.3%	84%
	J30Z	7.0	1.3	18.2%	12.0	0.7	6.0%	26%
	U30C	11.3	1.5	13.2%	10.5	0.2	1.7%	-14%

The average Cantabro loss and Tukey's rankings of OGFC mixtures prepared with the GRN1 mix design are presented in Figure 6-1. All the mixtures met FDOT's current mix design requirement at the STA condition with an average Cantabro loss of less than 20%. Comparatively, the HP mixture had the lowest average Cantabro loss and thus, was expected to have the best raveling resistance, followed by the PMA mixture and the two EMA mixtures. However, the difference between the HP and PMA mixtures was not statistically significant according to Tukey's rankings. At the LTA2 condition, the HP and EMA mixtures had similar Cantabro loss results, significantly lower than that of the PMA mixture. This indicated that the PMA mixture was more susceptible to raveling after extended long-term aging than both the HP and EMA mixtures.

Furthermore, the Cantabro loss of the PMA and HP mixtures increased significantly after the extended long-term aging for 20 days at 85°C, which indicated that the two mixtures became more susceptible to raveling because of asphalt aging and probably mix embrittlement. On the other hand, the two EMA mixtures had similar or slightly reduced Cantabro loss results at the LTA2 condition compared to the STA condition, which highlighted the superior aging resistance of the EMA binders. As discussed previously in Chapter 4, the changes in the Cantabro test results of EMA mixtures before and after aging were due to the combined effects of aging and curing of the EMA binder. A remaining question that warrants further investigation was how the LTA2 condition correlates to the field aging of OGFC mixtures in Florida. If the LTA2 condition was representative of medium-term field aging (e.g., 4 to 6 years of aging), then the EMA mixtures have the potential of providing better raveling resistance after longer-term aging because of their superior resistance to oxidative aging, which could possibly extend the current life span of OGFC mixtures in Florida. However, if the LTA2 condition simulates long-term field aging (e.g., over

10 to 12 years of aging), the EMA and HP mixtures were likely to have similar raveling resistance throughout their service lives.

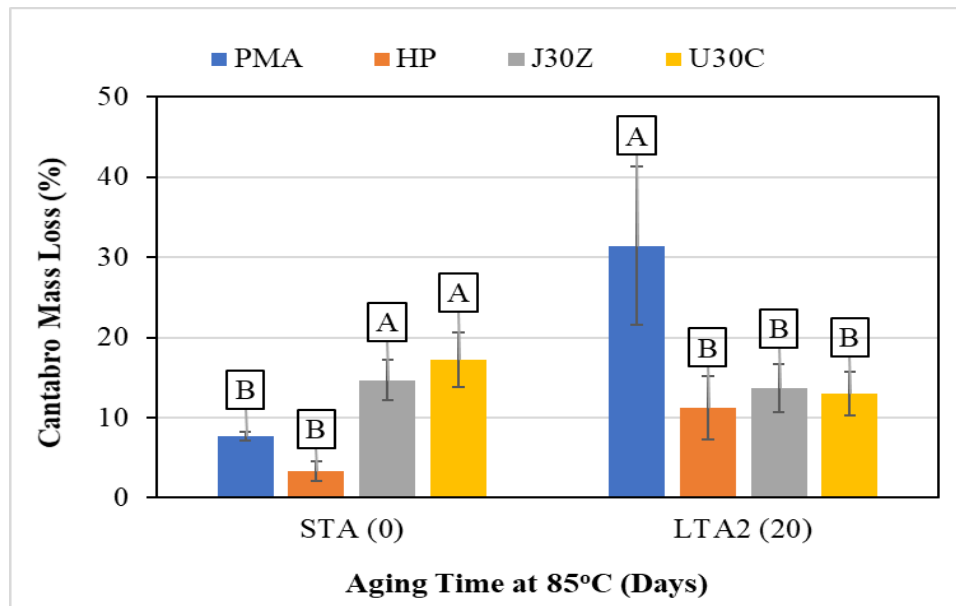


Figure 6-1. Cantabro Mass Loss of GRN1 Mixtures with Different Asphalt Binders at Two Mix Aging Conditions

Figure 6-2 shows the Cantabro loss results of the GRN2 mixtures containing different asphalt binders. Tukey's rankings of these mixtures at each mix aging condition are also given in Figure 6-2. At both conditions, the HP mixture had significantly lower average Cantabro loss results than the other three mixtures. Therefore, it was expected to have better raveling resistance before and after extended long-term aging. At the STA condition, the PMA and U30C mixtures had an average Cantabro loss of over 20%, which failed FDOT's current mix design requirement for FC-five mixtures. Upon extended long-term aging, the PMA mixture had a significantly higher Cantabro loss than the two EMA mixtures and thus, was expected to be more susceptible to raveling. At both aging conditions, the J30Z mixture outperformed the U30C mixture with lower Cantabro loss results.

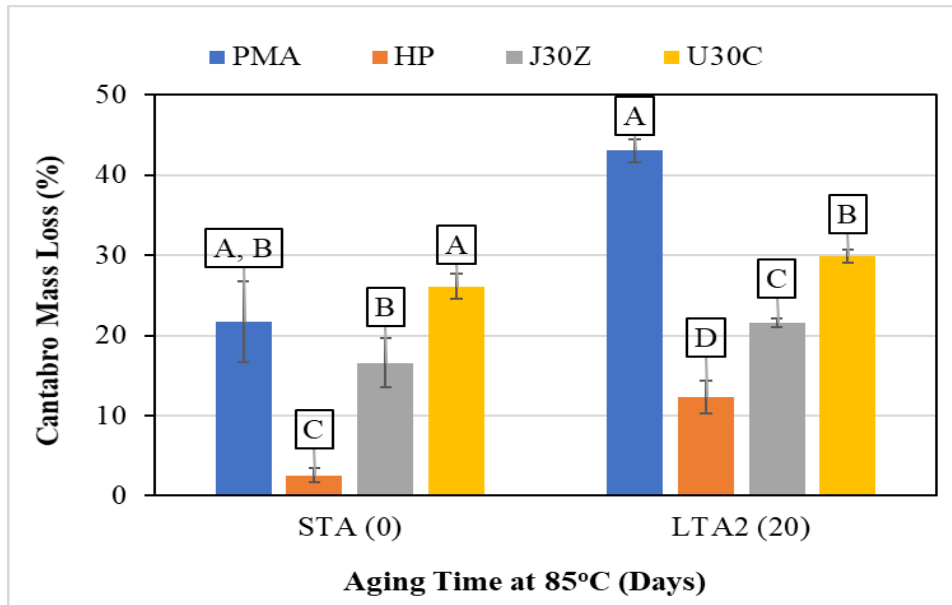


Figure 6-2. Cantabro Mass Loss of GRN2 Mixtures with Different Asphalt Binders at Two Mix Aging Conditions

Figure 6-3 shows the Cantabro loss results and Tukey's rankings of OGFC mixtures prepared with the GRN3 mix design at two mix aging conditions. Even for the GRN3 mixtures, the average Cantabro loss was less than 20% at the STA condition. The HP mixture had a significantly lower Cantabro loss and, thus, was expected to have better raveling resistance than the other three mixtures. However, the difference between the HP and J30Z mixtures was not statistically significant, according to Tukey's rankings. After the LTA2 conditioning, the PMA mixture had an average Cantabro loss of 26.8%, almost twice the other three mixtures. These results indicated that the PMA mixture was significantly more susceptible to raveling than the HP and PMA mixtures after extended long-term aging for 20 days at 85°C. Unlike the PMA and HP mixtures, the two EMA mixtures had similar Cantabro loss results at the STA and LTA2 conditions, indicating a potential superior aging resistance.

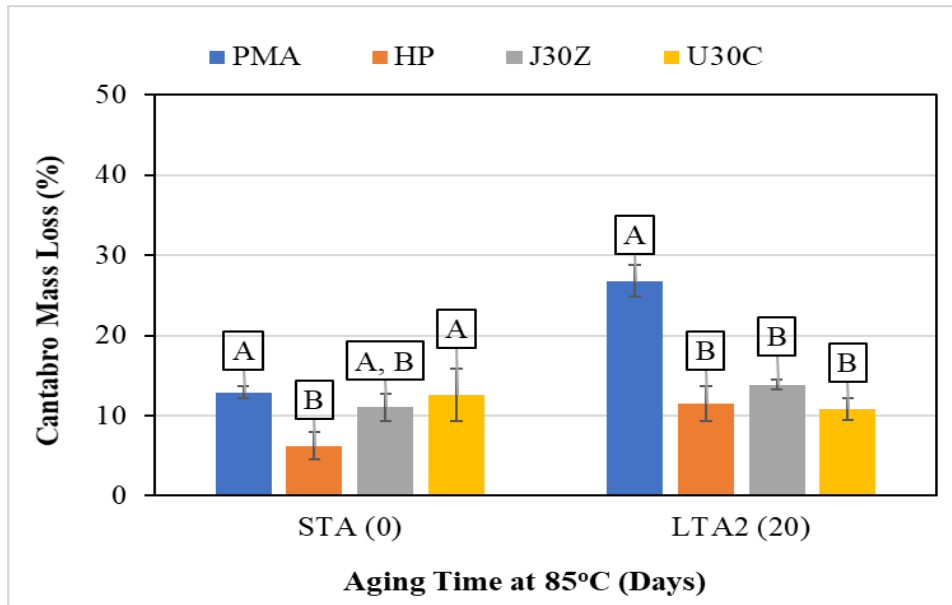


Figure 6-3. Cantabro Mass Loss of GRN3 Mixtures with Different Asphalt Binders at Two Mix Aging Conditions

The Cantabro loss results and Tukey's rankings of the LMS mixtures containing different types of asphalt binders are shown in Figure 6-4. At the STA condition, all the mixtures had an average Cantabro loss of less than 20% and thus, passed the FDOT's current mix design requirement for FC-5 mixtures. Comparatively, the HP mixture had the lowest average Cantabro loss, followed by the J30Z mixture and then the PMA and U30C mixtures. Upon extended long-term aging for 20 days at 85°C, the PMA mixture had a more substantial increase in the Cantabro loss than the other three mixtures. As a result, the PMA mixture had a significantly higher Cantabro loss and, thus, was expected to be more susceptible to raveling than the two EMA mixtures, while the HP mixture remained the best performer with the lowest Cantabro loss at the LTA2 condition.

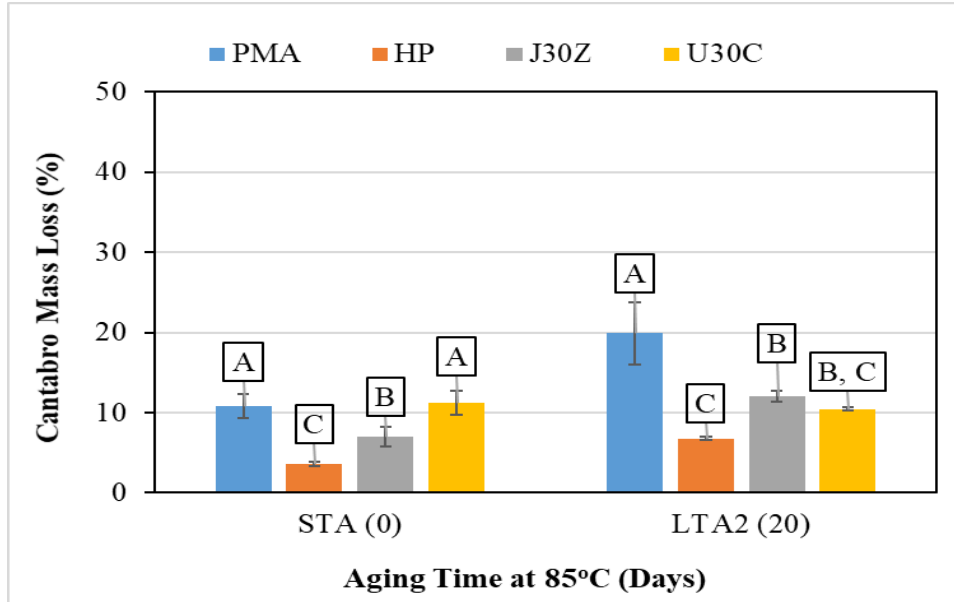


Figure 6-4. Cantabro Mass Loss of LMS Mixtures with Different Asphalt Binders at Two Mix Aging Conditions

6.2.2 IDT Strength Results

Table 6-2 summarizes the IDT strength results of the sixteen OGFC mixtures at two mix aging conditions. Overall, most EMA mixtures had higher IDT strength than the PMA and HP mixtures before and after extended long-term aging. There were two exceptions where the U30C mixtures had lower IDT strength than the other three mixtures at the STA condition when the EMA binder was still at the early stage of its curing process to gain strength. Detailed discussions of the IDT strength results for each mix design are provided as follows.

Table 6-2. Summary of IDT Strength Results

Mix Design ID	Binder Type	IDT Strength (psi)					
		STA			LTA2		
		Avg.	Std Dev.	COV	Avg.	Std Dev.	COV
GRN1	PMA	48.3	7.2	15.0%	71.7	4.2	5.8%
	HP	39.0	1.2	3.0%	57.9	2.7	4.7%
	J30Z	63.0	33.0	52.4%	105.5	9.3	8.8%
	U30C	69.9	3.9	5.6%	166.2	13.4	8.1%
GRN2	PMA	51.0	1.3	2.5%	55.8	7.4	13.3%
	HP	31.8	2.6	8.0%	47.9	3.8	8.0%
	J30Z	81.6	9.0	11.1%	90.6	6.7	7.4%
	U30C	22.4	2.9	12.8%	121.9	14.8	12.1%
GRN3	PMA	56.1	2.9	5.1%	77.0	1.7	2.2%
	HP	49.1	3.4	7.0%	64.8	3.6	5.5%
	J30Z	84.7	3.7	4.4%	117.3	5.8	5.0%
	U30C	33.7	3.4	10.0%	187.8	20.5	10.9%
LMS	PMA	81.7	2.7	3.3%	106.9	7.2	6.7%
	HP	54.1	2.8	5.3%	83.5	4.1	4.9%
	J30Z	154.4	9.2	6.0%	146.1	13.7	9.4%
	U30C	107.3	18.7	17.4%	212.7	16.5	7.8%

Figure 6-5 presents the IDT strength results of the GRN1 mixtures containing four types of asphalt binders. The U30C mixture had the highest average IDT strength at both aging conditions, followed by the J30Z, PMA, and HP mixtures, respectively. The difference among these mixtures was more pronounced at the LTA2 condition than at the STA condition. According to Tukey's rankings in Figure 6-5, only the HP and U30C mixtures had statistically different IDT strength at the STA condition upon considering the variability of the test results. At the LTA2 condition, all the differences in the IDT strength results among the four mixtures were statistically significant.

The increase in the IDT strength of the PMA and HP mixtures from the STA to LTA2 condition was because of asphalt aging. However, this increase was due to the combined effects of curing and aging of binders for the EMA mixtures. Comparatively, the U30C mixture experienced a greater extent of post-compaction curing than the J30Z mixture.

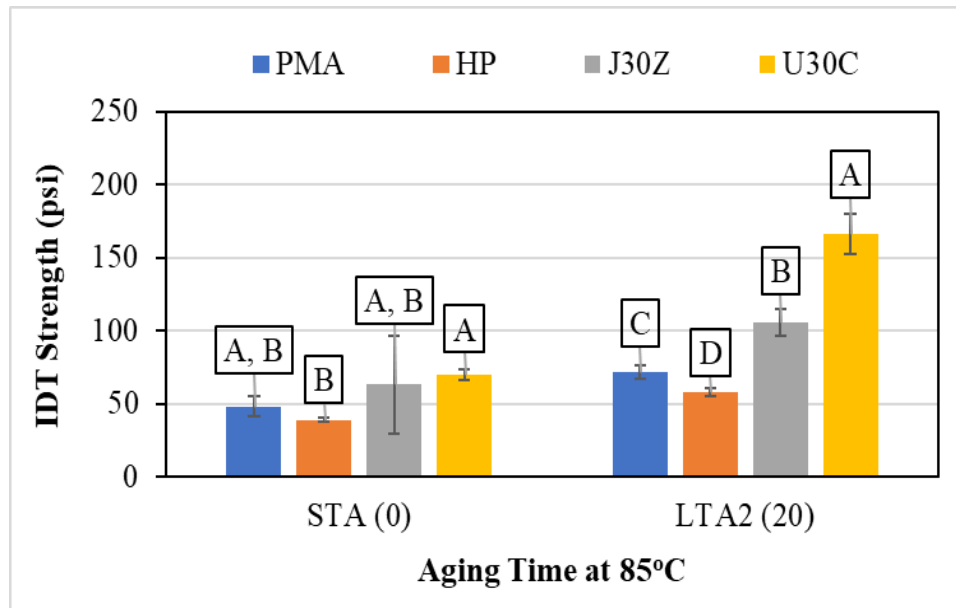


Figure 6-5. IDT Strength of GRN1 Mixtures with Different Asphalt Binders at Two Mix Aging Conditions

Figure 6-6 shows the IDT strength results and Tukey's rankings of OGFC mixtures prepared with the GRN2 mix design at two mix aging conditions. Overall, the J30Z mixture had the highest IDT strength at the STA condition, followed by the PMA, HP, and U30C mixtures, respectively. All the differences in the IDT strength results among these mixtures were statistically significant. Upon extended long-term aging for 20 days at 85°C, the IDT strength of the U30C mixture increased by approximately five times (i.e., from 22 psi to 122 psi), while those of the other three mixtures increased by only 10% to 50%. This substantial increase in the IDT strength of the U30C mixture was due to the combined effects of aging and the continued curing of the EMA binder. At

the LTA2 condition, the U30C mixture had the highest IDT strength, followed by the J30Z mixture and then the PMA and HP mixtures.

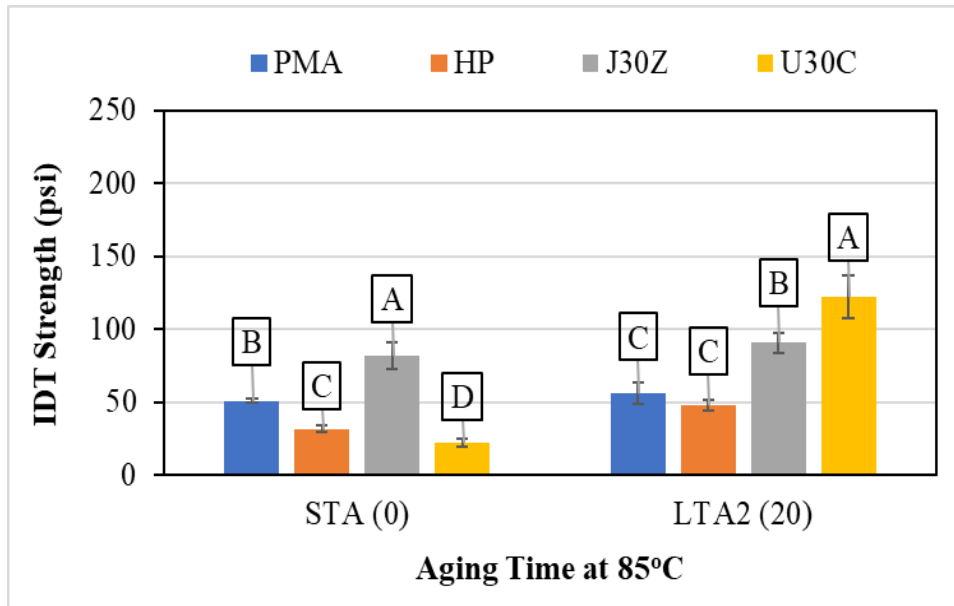


Figure 6-6. IDT Strength of GRN2 Mixtures with Different Asphalt Binders at Two Mix Aging Conditions

IDT strength results and Tukey's rankings of OGFC mixtures prepared with the GRN3 mix design are presented in Figure 6-7. The results showed a consistent trend as those of the GRN2 mixtures in Figure 6-6. The J30Z mixture had the highest IDT strength at the STA condition, followed by the PMA, HP, and U30C mixtures, respectively. Because of the continued curing of the EMA binder, the U30C mixture exhibited the highest IDT strength, followed by the J30Z mixture and then the PMA and HP mixtures at the LTA2 condition.

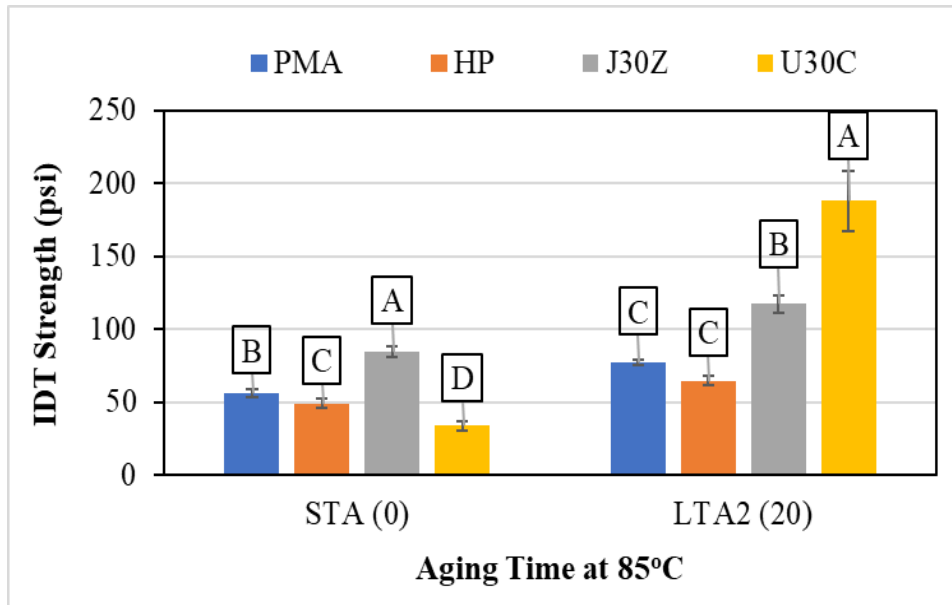


Figure 6-7. IDT Strength of GRN3 Mixtures with Different Asphalt Binders at Two Mix Aging Conditions

The IDT strength results of the LMS mixtures containing different types of asphalt binders are plotted in Figure 6-8. Tukey's rankings of these mixtures at each mix aging condition are also given in Figure 6-8. The two EMA mixtures showed statistically higher IDT strength than the PMA and HP mixtures at both aging conditions. The IDT strength of the J30Z mixture was higher than the U30C mixture in the STA condition, whereas the opposite tendency was observed in the LTA2 condition. These results indicated that the U30C mixture was significantly more susceptible to post-compaction curing for gaining strength than the J30Z mixture, which was consistent with the results of OGFC mixtures prepared with the other three FC-5 mix designs.

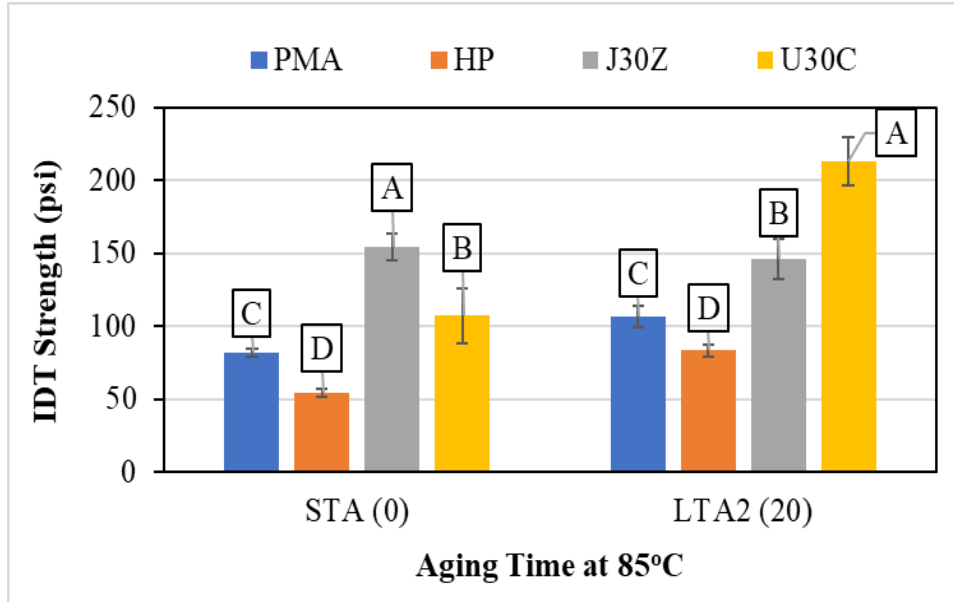


Figure 6-8. IDT Strength of LMS Mixtures with Different Asphalt Binders at Two Mix Aging Conditions

6.2.3 IDT Fracture Energy (G_f) Results

Table 6-3 summarizes the IDT G_f results of sixteen OGFC mixtures corresponding to a combination of four FC-5 mix designs and four asphalt binders. Overall, the J30Z mixture had a higher G_f than the other three mixtures at the STA condition. However, after extended long-term aging, the U30C mixture consistently showed the highest G_f . Thus, it was expected to have the best fracture resistance, followed by the J30Z mixture and then the PMA and HP mixtures for all the mix designs. Detailed discussions of the IDT G_f results for each mix design are provided in the following sections.

Table 6-3. Summary of IDT G_f Results

Mix Design ID	Binder Type	IDT G_f (J/m ²)					
		STA			LTA2		
		Avg.	Std Dev.	COV	Avg.	Std Dev.	COV
GRN1	PMA	6,535	591	9.0%	7,995	1,293	16.2%
	HP	6,792	644	9.5%	7,739	969	12.5%
	J30Z	4,670	3,466	74.2%	10,116	1,498	14.8%
	U30C	8,643	1,355	15.7%	19,065	3,944	20.7%
GRN2	PMA	6,819	256	3.7%	7,324	1,224	16.7%
	HP	5,660	424	7.5%	6,973	404	5.8%
	J30Z	7,511	1,185	15.8%	7,715	747	9.7%
	U30C	3,388	214	6.3%	12,861	2,302	17.9%
GRN3	PMA	6,795	473	7.0%	6,962	367	5.3%
	HP	6,764	422	6.2%	7,344	547	7.4%
	J30Z	8,387	531	6.3%	9,459	2,385	25.2%
	U30C	3,890	615	15.8%	12,318	1,995	16.2%
LMS	PMA	8,669	360	4.2%	7,664	543	7.1%
	HP	7,093	720	10.1%	8,979	1,498	16.7%
	J30Z	14,791	1,523	10.3%	10,744	1,280	11.9%
	U30C	8,972	969	10.8%	14,461	2,371	16.4%

Figure 6-9 presents the IDT G_f results and Tukey's rankings of OGFC mixtures prepared with the GRN1 mix design. Comparable G_f results were observed for the four mixtures at the STA condition. According to Tukey's statistical summary in Figure 6-9, only the difference between the two EMA mixtures was statistically significant, while the rest was not. However, the J30Z mixture had considerably higher variability in the IDT G_f results than the other three mixtures, making the statistical comparisons inconclusive. Upon extended long-term aging for 20 days at 85°C, the U30C mixture had significantly higher IDT G_f results and thus better fracture resistance than the

other three mixtures. The considerable improvement in IDT G_f results of the U30C mixture was due to the combined effects of aging and continued curing of the EMA binder.

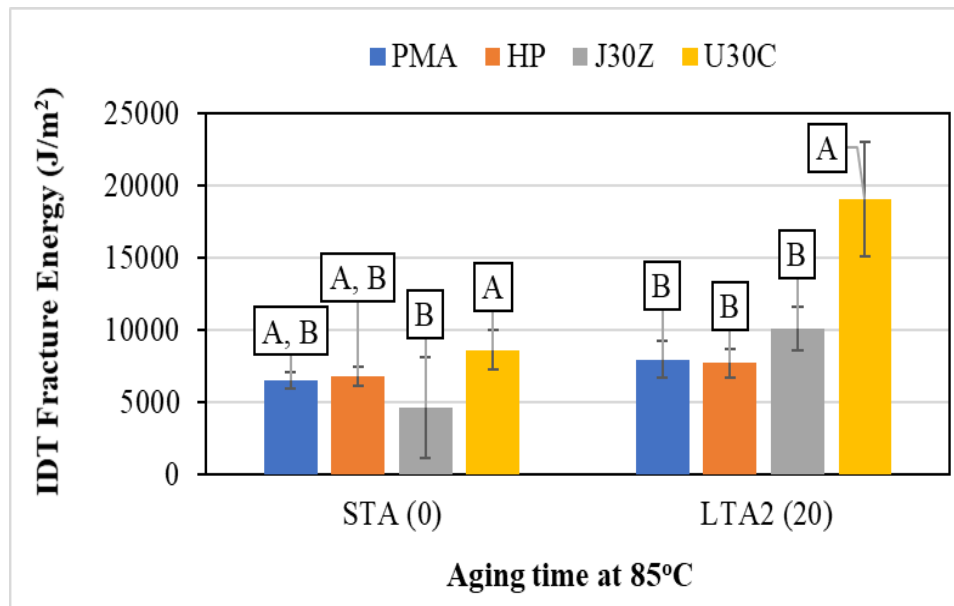


Figure 6-9. IDT G_f Results of GRN1 Mixtures with Different Asphalt Binders at Two Mix Aging Conditions

Figure 6-10 shows the IDT G_f results and Tukey's rankings of the GRN2 mixtures containing different types of asphalt binders at each mix aging condition. At the STA condition, the J30Z and PMA mixtures had similar G_f results, which were statistically higher than those of the HP and U30C mixtures. At the LTA2 condition, the U30C mixture had significantly higher G_f and, thus, better fracture resistance than the other three mixtures. Consistent with the results of the GRN1 mixtures in Figure 6-9, the G_f value of the U30C mixture increased substantially upon extended long-term aging primarily due to the continued curing of the EMA binder. In contrast, the PMA, HP, and J30Z mixtures exhibited similar G_f results at the STA and LTA2 conditions.

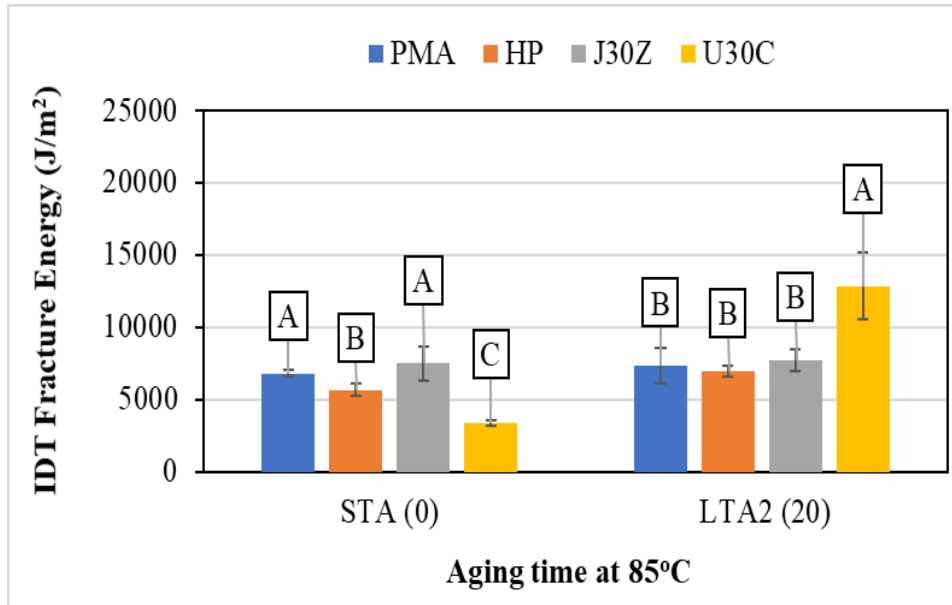


Figure 6-10. IDT G_f Results of GRN2 Mixtures with Different Asphalt Binders at Two Mix Aging Conditions

Figure 6-11 presents the IDT G_f results and Tukey's rankings of OGFC mixtures prepared with the GRN3 mix design at each mix aging condition. Similar trends were observed in the comparison of the mixtures containing different asphalt binders for the GRN2 and GRN3 mix designs. The PMA and HP mixtures had similar G_f results at the STA condition, which were statically lower than that of the J30Z mixture but statistically higher than that of the U30C mixture. At the LTA2 condition, the U30C mixture had the highest G_f and thus, was expected to have the best fracture resistance, followed by the J30Z mixture and then the PMA and HP mixtures. However, the difference between the J30Z versus the PMA and HP mixtures was not statistically significant, according to Tukey's rankings in Figure 6-11. Same with the GRN1 and GRN2 mix designs, the U30C mixture prepared with the GRN3 mix design showed significant improvement in fracture resistance, as indicated by higher IDT G_f results, due to the continued curing of the EMA binder during the extended long-term aging process.

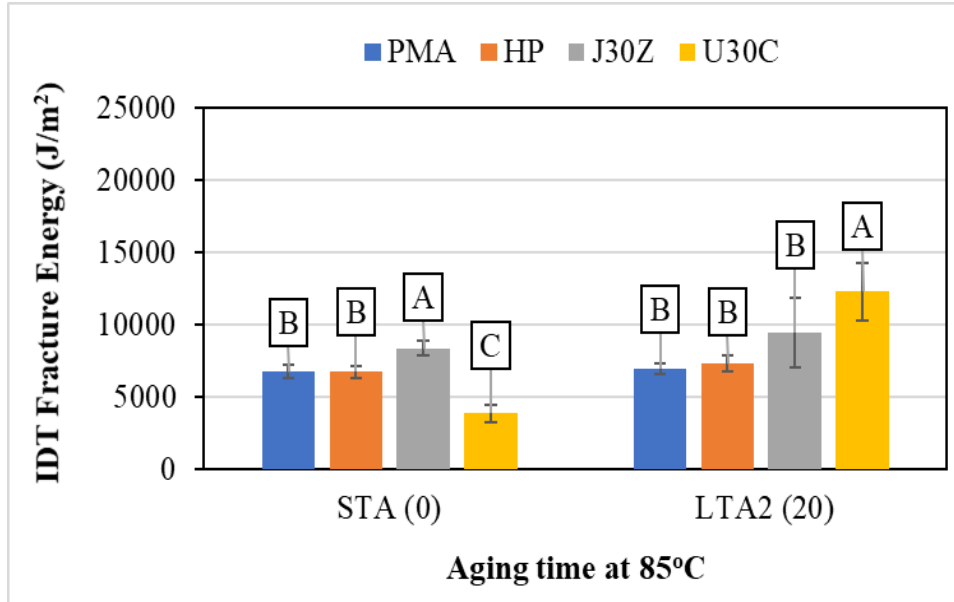


Figure 6-11. IDT G_f Results of GRN3 Mixtures with Different Asphalt Binders at Two Mix Aging Conditions

The IDT G_f results and Tukey's rankings of the OGFC mixtures prepared with the LMS mix design are shown in Figure 6-12. At the STA condition, the J30Z mixture had the highest G_f results, followed by the U30C and PMA mixtures and then the HP mixture. After extended long-term aging for 20 days at 85°C, the U30C mixture had the highest average G_f value and, thus, was expected to have the best fracture resistance, followed by the J30Z mixture, HP mixture, and PMA mixture, respectively. However, the difference between the HP versus the J30Z and PMA mixtures was not statistically significant, according to Tukey's rankings in Figure 6-12.

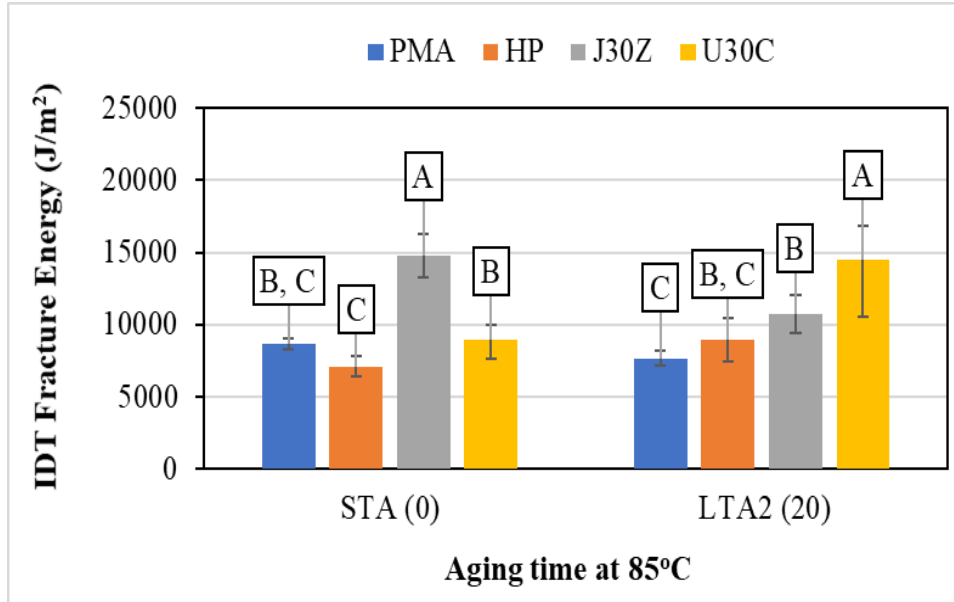


Figure 6-12. IDT G_f Results of LMS Mixtures with Different Asphalt Binders at Two Mix Aging Conditions

6.2.4 TSR Results

Table 6-4 summarizes the dry (unconditioned) strength, wet (moisture conditioned) strength, and TSR results of sixteen OGFC mixtures prepared with a combination of four FC-5 mix designs and four types of asphalt binders. First, all mixtures except one had a TSR of over 80%, thus, acceptable moisture resistance. The J30Z mixture had consistently higher dry strength than the other three mixtures. After moisture conditioning, the two EMA mixtures had higher wet strength results than the PMA and HP mixtures. For all U30C mixtures, a considerable increase in the tensile strength was observed after moisture conditioning. It was speculated that this increase could be attributed to the accelerated curing of the EMA binder when the mixture was conditioned in a water bath at 60°C as part of the moisture conditioning process for the TSR test. Because of the higher strength obtained after moisture conditioning, all the U30C mixtures had TSR values that

were considerably higher than 100%. A detailed discussion of the TSR test results for each mix design is provided below.

Table 6-4. Summary of TSR Test Results

Mix Design ID	Binder Type	Dry strength (psi)			Wet strength (psi)			TSR
		Avg.	Std Dev.	COV	Avg.	Std Dev.	COV	
GRN1	PMA	63.5	1.5	2.4%	53.6	3.3	6.1%	85%
	HP	51.7	12.7	24.6%	46.9	2.7	5.7%	91%
	J30Z	104.7	4.8	4.6%	82.3	4.2	5.1%	79%
	U30C	61.8	4.9	7.9%	85.0	10.6	12.5%	138%
GRN2	PMA	50.9	5.4	10.6%	50.2	3.0	6.1%	99%
	HP	40.4	4.6	11.4%	40.7	1.8	4.4%	101%
	J30Z	81.6	7.5	9.2%	72.8	3.4	4.6%	89%
	U30C	30.2	6.0	19.9%	71.6	9.5	13.2%	237%
GRN3	PMA	70.6	8.6	12.2%	72.4	6.4	8.8%	103%
	HP	55.2	4.8	8.8%	49.8	6.5	13.1%	90%
	J30Z	96.7	14.8	15.3%	102.4	3.6	3.5%	106%
	U30C	47.2	10.7	22.6%	66.7	6.1	9.1%	141%
LMS	PMA	99.2	15.7	15.8%	85.8	4.6	5.4%	86%
	HP	67.2	4.0	6.0%	64.7	1.1	1.7%	96%
	J30Z	124.1	8.2	6.6%	113.4	7.5	6.6%	91%
	U30C	97.4	4.8	4.9%	133.1	14.0	10.5%	137%

Figure 6-13 presents the TSR results of the GRN1 mixtures containing different asphalt binders. The J30Z mixture had the highest dry strength compared to the other three mixtures. After moisture conditioning, the J30Z and U30C mixtures had similar wet strength results, which were higher than those of the PMA and HP mixtures. Unlike the PMA, J30Z, and HP mixtures, the U30C

mixture had a higher tensile strength after moisture conditioning than before, which was likely attributed to accelerated curing of the EMA binder when the mixture was conditioned in a 60°C water bath for moisture conditioning. The U30C mixture had the highest TSR value of 138%, followed by the HP, PMA, and J30Z mixtures, respectively. However, the differences between the HP *versus* PMA mixtures and PMA *versus* J30Z mixtures were not considered significant because they were less than the allowable difference between two test results (i.e., d2s value) of 9.3% as recommended in NCHRP project 9-26 (Azari et al., 2010). Finally, all mixtures except one met the recommended test criteria in NCHRP project 1-55 (Watson et al., 2018) with a TSR of over 70% and average wet strength of over 50 psi. The only exception was the HP mixture, which had an average wet strength of 46.9 psi and thus, marginally failed the wet strength threshold. These results indicated that the four OGFC mixtures prepared with the GRN1 mix design were not expected to be moisture susceptible.

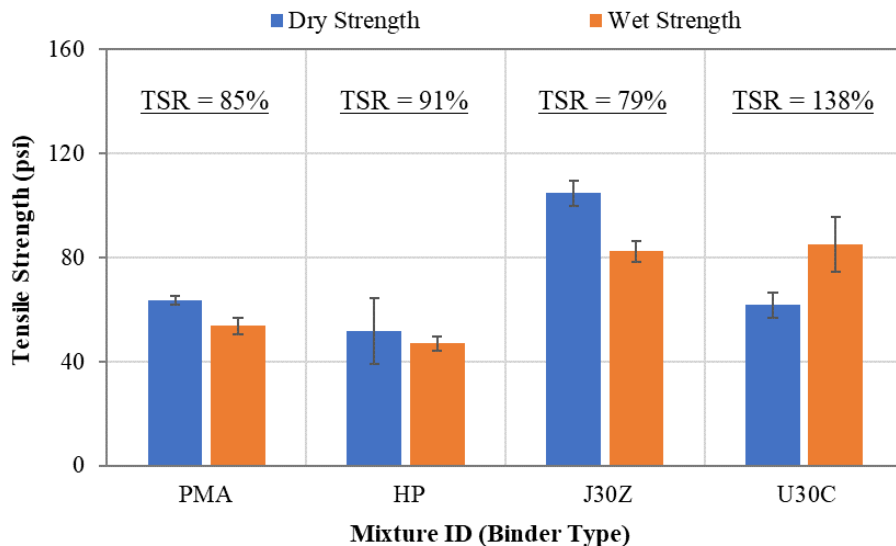


Figure 6-13. TSR Test Results of GRN1 Mixtures with Different Asphalt Binders

Figure 6-14 presents the TSR results of the GRN2 mixtures containing different asphalt binders. The J30Z mixture had the highest dry strength, followed by PMA, HP, and U30C mixtures,

respectively. After moisture conditioning, the two EMA mixtures had similar wet strength results, higher than those of the PMA and HP mixtures. As with the results in Figure 6-13, the U30C mixture had a significantly higher wet strength than the dry strength because of the continued curing of the EMA binder during the moisture conditioning process. As a result, the U30C mixture had an extraordinarily high TSR of 237%. The comparison of the TSR results indicated that the PMA and HP mixtures were expected to be more resistant to moisture damage than the J30Z mixture as their differences in TSR results were over the d2s value of 9.3%.

Nevertheless, all the GRN2 mixtures were expected to have satisfactory moisture resistance with TSR values of over 85%. In comparison against the test criteria recommended in NCHRP project 1-55 (Watson et al., 2018), the HP mixture failed the minimum wet strength threshold of 50 psi. However, this mixture did not show any deterioration in the tensile strength after moisture conditioning and thus, was not likely to be susceptible to moisture damage.

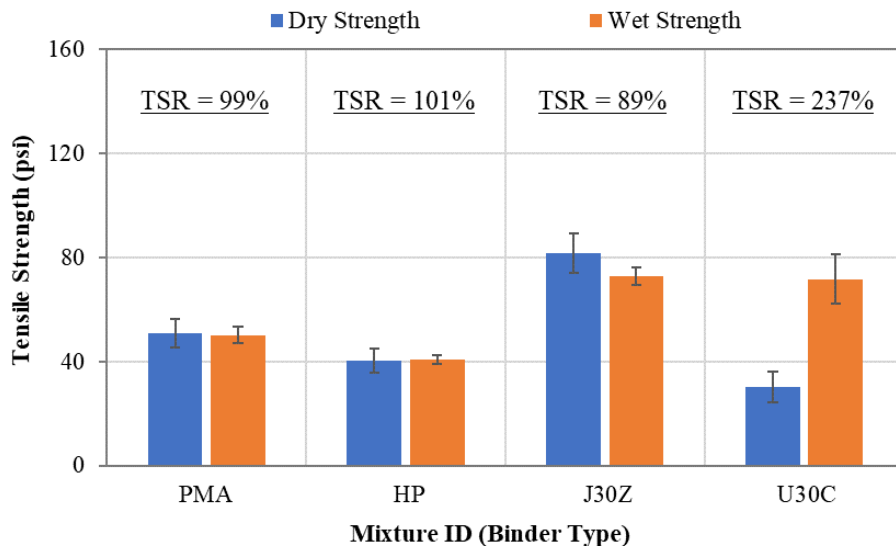


Figure 6-14. TSR Test Results of GRN2 Mixtures with Different Asphalt Binders

The TSR results of OGFC mixtures prepared with the GRN3 mix design are presented in Figure 6-15. The J30Z mixture had the highest dry and wet strength results, followed by the PMA mixture.

In comparing the remaining HP and U-EMA mixtures, the HP mixture had slightly higher dry strength while the U-EMA mixture had higher wet strength. As discussed previously, the considerable increase in the tensile strength of the U30C mixture was due to the continued curing of the EMA binder during the moisture conditioning process. Finally, the U-EMA mixture had the highest TSR, followed by the J-EMA and PMA mixtures, and then the HP mixture. Nevertheless, all the mixtures met the recommended TSR test criteria in NCHRP project 1-55 (i.e., a minimum TSR of 70% and a minimum wet strength of 50 psi) (Watson et al., 2018) and thus, were not expected to be prone to moisture damage.

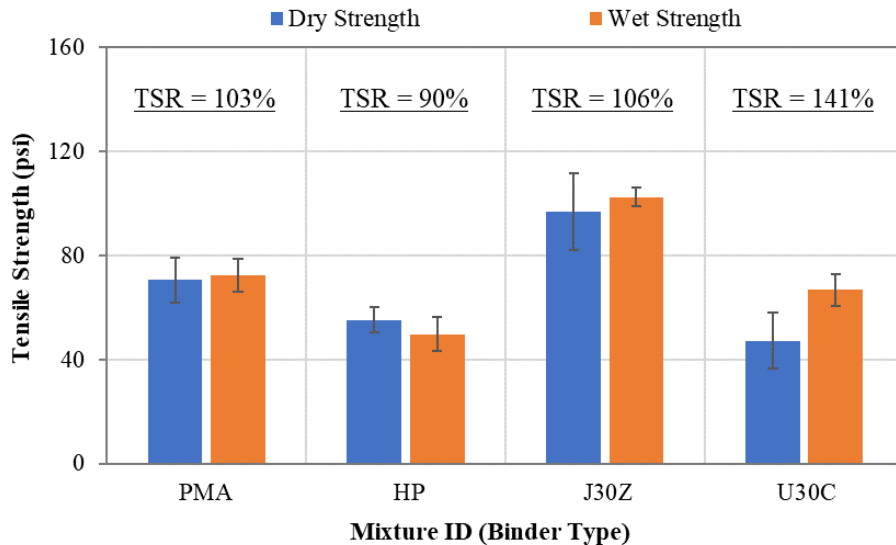


Figure 6-15. TSR Test Results of GRN3 Mixtures with Different Asphalt Binders

Figure 6-16 shows the TSR results of LMS mixtures containing different asphalt binders. The J30Z mixture had the highest dry strength, followed by PMA and U30C mixtures and then the HP mixture. Consistent with the results of the other mix designs discussed previously, the tensile strength of the U30C mixture increased significantly after moisture conditioning. As a result, it had higher wet strength than the other three mixtures. The ranking of the wet strength results for the PMA, HP, and J30Z mixtures was the same as that of the dry strength results. Finally, all the

mixtures met the recommended TSR test criteria in NCHRP project 1-55 (Watson et al., 2018) with a TSR of over 70% and a wet strength of over 50 psi and thus, were expected to have good moisture resistance.

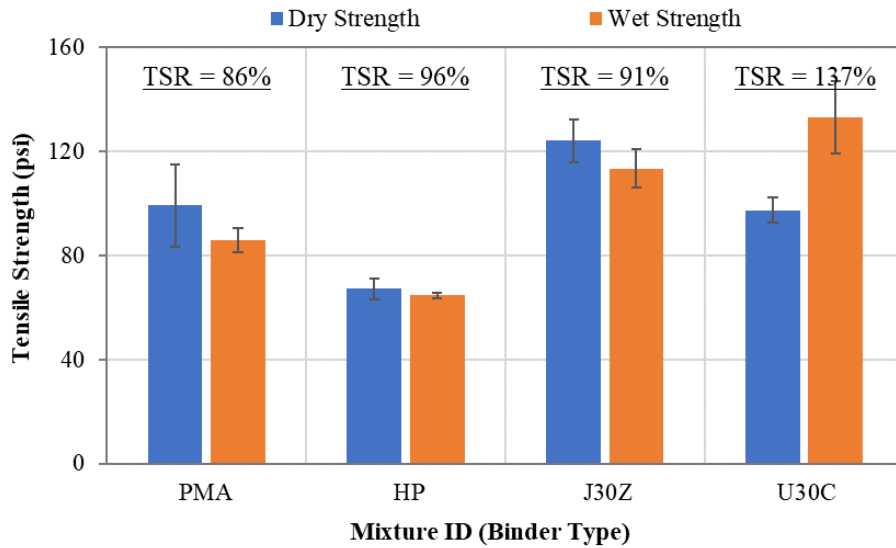


Figure 6-16. TSR Test Results of LMS Mixtures with Different Asphalt Binders

6.2.5 HWTT Results

Table 6-5 summarizes the HWTT results of 16 OGFC mixtures prepared with a combination of four FC-5 mix designs and four types of asphalt binders. All the mixtures were tested at the STA condition without additional long-term aging to evaluate their rutting resistance at their most vulnerable conditions. Overall, the HWTT results for mixtures prepared with the GRN1 and LMS mix designs were significantly better than those prepared with the GRN2 and GRN3 mix designs. All the GRN1 and LMS mixtures rutted less than 12.5 mm and had no signs of stripping. For the GRN2 and GRN3 mix designs, the J30Z mixture showed better rutting and moisture resistance performance than the HP and PMA mixtures. The U30C mixtures exhibited high severity stripping failures in HWTT and did not last more than 7,000 passes before reaching 12.5 mm rut depth.

Detailed discussions of the HWTT results for each mix design are provided in the following sections.

Table 6-5. Summary of HWTT Results

Mix Design ID	Binder Type	Average Rut Depth at 20,000 Passes (mm)	Average Passes to 12.5 mm Rut Depth
GRN1	PMA	9.4	> 20,000
	HP	4.9	> 20,000
	J30Z	6.3	> 20,000
	U30C	6.8	> 20,000
GRN2	PMA	> 12.5	10,000
	HP	> 12.5	17,000
	J30Z	6.3	> 20,000
	U30C	> 12.5	5,000
GRN3	PMA	11.6	> 20,000
	HP	7.0	> 20,000
	J30Z	3.7	> 20,000
	U30C	> 12.5	6,800
LMS	PMA	6.1	> 20,000
	HP	7.4	> 20,000
	J30Z	4.8	> 20,000
	U30C	4.9	> 20,000

Figure 6-17 presents the HWTT rutting curves of the OGFC mixtures prepared with the GRN1 mix design. As shown, all the mixtures lasted over 20,000 passes before reaching 12.5 mm rut depth and had no signs of stripping; therefore, they were expected to have good rutting resistance and moisture resistance. The rut depth results at 20,000 passes indicated that the HP mixture had the best rutting resistance, followed by the J30Z and U30C mixtures and then the PMA mixtures.

However, the difference between the HP and J30Z mixtures was only 1.4 mm, which was not considered practically significant for HWTT. On the other hand, the difference between the HP and U30Z mixtures was largely limited to the post-compaction phase of the HWTT curve, while the two mixtures exhibited similar behavior in the creep phase.

Figure 6-18 presents the HWTT rutting curves of OGFC mixtures prepared with the GRN2 mix design. All mixtures except one had significantly more rutting in HWTT than those prepared with the GRN1 mix design, as shown in Figure 6-17. Overall, the J30Z mixture had the best HWTT results and thus, was expected to have the best rutting resistance and moisture resistance, followed by the HP, PMA, and U30C mixtures, respectively. As shown in Figure 6-20(a) and Figure 6-20(b), both the PMA and HP mixtures showed low to medium severity stripping failures during the test, which was also confirmed by the shape of the HWTT curves in Figure 6-18. High severity stripping was observed in the U30C mixture [Figure 6-20(c)], which only lasted approximately 5,000 passes before reaching 12.5 mm rut depth. During testing, it was also observed that some mixture particles got "picked out" and stuck to the HWTT wheels upon the deterioration of the mixture. It was speculated that the U30C mixture exhibited an early failure in HWTT when tested at the STA condition because the EMA binder was still at the early stage of its curing process and had not gained sufficient cohesive strength to resist the severe condition in HWTT. This result is supported by the low IDT strength and G_f results of the mixture at the STA condition (Figure 6-6 and Figure 6-10). It raises a concern that the U30C mixture prepared with the GRN2 mix design may experience premature rutting and possibly shoving failures immediately after construction due to lack of strength. To understand the effect of curing on the rutting behavior of epoxy-modified mixtures, U30C mixtures were prepared with GRN2 mix design and left for curing for 7, 14, 21, and 28 days under room temperature. The HWTT rutting curves of these cured samples

are plotted in Figure 6-19. Based on the results, the samples allowed for more curing time (i.e., 28 days) clearly performed well with rutting below 3 mm after 20,000 passes and no sign of stripping. However, the U30C samples with up to 21 days of curing failed within 135 to 8500 passes. This reasserts that the curing time is a critical parameter for the performance of the U-EMA mixture. To address this concern further, heavy vehicle simulator (HVS) testing of this mixture is recommended. The test can evaluate the post-compaction curing behavior and also determine the amount of time after construction required for the mixture to gain sufficient strength before it can be allowed to open to traffic on the roadway.

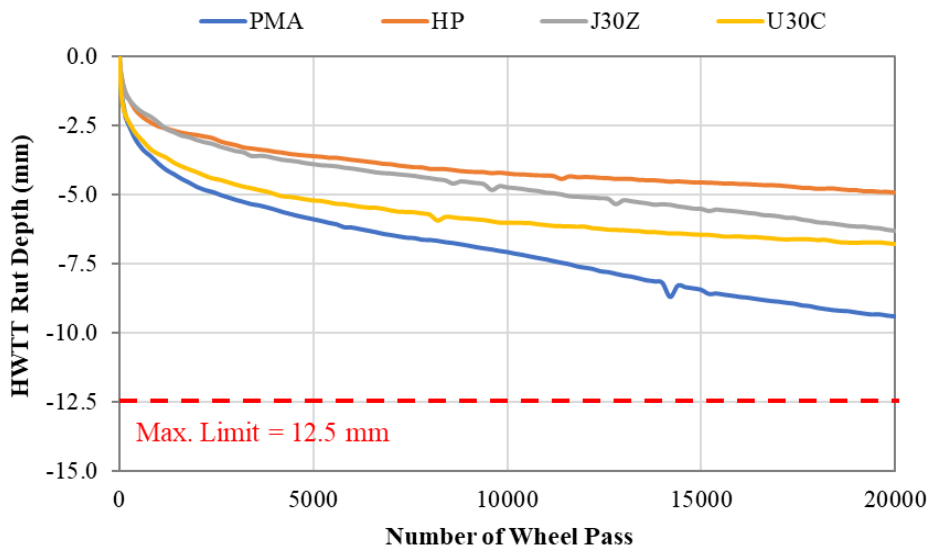


Figure 6-17. HWTT Rutting Curves of GRN1 Mixtures with Different Asphalt Binders

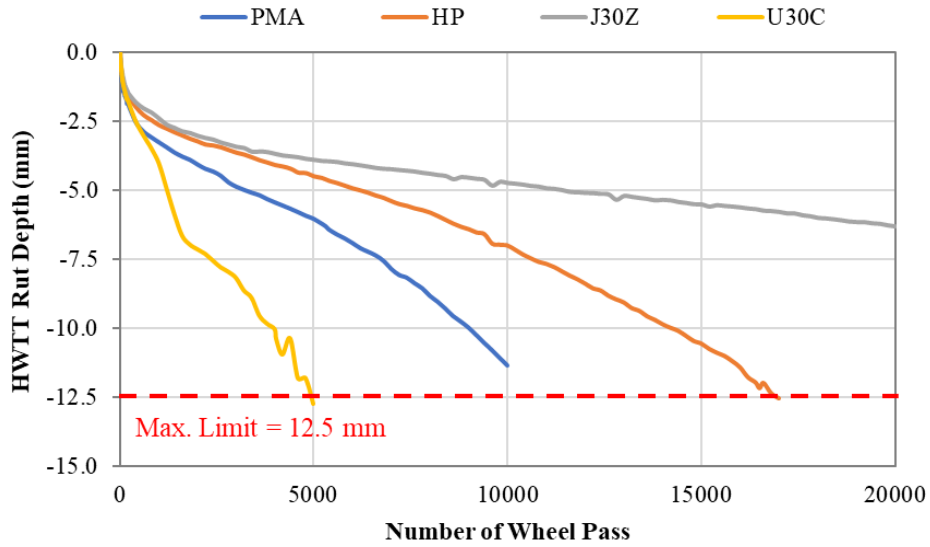


Figure 6-18. HWTT Rutting Curves of GRN2 Mixtures with Different Asphalt Binders

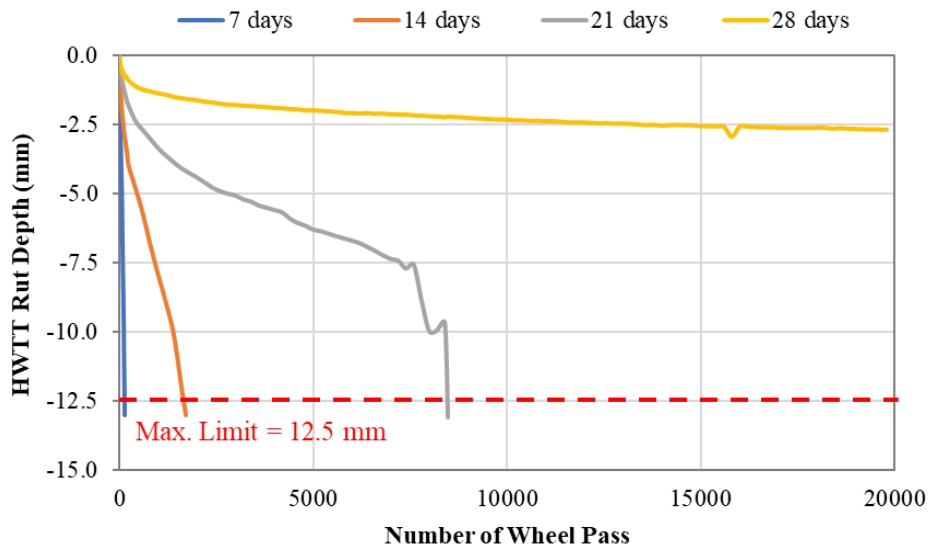


Figure 6-19. HWTT Rutting Curves of GRN2 Mixtures with U30C Binder at Different Curing Times

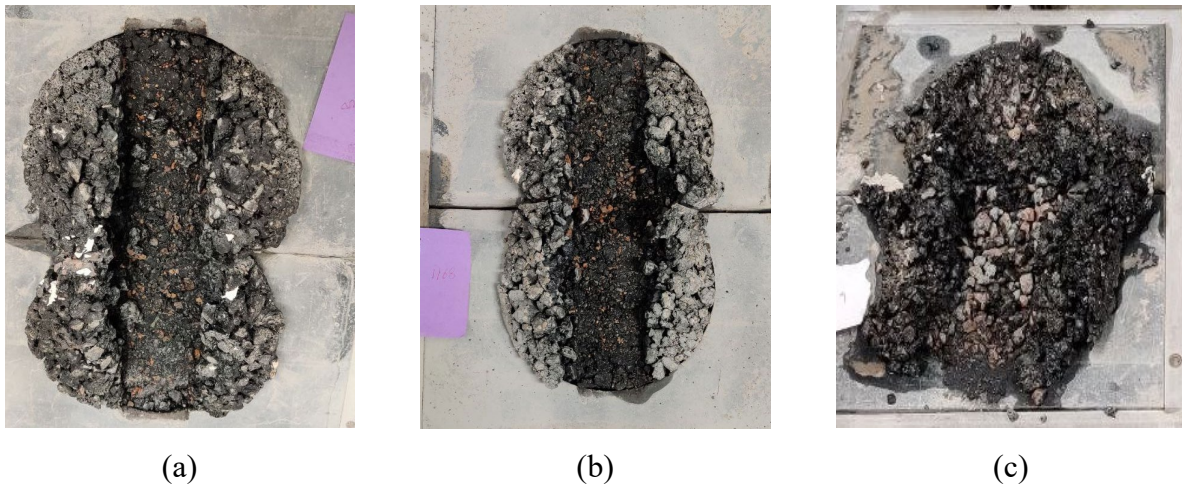


Figure 6-20. Pictures of GRN2 Mixture Samples prepared with (a) PMA Binder, (b) HP Binder, (c) U30C Binder after Testing in HWTT

Figure 6-21 presents the HWTT rutting curves of OGFC mixtures prepared with the GRN3 mix design. In general, these mixtures showed similar trends but better HWTT results overall than those prepared with the GRN2 mix design in Figure 6-20. The J30Z remained the best performer, followed by the HP mixture and then the PMA mixture. These three mixtures lasted over 20,000 passes before reaching 12.5 mm rut depth and had no stripping signs, indicating adequate rutting and moisture resistance. The U30C mixture failed HWTT at approximately 6,800 passes mainly because of stripping. Figure 6-22 presents a picture of the U30C mixture samples after testing, where a considerable amount of uncoated fine aggregate particles are visible. This mixture also exhibited the particle "picking up" issue shown in Figure 6-23. As discussed previously, the early failure of this mixture in HWTT was also likely attributed to its low cohesive strength because of the lack of curing of the EMA binder when tested at the STA condition. Therefore, HVS testing of the U30C mixture prepared with the GRN3 mix design was recommended to determine when the OGFC pavement constructed with this mixture can be allowed for trafficking after construction.

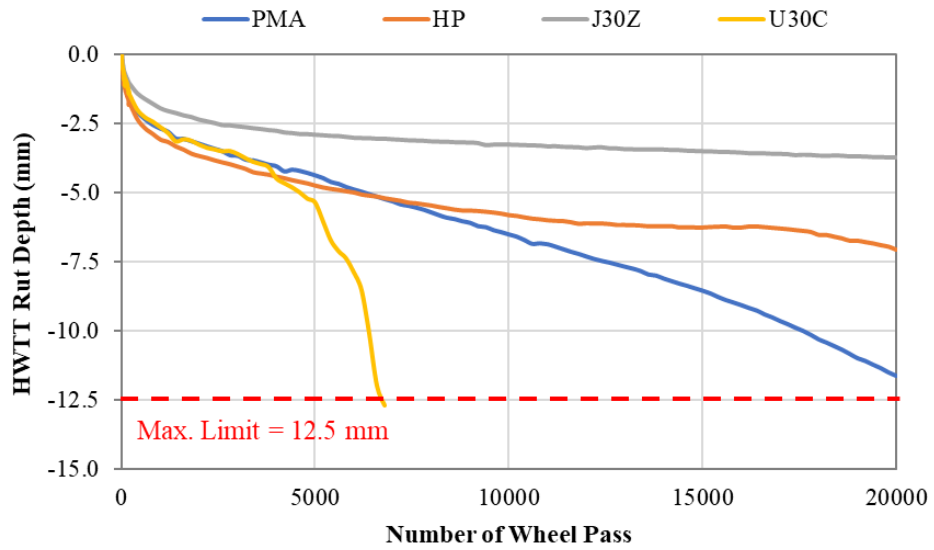


Figure 6-21. HWTT Rutting Curves of GRN3 Mixtures with Different Asphalt Binders



Figure 6-22. Picture of U30C GRN3 Mixture Samples after Testing in HWTT

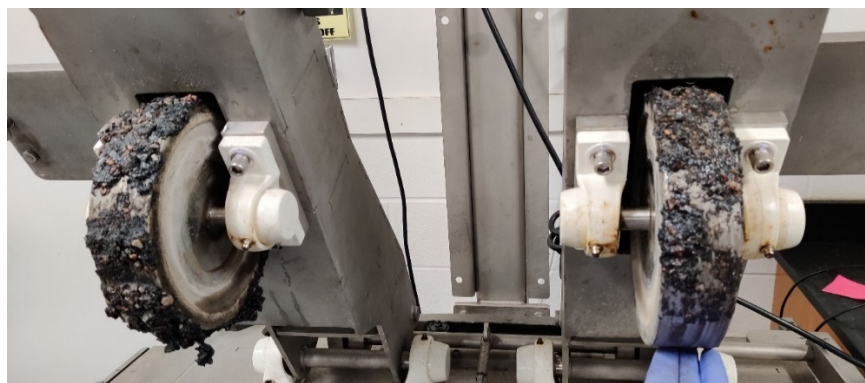


Figure 6-23. Picture of HWTT Wheels Stuck with U30C GRN3 Mixture Particles

The HWTT rutting curves of OGFC mixtures prepared with the LMS mix design are shown in Figure 6-24. All LMS mixtures containing different asphalt binders had good results in the HWTT, with less than 12.5 mm of rutting at 20,000 passes and no signs of stripping. Therefore, these mixtures were expected to have good rutting resistance and moisture resistance. Comparatively, the two EMA mixtures had the best rutting resistance with the lowest rut depths at 20,000 passes, followed by the PMA mixture and then the HP mixture. However, the differences among all the mixtures were less than 2.5 mm, which were not considered practically significant given the variability of the test results and the high air voids of OGFC mixtures.

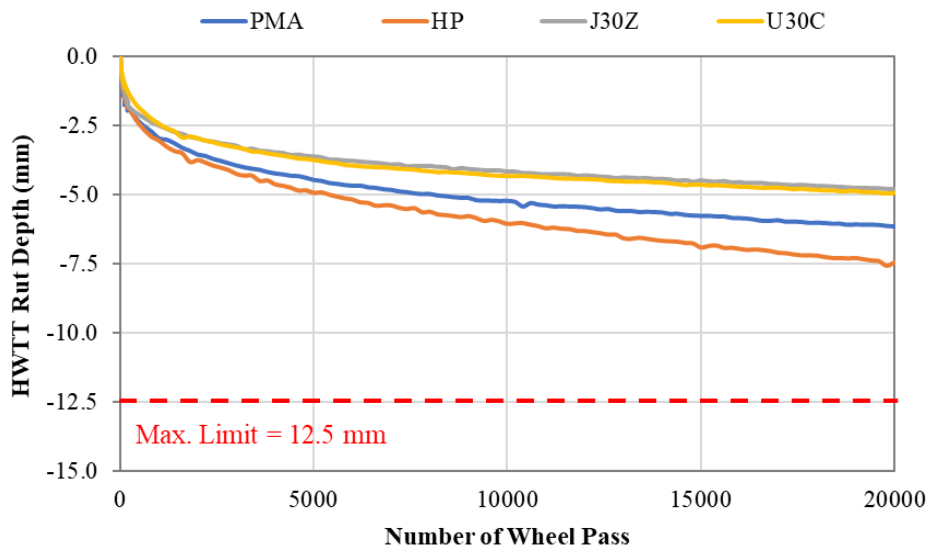


Figure 6-24. HWTT Rutting Curves of LMS Mixtures with Different Asphalt Binders

6.3 Summary of Findings

Performance tests were conducted on OGFC mixtures with PMA, HP binder, and two EMA binders with 30% EDR at unaged and extended long-term aging conditions. Overall, OGFC mixtures prepared with the HP binder had the lowest Cantabro loss results at the STA and LTA2 conditions. Hence, they were expected to have the best raveling resistance before and after extended long-term aging. The two EMA mixtures had much better Cantabro results than the

mixtures containing a PMA binder at the LTA2 condition. Furthermore, the EMA mixtures showed similar Cantabro loss results as the HP mixture in most cases, which indicated comparable raveling resistance after extended long-term aging.

Although the J30C mixtures had consistently higher IDT strength and G_f results than the other mixtures at the STA condition, the U30C mixtures became the best performer with the best tensile strength and fracture resistance after extended long-term aging. All OGFC mixtures prepared with different FC-5 mix designs and asphalt binders except one had a TSR of over 80% when tested at the STA condition and thus, were expected to have acceptable resistance to moisture damage. Unlike the PMA, HP, and J30Z mixtures, the U30C mixtures exhibited considerably higher wet strength than the dry strength, which yielded unusual TSR values significantly higher than 100%. The substantial increase in tensile strength of U30C mixtures was likely attributed to the accelerated curing of the EMA binder when the mixture was conditioned in a 60°C water bath for moisture conditioning of the TSR test.

The HWTT results for the OGFC mixtures were highly dependent on the mix design used. All mixtures prepared with the GRN1 and LMS mix designs had less than 12.5 mm of rutting at 20,000 passes and showed no signs of stripping. The J30Z and U30C mixtures had similar or slightly better results than the HP and PMA mixtures in HWTT. For the GRN2 and GRN3 mix designs, on the other hand, the J30Z mixtures significantly outperformed the other three mixtures in terms of rutting resistance and moisture resistance. The PMA and HP mixtures prepared with the GRN2 mix design reached 12.5 mm rut depth before 20,000 passes and had low to medium severity stripping failures. The U30C mixtures prepared with the same mix designs showed high severity stripping failures and, as a result, lasted less than 7,000 passes before reaching 12.5 mm rut depth. It was believed that this early failure of U30C mixtures was because the EMA binder, when tested

at the STA condition, was in the early stage of its curing process and had not gained sufficient cohesive strength to resist the severe condition in HWTT. These results raise a concern that the U30C mixtures prepared with the GRN2 and GRN3 mix designs may not be allowed to open to traffic immediately after construction due to lack of strength. HVS testing of these mixtures is needed to determine the amount of time required for the mixtures to gain sufficient strength before they should be allowed for trafficking on the roadway.

CHAPTER 7. CONCLUSIONS AND RECOMMENDATIONS

7.1 Conclusions

This thesis sought to investigate the effectiveness of using epoxy-modified asphalt to improve the durability and life span of open-graded friction course mixtures in Florida. The literature review was focused on two topics: 1) mix design and performance testing of OGFC mixtures and 2) use of epoxy resin for asphalt modification. The state-of-the-practice of OGFC mixtures, OGFC mix design, OGFC performance testing approaches, existing OGFC durability enhancement techniques, and the fundamentals of EMA binders and mixture were synthesized. Addressing the limitations identified, an experimental plan was developed, starting with the selection of suitable asphalt binders for epoxy modification based on fluorescence microscopy. Later, an optimum epoxy dosage rate to be added to the chosen asphalt binders was determined with respect to material cost and OGFC performance properties. A mix design procedure was then developed to prepare OGFC mixtures containing EMA binders at optimum EDR. The EMA mixtures were subjected to three aging conditions and tested for raveling resistance, tensile strength, fracture resistance, moisture sensitivity, and rutting potential. The performance properties of EMA mixtures were characterized and compared with the OGFC mixtures prepared with PG 76-22 PMA and HP binders. The major conclusions of the study are orderly summarized below:

- Base binder Z had the best compatibility with the epoxy materials from a foreign source, while the base binder C was most compatible with the epoxy materials from a domestic source.
- The compatibility of EMA binder combinations was reduced with an increase in the EDR from 15% to 25%. This was indicated by the network distribution of epoxy resins observed using fluorescence micrographs.

- Most of the EMA mixtures had reduced Cantabro loss, increased IDT strength, and increased fracture energy with an increase in EDR between 15% to 40%.
- On ranking the CAI, the U-EMA mixtures had the best aging resistance, followed by the J-EMA mixtures and then the PMA mixtures.
- After long-term aging for 10 days and 20 days at 85°C, the EMA mixtures at 30% and 40% EDRs outperformed the PMA and low-dosage EMA mixtures in the Cantabro and IDT tests.
- Based on the performance properties of OGFC mixtures (statistically significant) and the material cost, 30% was selected as the optimum EDR for both J-EMA and U-EMA binders. At this EDR, the estimated material cost of EMA OGFC mixtures was approximately 3.5 to 5 times higher than those containing a PMA binder.
- The new mix design procedure developed for OGFC mixtures containing 30% EMA binder was successfully validated with four FDOT approved FC-5 mix designs.
- In comparison to the OGFC mixtures containing a PG 67-22 binder, the mixtures with an EMA binder at the optimum EDR exhibited less asphalt draindown in the pie plate test. Further, the Cantabro loss of EMA mixtures was less than 20% in STA (unaged) condition. Thus, the developed procedure has the potential of designing EMA OGFC mixtures with adequate raveling resistance before aging and minimal potential for asphalt draindown during production.
- Relatively, the OGFC mixtures with HP binder had the lowest Cantabro loss at both short-term and extended long-term aging conditions. Nevertheless, in most cases, the EMA mixtures at 30% EDR performed comparatively as the HP mixtures at the extended long-term aging condition. Though the PMA mixtures performed similarly or better than the EMA mixtures at short-term aging condition, the EMA mixtures showed significantly lower

Cantabro loss upon extended aging, which indicated potentially better raveling resistance and durability in a longer span.

- On comparing the IDT results, the J-EMA and U-EMA mixtures at 30% EDR had the highest IDT strength and fracture energy at short-term and extended long-term aging conditions, respectively.
- All the OGFC mixtures prepared with different asphalt binders, except for one, had a TSR of over 80%. Hence, all the mixtures were expected to have sufficient resistance to moisture damage. Furthermore, exceptionally high wet strength was obtained for U-EMA mixtures at 30% EDR leading to a TSR above 100%. The significant increase in wet strength was possibly due to the accelerated curing of the EMA binder when the mixture was conditioned in a 60°C water bath for moisture conditioning.
- The HWTT performance of OGFC mixtures was found to be highly dependent on the mix design and the type of asphalt binder used. All mixtures prepared with the GRN1 and LMS mix designs had minimal rut depth and no signs of stripping. The J-EMA and U-EMA mixtures at 30% EDR had similar or slightly better HWTT results than the HP and PMA mixtures. However, for both the GRN2 and GRN3 mix designs, the J-EMA mixtures had significantly better HWTT results than the other three mixtures and exhibited no signs of stripping. The PMA and HP mixtures prepared with the GRN2 mix design showed low to medium severity stripping failures, while the U-EMA mixtures prepared with both the GRN2 and GRN3 mix designs had high severity stripping failures. It is speculated that the U-EMA binder was still in the early stages of curing at the STA condition and did not have sufficient cohesive strength to withstand the HWTT conditions, resulting in the early

stripping failure of U-EMA mixtures. U-EMA mixtures cured for four weeks at room temperature showed good rutting and moisture resistance in HWTT.

- Overall, the test results supported the hypothesis that the EMA binder could potentially improve the long-term durability of OGFC mixtures in Florida. Nevertheless, the improved performance of OGFC mixtures could also be achieved by using HP binders at a lower cost.

7.2 Recommendations

Future research and implementation activities based on the findings of the thesis are provided as follows:

- Determine the critical field aging conditions (in terms of aging time and climatic conditions) corresponding to the OGFC mixture's initial raveling and develop a representative laboratory mix aging procedure for mixture performance evaluation.
- Construct a field demonstration project for assessing the long-term field performance of OGFC mixtures containing HP versus EMA binders, as well as identify the possible challenges associated with the production and construction of EMA OGFC mixtures.
- Monitor the post-compaction curing behavior of U-EMA mixtures using an HVS and determine the time after construction when the pavement can be opened to traffic.
- Perform life-cycle cost analysis to compare the cost-effectiveness of OGFC mixtures prepared with PMA, HP, and EMA binders based on the actual bid price and long-term field performance data.

REFERENCES

- Al-Busaltan, S., Al-Yasari, R., Al-Jawad, O., and Saghafi, B. (2020). Durability Assessment of Open-Graded Friction Course using a Sustainable Polymer. *International Journal of Pavement Research and Technology*, Vol. 13(6), pp. 645-653.
- Alvarez, A., Martin, E., Estakhri, C., Button, J., Glover, C., and Jung, S. (2006). Synthesis of Current Practice on the Design, Construction, and Maintenance of Porous Friction Courses. Report No. FHWA/TX-06/0-5262-1, Texas Department of Transportation, Austin, TX.
- Alvarez, A., Martin, A., and Estakhri, C. (2011). A Review of Mix Design and Evaluation Research for Permeable Friction Course Mixtures. *Construction and Building Materials*, Vol. 25, pp. 1159-1166.
- Arambula-Mercado, E., Caro, S., Torres, C. A. R., Karki, P., Sanchez-Silva, M., and Park, E. S. (2019). Evaluation of FC-5 with PG 76-22 HP to Reduce Raveling. Report No. BE287, Prepared by Texas A&M Transportation Institute for the Florida Department of Transportation, Tallahassee, FL.
- Azari, H. (2010). Precision Estimates of AASHTO T283: Resistance of Compacted Hot Mix Asphalt (HMA) to Moisture-Induced Damage. National Cooperative Highway Research Program, Transportation Research Board of the National Academies, Web-only Document 166, Washington, D.C.
- Baldock, R. H. (1939). Open Type Asphaltic Concrete. *The Asphalt Forum*, Vol. 3, pp. 4-5.
- Bennert, T., and A. Cooley. (2014). Evaluate the Contribution of the Mixture Components of the Longevity and Performance of FC-5. Florida Department of Transportation, Tallahassee, FL.

- Buddhavarapu, P., Smit, A., and Prozzi, J. (2015). A Fully Bayesian Before-After Analysis of Permeable Friction Course Pavement Wet Weather Safety. *Accident Analysis and Prevention*, Vol. 80, pp. 89-96.
- Chen, J., Tang, T., and Zhang, Y. (2017). Laboratory Characterization of Directional Dependence of Permeability for Porous Asphalt Mixtures. *Materials and Structures*, Vol. 50, Article No. 215.
- Chen, Y., Hossiney, N., Yang, X., Wang, H., and You, Z. (2021). Application of Epoxy-Asphalt Composite in Asphalt Paving Industry: A Review with Emphasis on Physicochemical Properties and Pavement Performances. *Advances in Materials Science and Engineering*, Vol. 2021.
- Cooley, L., Brumfield, J., Wogawer, R., Partl, M., Poulikakos, L., and Hicks, G. (2009). Construction and Maintenance Practices for Permeable Friction Courses. NCHRP Report 640, The National Academies Press, Washington, D.C.
- Daines, M. E. (1986). Pervious Macadam: Trials on Trunk Road A38 Burton Bypass. Research Report No. 57, Transport and Road Research Laboratory, Wokingham, UK.
- Daines, M. E., and Colwill, D. (1989). Progress in the Trials of Pervious Macadam. *Highways*, Vol. 57.
- Dinnen, A. (1991). Epoxy Bitumen Binders for Critical Road Constructions. Proceedings of the 2nd Eurobitume Symposium, pp. 294-296.
- Florida Department of Transportation (FDOT). (2022). Standard Specifications for Road and Bridge Construction. Link at:
<https://fdotwww.blob.core.windows.net/sitefinity/docs/default->

[source/programmanagement/implemented/specbooks/january-2022/january2022-ebook.pdf](#).

Gu, F., Moraes, R., Chen, C., Yin, F., Watson, D., and Taylor, A. (2021). Effects of Additional Antistrip Additives on Durability and Moisture Susceptibility of Granite-Based Open Graded Friction Course. *Journal of Materials in Civil Engineering*, Vol. 33(9), pp. 04021245.

Hernandez-Saenz, M., Caro, S., Arambula-Mercado, E., and Martin, A. (2016). Mix Design, Performance and Maintenance of Permeable Friction Courses in the United States: State of the Art. *Construction and Building Materials*, Vol. 111, pp. 358-367.

Herrington, P. (2010). Epoxy-Modified Porous Asphalt. NZ Transport Agency Research Report No. 410, NZ Transport Agency, Wellington, NZ.

Herrington, P., Alabaster, D., Arnold, G., Cook, S., Fussell, A., and Reilly, S. (2007). EMA Open-Graded Porous Asphalt. Land Transport New Zealand Research Report No. 321, Land Transport New Zealand, Wellington, NZ.

Herrington, P., and Alabaster, D. (2008). EMA Open-Graded Porous Asphalt. *Road Materials and Pavement Design*, Vol. 9(3), pp. 481-498.

Huber, G. (2000). NCHRP Synthesis 284: Performance Survey on Open-Graded Friction Course Mixes, Transportation Research Board, Washington, D.C.

Jackson, N. C., Vargas, A., and Pucinelli, J. (2008). Quieter Pavement Survey. Publication WA-RD 688.1, Washington State Transportation Commission, Department of Transportation, Olympia, WA.

- Kabir, M. S., King, W., Abadie, C., Icenogle, P., and Cooper, S. B. (2012). Louisiana's Experience with Open-Graded Friction Course Mixtures. *Transportation Research Record*, Vol. 2295, pp. 63-71.
- Kandhal, P. (2002). Design, Construction, and Maintenance of Open-Graded Asphalt Friction Courses. National Asphalt Pavement Association Information Series 115, National Asphalt Pavement Association, Lanham, MD.
- Kayhanian, M., and Harvey, J. T., (2020). Optimizing Rubberized Open-Graded Friction Course (RHMAO) Mix Designs for Water Quality Benefits: Phase I: Literature Review. Report No. UCPRC-RR-201903, University of California Pavement Research Center, Davis, CA.
- Kline, L. (2010). Comparison of Open Graded Friction Course Mix Design Methods Currently used in the United States. Link at: https://tigerprints.clemson.edu/all_theses/846.
- Kuennen, T. (2012). The Chemistry of Road Building Materials: Asphalt a la Carte - Modifiers Control Mix Performance. *Better Roads – Road Science*, pp. 16-27.
- Lu, Q., and Bors, J. (2015). Alternate uses of Epoxy Asphalt on Bridge Decks and Roadways. *Construction and Building Materials*, Vol. 78, pp. 18-25.
- Luo, S., Lu, Q., and Qian, Z. (2015). Performance Evaluation of EMA Open-Graded Porous Asphalt Concrete. *Construction and Building Materials*, Vol. 76, pp. 97-102.
- Lyon, C., Persaud, B., and Merritt, D. (2018). Quantifying the Safety Effects of Pavement Friction Improvements – Results from a Large-Scale Study, *International Journal of Pavement Engineering*, Vol. 19(2), pp. 145-152.

- Mallick, R., Kandhal, P., Cooley Jr., L. A., and Watson, D. (2000). Design, Construction, and Performance of New-Generation Open-Graded Friction Courses. NCAT Report 00-01, National Center for Asphalt Technology, Auburn, AL.
- McGraw, H. Chapter 16: Ethers, Epoxides and Sulfides. Link at:
<https://slideplayer.com/slide/8922034/>, accessed on April 11, 2018.
- Moraes, R. and Yin, F. (2020). Evaluation of Epoxy Asphalt Binders for Open-Graded Friction Course (OGFC) Application. Proceedings of the RILEM International Symposium on Bituminous Materials – ISM Lyon 2020, Lyon, France.
- National Center for Asphalt Technology (NCAT). (2015). A Commitment to Conservation and Sustainability: Exploring Japan’s Asphalt Pavement Innovations. Asphalt Technology News, Vol. 27(2), pp. 1-16.
- Ndon, U. J. (2017). Trends in the Application of Permeable Pavement as Sustainable Highway Storm Water Management Option for Safe-Use of Roadways. Journal of Civil and Environmental Engineering, Vol. 7(6), pp. 1-15.
- OECD. (2008). Long-life Surfaces for Busy Roads. OECD Transport Research Centre, Paris, France, pp. 185.
- ONI. (2021). Retrieved from Fluorescence Microscopy a Simple Overview. Link at:
<https://oni.bio/fluorescence-microscopy>, accessed on April 27, 2021.
- Onyango, M., and Woods, M. (2017). Analysis of the Utilization of Open-Graded Friction Course (OGFC) in the United States. International Conference on Highway Pavements and Airfield Technology 2017, pp. 137-147.
- Peng, W., and Riedl, B. (1995). Thermosetting Resins. Journal of Chemical Education, Vol. 72, pp. 587-592.

- Plug, C. P., Bondt, A. H., and Khedoe, R. N. (2012). Effect Kwaliteit Bitumen op Duurzaamheid ZOAB. Link at: [https://www.crow.nl/downloads/pdf/bijeenkomsten-congressen/2012/infradagen/\(102\)-effecten-kwaliteit-bitumen-op-duurzaamheid-z](https://www.crow.nl/downloads/pdf/bijeenkomsten-congressen/2012/infradagen/(102)-effecten-kwaliteit-bitumen-op-duurzaamheid-z).
- Polacco, G., Filippi, S., Merusi, F., and Stastna, G. (2015). A Review of the Fundamentals of Polymer-Modified Asphalts: Asphalt/Polymer Interactions and Principles of Compatibility. *Advances in Colloid and Interface Science*, Vol. 224, pp. 72-112.
- Qureshi, N. A., Farooq, S. H., and Khurshid, B. (2015). Laboratory Evaluation of Durability of Open-Graded Friction Course Mixtures. *International Journal of Engineering and Technology*, Vol. 7(3), pp. 956-964.
- Seim, C. (1973). Skid Resistance of Epoxy Asphalt Pavements on California Toll Bridges. NSTP 530, Skid Resistance of highway pavements, ASTM International, pp. 41-59.
- Seim, C. (1974). Experiences with Skid-Resistant Epoxy Asphalt Surfaces on California Toll Bridges. *Transportation Research Record*, Vol. 523, pp. 110-122.
- Shimeno, S., and Tanaka, T. (2010). Evaluation and Further Development of Porous Asphalt Pavement with 10 Years Experience in Japanese Expressways. *Proceedings of the 11th International Conference on Asphalt Pavements*, pp. 43-52, Nagoya, Japan.
- Shuler, S., and Hanson, D. I. (1990). Improving Durability of Open-Graded Friction Courses. *Transportation Research Record*, pp. 35-41.
- Smith, R.W., Rice, J. M., and Spelman, S. R. (1974). Design of Open-Graded Asphalt Friction Courses. Report FHWA-RD-74-2, Federal Highway Administration, Washington, D.C.
- Takahashi, S. (2013). Comprehensive Study on Porous Asphalt Effect on Expressways in Japan: Based on Field Data Analysis in the Last Decade, *Road Materials and Pavement Design*, Vol. 14(2), pp. 239-255.

- Tian, J., Luo, S., Lu, Q., and Liu, S. (2021). Effects of Epoxy Resin Content on Properties of Hot Mixing Epoxy Asphalt Binders. Unpublished manuscript.
- Tian, X., Huang, X., and Yu, B. (2011). Experimental Study on the Durability of Open Graded Friction Course Mixtures. *Pavements and Materials: Recent Advances in Design, Testing and Construction*, pp. 71-77.
- Timm, D. H., Robbins, M. M., Tran, N., and Rodezno, C. (2014). Recalibration Procedures for the Structural Asphalt Layer Coefficient in the 1993 AASHTO Pavement Design Guide. NCAT Report 14-08, National Center for Asphalt Technology, Auburn, AL.
- Watson, D. (2014). In Search of Longer Life PFC's. *Asphalt Technology News*, Vol. 26(2), National Center for Asphalt Technology, Auburn University, AL.
- Watson, D., Johnson, A., and Jared, D. (1998). Georgia DOT's Progress in Open-Graded Friction Course Development. *Transportation Research Record*, Vol. 1616, pp. 30-33.
- Watson, D., Tran, N., Rodezno, C., Taylor, A., and James, Jr, T. (2018). Performance-Based Mix Design of Porous Friction Courses. NCHRP Project 1-55, Transportation Research Board of the National Academies of Sciences, Engineering, and Medicine, In Press, Washington, D.C.
- Wu, J. P., Herrington, P. R., and Alabaster, D. (2019). Long-term Durability of Epoxy-Modified Open-Graded Porous Asphalt Wearing Course. *International Journal of Pavement Engineering*, Vol. 20(8), pp. 920-927.
- Xie, Z., Tran, N., Watson, D. E., and Blackburn, L. D. (2019). Five-Year Performance of Improved Open-Graded Friction Course on the NCAT Pavement Test Track. *Transportation Research Record*, Vol. 2673(2), pp. 544-551.

- Yin, F., Anand, A., Moraes, R., Tran, N., and West, R. (2021). Design and Performance of Open-Graded Friction Course Mixtures Containing Epoxy Asphalt. National Center for Asphalt Technology, Auburn, AL.
- Youtcheff, J., Gibson, N., Shenoy, A., and Al-Khateeb, G. (2006). Evaluation of Epoxy Asphalt and Epoxy Asphalt Mixtures. Proceedings of the 51st Annual Conference of the Canadian Technical Asphalt Association (CTAA), Polyscience Publications, Laval, Québec, Canada, pp. 351-367.
- Zegard, A., Smal, L., Naus, R., Apostolidis, P., Liu, X., Van de Ven, M., Erkens, S., and Scarpas, A. (2019). Field Trials with Epoxy Asphalt for Surfacing Layers - Province of North Holland Case Study. Poster Session during the 99th Transportation Research Board Annual Meeting, Transportation Research Board, Washington, D.C.
- Zhou, F., Im, S., Sun, L., and Scullion, T. (2017). Development of an IDEAL Cracking Test for Asphalt Mix Design and QC/QA. Road Materials and Pavement Design, Vol. 18(sup4), pp. 405-427.
- Zhu, J., Birgisson, B., and Kringos N. (2014). Polymer Modification of Bitumen: Advances and Challenges. European Polymer Journal, Vol. 54, pp. 18-38.